Adipose tissue as a mediator of inflammation and oxidative cellular damage in obesity and type 2 diabetes.

Jones, Danielle Alice

ADIPOSE TISSUE AS A MEDIATOR OF INFLAMMATION AND OXIDATIVE CELLULAR DAMAGE IN OBESITY AND TYPE 2 DIABETES

DANIELLE ALICE JONES

(NISCHR PhD studentship: HS/09/006)

Submitted to Swansea University in fulfilment of the requirements for the Degree of Dr of Philosophy

Diabetes Research Group

College of Medicine

Swansea University

2013

Declaration and Statements

Declaration

This work has not previously been accepted in substance for any degree and is not being concurrently submitted in candidature for any degree.

Signed.....(candidate)

Date.....18/12/13.....

Statement 1

This thesis is the result of my own investigations, except where otherwise stated. Where correction services have been used, the extent and nature of the correction is clearly marked in a footnote(s)

Other sources are acknowledged by footnotes giving explicit references. A bibliography is appended.

Signed.....(candidate)

Date.....18/12/13.....

Statement 2

I hereby give consent for my thesis, if accepted, to be available for photocopying and for inter-library loan, and for the title and summary to be made available to outside organisations.

Signed.....(candidate)

Date.....18/12/13.....

Acknowledgments

I would like to thank everyone who made this thesis possible. Particularly I would like to thank Prof. Jeff Stephens for his constant support and for always keeping me motivated, and Dr Sarah Prior, for not only being a fantastic teacher but also a wonderful friend. I am very grateful to Professor John Baxter, Mr Jonathan Barry, Mr Scott Caplin, Nia Eyre and all of the surgical staff at Morriston hospital and the Princess of Wales hospital. Without this team of wonderful people I would never have been able to collect the samples required to carry out this work. Also, a big thank you to all of patients that participated in the study. I would like to thank Professor Steve Humphries and his research group at the Centre for Cardiovascular Genetics, UCL, for their time and patience while teaching me the technique for measuring telomere length. I would like to thank everyone on the 3rd floor of the ILS, particularly the Diabetes Research group for all the giggles (and moans) along the way and always being there with advice whenever I had a problem. I will be eternally grateful to NISCHR for providing the funding, without which this research would have never left the ground. Finally and most importantly I would give my love and thanks to my ever supportive family for always being there for me financially and emotionally and Simon for putting up with the tears and always being there to make me laugh and get on with it.

Summary

In the past 30 years the prevalence of obesity has almost trebled resulting in an increased incidence of type 2 diabetes mellitus (T2DM) and other co-morbidities. Visceral adipose tissue is believed to play a vital role in these conditions, but underlying mechanisms remain unclear. A close association exists between obesity, diabetes and oxidative stress, resulting in increased reactive oxygen species formation.

The experiments in this thesis address this by searching for possible biochemical changes which may be specific for the onset of obesity related T2DM, as well as looking for genetic alterations at molecular and gene expression levels. This thesis also explored various techniques such as polymerase chain reaction (PCR), colorimetric assays and real-time RT-PCR. The aim was to investigate the role of adipose tissue in obesity and T2DM, focusing on markers of oxidative stress and gene expression in human visceral adipose tissue from subjects categorised as lean, obese and obese with T2DM. This cross-sectional study measured two markers of oxidative stress, two markers of DNA damage, gene expression analysis and identification of genes associated with T2DM and obesity. Specific gene sequencing was carried out on the glutathione reductase gene to determine possible gene variants.

Results showed a paradoxical decrease in adipose markers of oxidative stress in subjects with obesity and T2DM. There appeared to be a protective mechanism in these subjects, displaying reduced levels of oxidative stress compared to other groups. This could be due to a significant proportion of these subjects being on ACE inhibitor and statin therapy, which may be confounding results and minimising the effects of the oxidative burden. Additionally, the same subjects showed an increased expression of the glutathione reductase gene. It is difficult to conclude if the decreased levels of oxidative stress in these subjects were a result of the increased glutathione reductase expression in the visceral adipose tissue or if there remains an unseen factor influencing the dramatic expression change seen in this group of subjects. No glutathione reductase gene variants were identified in these samples.

This analysis highlighted that within this sample set, the impact of oxidative stress is in fact reversible as the antioxidant capacity in these subjects is evident, and in combination with correct drug therapy it may be possible to combat oxidative burden and reduce the subsequent damage inflicted upon the cells.

Abbreviations

µg	Micrograms
µl	Microlitres
µm	Micrometres
$\Delta ABTS^+$	Relative change in $ABTS^+$ formation
A	Adenine
ABTS	2, 2-azino-bis-3-ethylbensthiazoline-6-sulphonic acid
ACE	Angiotensin-converting-enzyme
ACP1	Erythrocyte acid phosphatase
ADP	Adenine diphosphate
AGE	Advanced glycation end-products
ANOVA	Analysis of variance
APOE	Apolipoprotein E
AT	Adipose tissue
ATP	Adenine triphosphate
BAT	Brown adipose tissue
BMI	Body mass index
cDNA	Complementary DNA
C	Cytosine
CAT	Catalase
CHD	Coronary heart disease
CV	Coefficient of variation
CVD	Cardiovascular disease
DBP	Diastolic blood pressure
DM	Diabetes mellitus
DNA	Deoxyribonucleic acid
ELISA	Enzyme-linked immunosorbent assay
FAD	Flavin adenine dinucleotide
FFA	Free fatty acid
G	Guanine
G6PDH	Glucose-6-phosphate dehydrogenase
GCL	Glutamate cysteine ligase

GC-MS	Gas chromatography–mass spectrometry
GPX	Glutathione peroxidase
GS	GSH synthetase
GSH	Reduced glutathione
GSR	Glutathione reductase
GSSR	Oxidised glutathione
hVAT	Human visceral adipose tissue
H_2	Hydrogen
H_2O	Water
H_2O_2	Hydrogen peroxide
HDL-C	High density lipoprotein-cholesterol
HO_2	Hydroperoxyl
HRP	Horse radish peroxidase
IL	Interleukin
IR	Insulin resistance
kg	Kilograms
L	Lean
LDL-C	Low density lipoprotein-cholesterol
LPS	Lipopolysaccharide
$^{\bullet}OH$	Hydroxyl radical
O	Obese
O_2	Oxygen
ODM	Obese with type 2 diabetes mellitus
OSA	Obstructive sleep apnoea
PBS	Phosphate buffered saline
PRDX	Peroxiredoxin
m	Metres
ml	Millilitre
mm	Millimetres
mmol	Millimolar
mRNA	Messenger RNA
MDA	Malondialdahyde
n	Number
ng	Nanograms

NADPH	Nicotinamide adenine dinucleotide phosphate
NF-κB	Nuclear factor kappa beta
NHS	National Health Service
NO	Nitric oxide
NOS	Nitric oxide synthase
NOX	NADPH oxidase
PCR	Polymerase chain reaction
PPARγ	Peroxisome proliferator-activated receptor gamma
rpm	Revolutions per minute
RNA	Ribonucleic acid
ROS	Reactive oxygen species
rtp	Room temperature
RT-PCR	Real-time polymerase chain reaction
SBP	Systolic blood pressure
SCG	Single copy gene
SOD	Superoxide dismutase
T	Thymine
T1DM	Type 1 diabetes mellitus
T2DM	Type 2 diabetes mellitus
TAOS	Total antioxidant status
TBARS	Thiobarbituric acid reactive substances
TLR-4	Toll-like receptor 4
TNFα	Tumour necrosis factor alpha
U	Uracil
UCL	University College London
UK	United Kingdom
UV	Ultraviolet
VAT	Visceral adipose tissue
WAT	White adipose tissue
WHO	World Health Organisation
WHR	Waist:Hip ratio
WIMOS	Welsh Institute of Metabolic and Obesity Surgery

Contents

Chapter 2-Materials and Methods

Chapter 7- Discussion

Appendix

References

CHAPTER ONE

GENERAL INTRODUCTION

Type 2 diabetes (T2DM) and obesity are very common chronic inflammatory conditions. Whilst obesity is associated with T2DM, not all obese subjects develop diabetes. Susceptibility to T2DM is likely to be the result of combined genetic and environmental factors and it is probable that gene-environment interactions play a major influence in the progression from simple obesity to obesity with glucose dysregulation. This is supported by the observation that groups of similar genetic backgrounds exposed to particular environments have an increase in the prevalence of T2DM. This may explain why lifestyle intervention alone may not help a proportion of these high-risk subjects. Impaired glucose regulation is not universal amongst those with obesity. Possible reasons for this include differing proportions of visceral fat, and levels of adipokines and inflammatory markers (implicated in insulin resistance) which may influence β-cell function. This thesis will discuss the pro-inflammatory and pro-oxidant phenotype associated with morbid obesity and examine its contribution to the risk of T2DM.

1.1 Oxidative stress

Oxidative stress is free radical-mediated damage caused by reactive oxygen species (ROS) (Stephens *et al,* 2006). ROS are molecules that have one or more unpaired electrons within the outer shell of their structure thus making them highly reactive (Turrens, 2003). Oxidative stress occurs as a result of an overproduction of ROS, and even though they are produced naturally, their overproduction combined with an insufficient antioxidant defence, can have severe pathological consequences such as the onset of coronary heart disease (CHD), diabetes and cancer (Flekac *et al,* 2008;

Stephens *et al*, 2009). Excessive levels of ROS have the ability to cause oxidative DNA damage (Salpea et al, 2009) and alter both a molecule's function and structure causing damage to tissue and resulting in overall dysfunction (Zalba *et al*, 2006). This overproduction can be further intensified by the addition of exogenous sources of ROS such as those found in cigarette smoke, which is a major risk factor involved in the onset of CHD (Stephens *et al*, 2008).

1.1.1 Pro-oxidants

There are different species of ROS, which arise from different sources and each having their individual effects within a cell. Table 1.2 gives examples of the main pro-oxidants. The effects of free radicals on macromolecules are controlled by a range of different endogenous and exogenous enzymatic and non-enzymatic antioxidant systems (Maritim et al, 2003).

Table 1.1 Examples of oxidising agents

Radical	Name	Comments
$^{\bullet}O_2$-	Superoxide anion	Formed via the reduction of O_2 during oxidative phosphorylation by the electron transport chain. Undergoes dismutation forming H_2O_2 or results in $^{\bullet}OH$ formation via enzymatic catalysis
H_2O_2	Hydrogen peroxide	Formed by the reduction of O_2 or by dismutation of $^{\bullet}O_2$-. Soluble in lipids and able to diffuse across membranes
$^{\bullet}OH$	Hydroxyl radical	Formed during peroxynitrite decomposition and the Fenton reaction. Damages most cellular components due to its highly reactive state
ROOH	Organic hydroperoxide	Formed via radical reactions with cellular components such as lipids and nucleobases
$RO^{\bullet}/ROO^{\bullet}$	Alkoxy/Peroxy radicals	Formed via radical addition to double bonds or hydrogen abstraction in the presence of oxygen. Plays a role in lipid peroxidation
HOCl	Hypochlorous acid	Formed from H_2O_2 by myeloperoxidase. Soluble in lipids and able to oxidise protein components such as amino groups, thiol groups and methionine due to its highly reactive state
$ONOO^-$	Peroxynitrite	Formed via reactions between $^{\bullet}O_2$- and $NO^{\bullet}$. Soluble in lipids and highly reactive. Forms hydroxyl radicals and nitrogen dioxide via homolytic cleavage

1.1.2 Antioxidants

Endogenous anti-oxidative enzymes limit the burden of ROS by scavenging excessive oxidants (Lee and Choi, 2006). However, in diseases such as T2DM these scavenger enzymes are less effective as their defensive role is hampered by excessive oxidative stress (Flekac *et al*, 2008). Polymorphisms or genetic variations, which are single base DNA changes within a population, in antioxidant genes can

predispose to increased levels of oxidative stress, as a result of diminished enzyme activity, ultimately resulting in diabetes (Chistyakov *et al*, 2001). Also, exogenous antioxidants, such as dietary vitamin E have been found to play an anti-oxidant role and can decrease ROS levels; however these may have little effect if there is an excessive level of oxidative stress (Farbstein *et al*, 2013). The maintenance of a healthy level of cellular ROS plays an important role in endothelial health and availability of nitric oxide (NO), which itself is a pro-oxidant but also acts as an important cellular signalling molecule. It has been reported that oxidative stress induced endothelial dysfunction is associated with ageing and cardiovascular disease (CVD) (Sturgeon *et al*, 2010).

Different antioxidant systems are responsible for the maintenance of different oxidant levels. For example, H_2O_2 is formed during normal cell metabolism and is responsible for the generation of hydroxyl radicals resulting in cellular damage such as lipid peroxidation, protein oxidation and DNA damage and mutation (Diaz-Llera *et al*, 2000). The glutathione antioxidant system is responsible for the reduction of cellular H_2O_2 to oxygen and water (Sturgeon *et al*, 2010). In the case of this antioxidant system failing to maintain H_2O_2 levels then lipid peroxidation may be initiated.

1.1.3 Lipid peroxidation

Lipid peroxidation is the process in which lipids are degraded in environments of high oxidative burden. During this cellular process electrons are 'stolen' from lipids

by free radicals, particularly in cell membranes, resulting in cellular damage. Polyunsaturated fatty acids are more susceptable to lipid peroxidation due to their higher carbon double bond content. There are three stages that make up the lipid peroxidation process: initiation, propagation and termination. During the initiation stage, ROS such as hydroxyl ($^{\bullet}OH$) and hydroperoxyl (HO_2) radicals, combine with hydrogen (H_2) to produce water and fatty acid radicals. These radicals are highly unstable and react with oxygen producing a peroxyl fatty acid radical in the propagation stage of lipid peroxidation. The peroxyl fatty acid radical is an unstable molecule that in turn produces further fatty acid radicals and lipid peroxides. These radical reactions continue producing new fatty acid radicals each time. Termination occurs when a radical reacts with another radical producing a non-radical species. For this to occur there must be a high enough concentration of radicals to make the probability of two colliding more likely. As previously described (section 1.1.2) these radicals are 'scavenged' by antioxidant agents in order to terminate lipid peroxidation and therefore preserve the cellular membrane. Products of lipid peroxidation are considered important markers of oxidative damage in diabetes (Lyons, 1991; Armstrong and al-Awadi, 1991; Kakkar *et al*, 1995). Previous studies have found a decrease in antioxidant levels and an increase in lipid peroxidation products, such as F_2-isoprostanes in patients with diabetes (Baynes, 1991; Gopaul *et al*, 1995; Patrono and Fitzgerald, 1997). F_2-isoprostanes are an example of widely used plasma markers of oxidative stress. A clear association between oxidative stress and T2DM has been shown by measuring elevated levels of lipid peroxidation products (Griesmacher *et al*, 1995). Lipid peroxidation can be promoted by a

combination of increased oxidative stress and decreased antioxidant levels or efficiencies (Manfredini et al, 2010). Furthermore, increased ROS production may be a result of inflammation. It has been seen in inflammatory diseases, such as asthma, that an overproduction of ROS by inflammatory cells may result in increased lipid peroxidation (Wood *et al,* 2003).

1.2 Inflammation and the production of reactive oxygen species

Inflammation is a protective response to exposure to substances such as allergens, pollutants, bacteria and viruses, which may cause damage and infection. The inflammatory response, as summarised in Figure 1.1, is characterised by the production of proinflammatory cytokines including interleukin-5 (IL-5) and IL-8 and the activation of inflammatory cells, such as: mast cells, eosinophils, neutrophils and macrophages. This activation results in the production of ROS due to the cell's 'respiratory burst', during which oxygen (O_2) is taken into the cell and ROS are released. During this 'burst' a number of pro-oxidant reactions occur resulting in the accumulation of ROS (Figure 1.1). If levels of ROS become high enough to overwhelm the antioxidant systems this results in lipid peroxidation (Wood *et al,* 2003).

Figure 1.1 Induction of oxidative stress and lipid peroxidation by inflammatory response

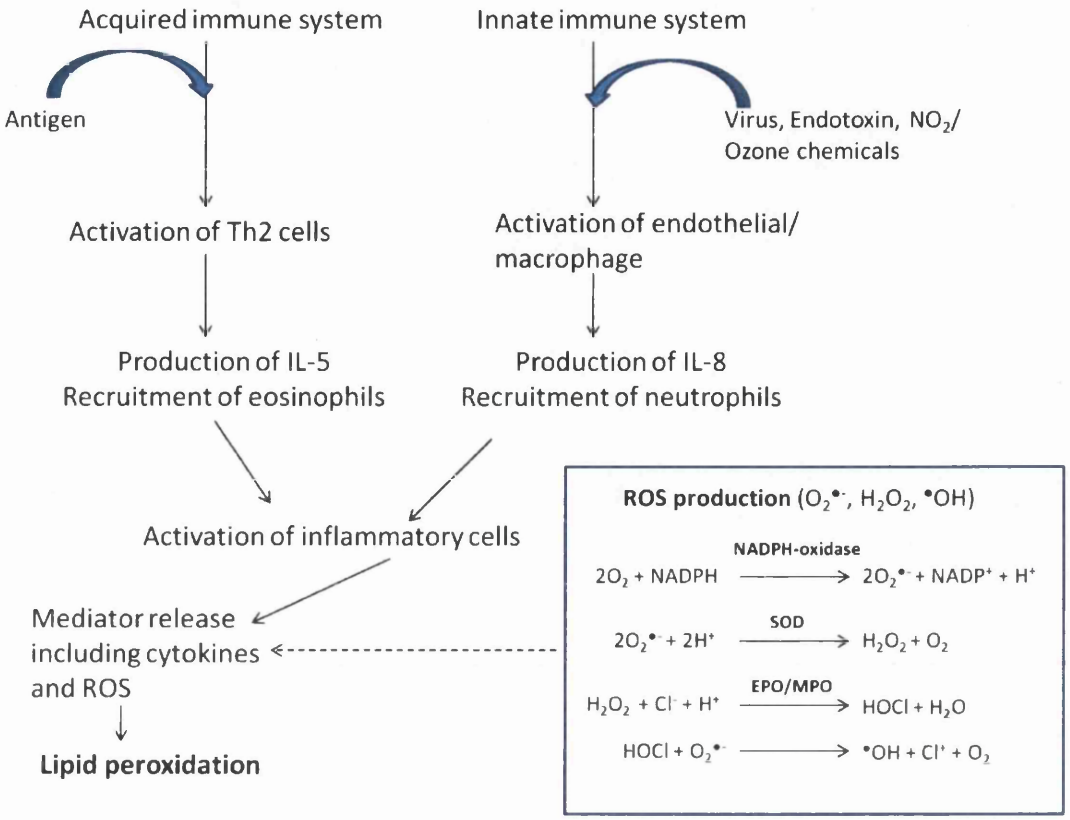

Figure. 1.1 Mechanisms of inflammation that result in lipid peroxidation. EPO: eosinophil peroxidase; H_2: hydrogen; H_2O_2: hydrogen peroxide; $^{\bullet}OH$: hydroxyl radical; IL: interleukin; MPO: myeloperoxidase; NADPH: reduced nicotinamide-adenine dinucleotide phosphate; NADP: nicotinamide-adenine dinucleotide phosphate; O_2^-: superoxide; SOD: superoxide dismutase; Th2: T-helper type-2 cells

Activated inflammatory cells such as macrophages, which are present at high levels in adipose tissue (AT), have been associated with the development of obesity and diabetes (Hotamisligil and Erbay, 2008). Increased inflammation observed in obesity is characterised by inflammatory mediators in AT (Ye, 2009).

1.3 Adipose tissue

AT is an active endocrine and paracrine organ that releases a large number of cytokines and bioactive mediators, which influence body weight and many homeostatic mechanisms including glucose homeostasis and insulin resistance (IR) (Van Gaal *et al,* 2006; Eldor *et al*, 2006). There are two types of adipose tissue; brown adipose tissue (BAT) and white adipose tissue (WAT), both of which store energy in the form of triglycerides but have different morphology, function and regulation and are both found in different anatomical locations.

1.3.1 Brown adipose tissue

BAT appears brown in colour due to vast vascularisation and cytochromes present in the large number of mitochondria (Figure 1.2). It releases energy as heat and is responsible for the regulation of body heat in newborn mammals and during hibernation. It is predominantly involved in non-shivering thermogenesis, which is a thermogenic function required by an organism to counteract heat loss associated with birth and atmospheric life (Lee *et al*, 2013). In most mammals BAT develops during the gestational period and is therefore prominent in newborns and the young, located primarily around arterial vessels and vital organs. The amount of BAT in a mammal is dependent on the amount of non-shiver thermogenesis required and corresponds to the balance between metabolic body mass (i.e. heat produced and heat lost). As most mammals age their heat lost per unit body weight is decreased and BAT becomes undistinguishable to WAT. Although, recent studies

show human adults still have a large proportion of BAT within the thoracic area (Saito *et al*, 2009).

1.3.2 White adipose tissue

WAT is the main source of energy in any mammal and is the most abundant fatty tissue, accounting for approximately 50% of an individual's body weight in severe obesity (Hahn and Novak, 1975). WAT cells are predominantly developed after birth via adipose cell hypertrophy. This study will focus on WAT as the human AT samples are all from adult patients.

Figure 1.2 Comparison of BAT and WAT

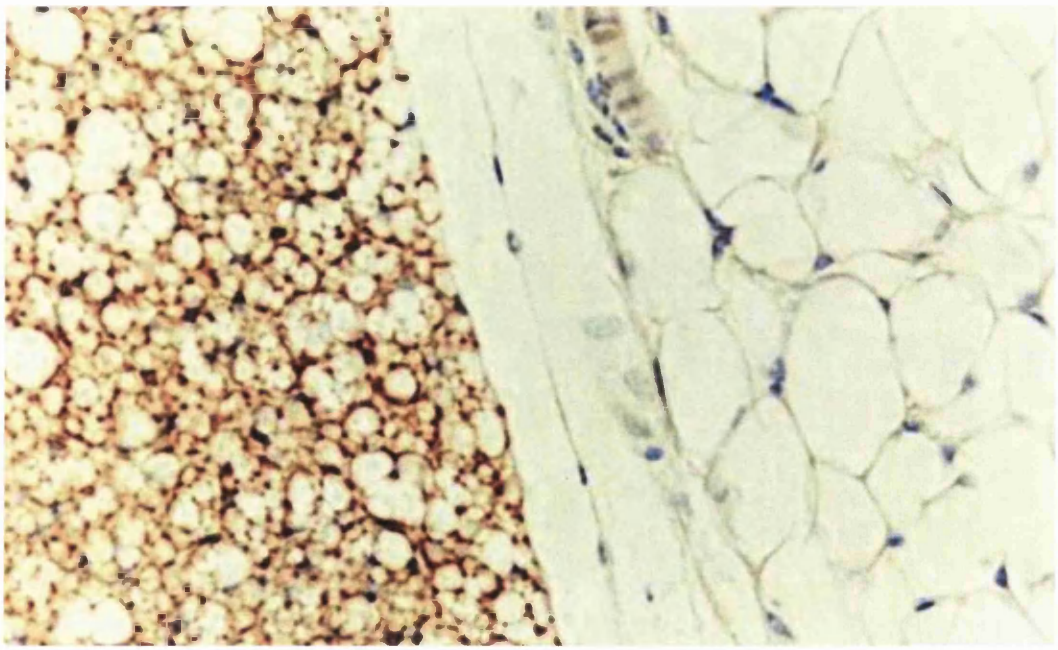

Figure 1.2 Immunohistochemical image of brown adipose tissue (left) and white adipose tissue (right) (adapted from www.circ.ahajournals.org, accessed 16th April 2013)

1.3.3 Structure and function

AT is predominantly made up of mature adipocytes. Adipocytes are a unique cell type as 95% of the total cell body consists of a lipid droplet (Trujillo *et al*, 2006) (Figure 1.2). The primary role of the lipid droplet is the storage of triglycerides, which are released via lipolysis adding to overall triglyceride levels produced by triglyceride synthesis. An adipose cell can vary vastly in size from approximately 25-200μm in diameter, which is determined by an increased storage of lipid resulting in overall cell size increase. The remaining 5% of the adipocyte capacity is responsible for the expression and release of endocrine and paracrine hormones, which are able to communicate with neighbouring adipose cells as well as acting as regulators of cellular processes in peripheral tissues (e.g. liver and nervous system) (Trujillo *et al*, 2006). AT also contains preadipocytes (undifferentiated adipocytes), endothelial cells, pericytes, tissue resident macrophage, monocytes, fibroblasts and is rich in blood vessels (Kowalska, 2007; Trujillo *et al*, 2006). Endothelial cells and pericytes have been observed to be crucial components in AT homeostasis allowing growth and development in AT (Claffey *et al*, 1992), whereas cell types such as monocytes and macrophages are responsible for the clearance of necrotic adipocytes particularly abundant in obesity (Cinti *et al*, 2005). These characteristics make it ideally suited for its function as an endocrine organ and the distribution of these cell types within AT has been found to differ depending on its localisation, such as tissue developed in different adipose depots (Prunet-Marcassus *et al*, 2006).

1.3.4 Adipose depots

AT is located within specific depots within the body. There are considered to be three main depots of AT: (i) subcutaneous AT (layer under the skin), (ii) visceral AT (VAT) (around internal abdominal organs) and (iii) bone marrow. These depots have different biochemical functions, structure, composition and relationship with neighbouring organs (Trujillo *et al*, 2006). Recent studies focusing on differences in AT depots have described modest gene expression differences between depots although not enough to be employed as biomarkers for the specific depots (Gesta *et al*, 2006). Gesta *et al* suggested that adipocytes located in different depots have distinct developmental gene expression differences, which are thought to play a role in the distribution of AT and contribute the development of obesity and other metabolic disorders (Gesta *et al*, 2006). In abdominal visceral depots, often described as abdominal pads or omentum, there is a characteristically higher expression of interleukin-6 (IL-6) in comparison to subcutaneous depots (Huh *et al*, 2012), as a result abdominal VAT is closely associated with IR, T2DM and CVD. Therefore, the focus of this work will concentrate on VAT.

1.3.5 Adipokines

As aforementioned, AT is an endocrine and paracrine organ that communicates with other organs and neighbouring tissues via local and systemic interactions mediated by adipose-specific cytokines, or protein factors called adipokines (Trujillo *et al*, 2006). AT has been found to be a source of pro-inflammatory cytokines such

as IL-6 and tumour necrosis factor alpha (TNF-α) and anti-inflammatory factors such as adiponectin (Kowalska *et al*, 2007) (Table 1.2).

Adipokines have been associated with atherosclerosis, inflammation, insulin resistance and oxidative stress (Eldor *et al*, 2006). An increase in oxidative stress is associated with adipokine dysfunction (Furukawa *et al*, 2013; Iyer *et al*, 2010). Obesity induces the expression of several adipokines and pro-inflammatory markers that contribute to cardiovascular risk in overweight and obese subjects (Van Gaal *et al*, 2006).

Table 1.2 Adipokines and their function

Adipokine	Function	References
Adiponectin	AT secreted hormone. Role in glucose regulation and fatty acid oxidation. Associated with obesity, T2DM and CVD	Hui *et al,* 2011
Leptin	AT secreted hormone. Role in appetite and metabolism. Controls energy intake and expenditure via central nervous system	Mantzoros *et al*, 2011
Resistin	AT secreted factor. Responsible for increased levels of low-density lipoprotein (LDL). Plays a role in IR. Associated with obesity and T2DM and CVD	Jamaluddin *et al*, 2011
Visfatin	Cytokine involved in β-cell maturation and inhibits neutrophil apoptosis, activates insulin receptors and lowers blood glucose and improves insulin sensitivity	Zhang*et al,* 2011
IL-6	Cytokine involved in pro and anti-inflammatory response as a mediator of acute phase inflammatory response during infection or trauma. Associated with diabetes and atherosclerosis	Hirano, 2010
TNF-α	Cytokine involved in acute phase inflammatory response responsible for apoptotic cell death during inflammation	Marusic *et al*, 2012

1.4 Obesity

Obesity is an excess of body fat, or AT, which is associated with an adverse effect on an individual's health. In the past 30 years the prevalence of obesity has almost trebled (Rennie and Jebb, 2005) resulting in an increased incidence of T2DM, CHD and other co-morbidities. Increased body fat (particularly VAT) is believed to play a vital role in these conditions in obese people, but many of the underlying mechanisms remain unclear. A close association exists between obesity, diabetes, inflammation and oxidative stress, which results in increased formation of ROS (Mathieu *et al,* 2009; Inge *et al,* 2010).

In recent decades the prevalence of obesity has increased rapidly in both developed and developing countries. In 1980, the UK statistics showed that 6% of the males and 8% of females were obese. However, by the year 2002 these numbers had increased to 23% and 25% respectively (Rennie and Jebb, 2005). In recent years this has continued to escalate to more than 55% of the UK population being classified as being overweight or obese. This high prevalence trend is also beginning to appear in children. In 2002, approximately 22% boys and 28% girls aged 2-15 were overweight or obese (Rennie and Jebb, 2005).

1.4.1 Body Mass Index

Body Mass Index (BMI) is a surrogate marker often used to define obesity. BMI is calculated using the following equation:-

$$\text{BMI (kg/m}^2\text{)} = \text{weight (kg)} / [\text{height (m)}]^2$$

The World Health Organisation (WHO) categorise individuals as underweight if they have a BMI <18.5, healthy between 18.5-24.9, overweight 25-29.9, obese >30 and morbidly obese >40 (Figure 1.3).

Figure 1.3 Standard graph to calculate BMI

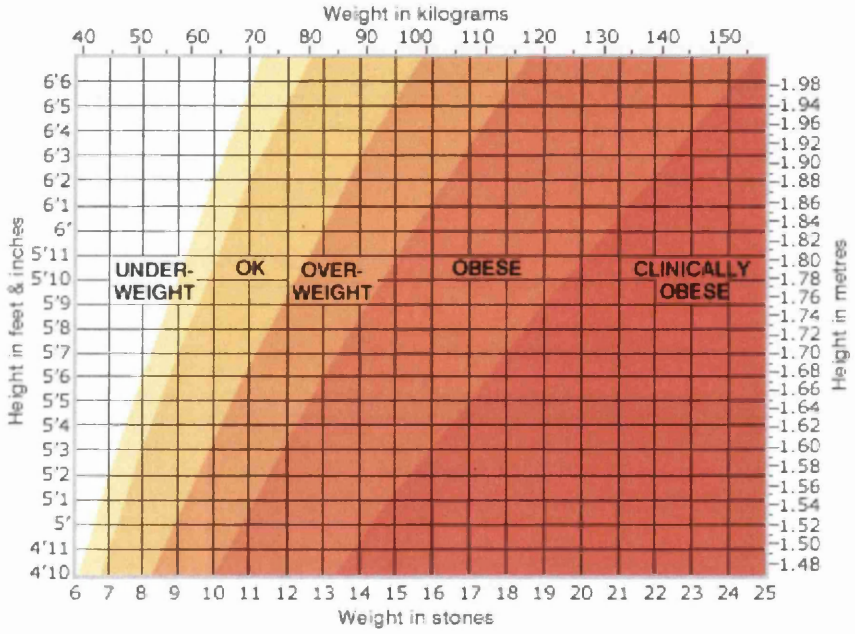

(www.bbc.co.uk, accessed 20th April 2013)

BMI may not be accurate in the case of large muscle mass as it does not consider body build. BMI classification may differ by ethnic group as there are lower cut-off values for each class. A measure to assess central obesity is waist circumference or waist circumference: hip circumference ratio (WHR). Central obesity can be defined as a WHR ratio of >0.95 in males or >0.85 in females or waist circumference of >102cm and >88cm respectively in Caucasian subjects (World Health Organisation,

2008). Waist circumference may be a more accurate measure of VAT than BMI as it provides information about the distribution of fat and allows risk assessment for CHD and associated conditions. An increase in BMI has been associated with increased mortality and is a principal component in the development of metabolic syndrome (Furukawa, 2013). In particular the distribution of adiposity has a significant impact of the risk of metabolic disorders, including diabetes (Kissebah, *et al*, 1982; Hartz *et a;*, 1983).

1.4.2 Fat distribution

The distribution of AT in obese subjects differs by gender (Bouchard *et al*, 1993). An increase in abdominal VAT is seen particularly in males, whereas females are more likely to have an increase in subcutaneous AT. Sex hormones have been shown to play a role in this process, particularly during the menopause when there is an increase in AT distribution within the abdomen (Toth *et al*, 2000). Obesity can be defined according to fat distribution, as the type of obesity may alter a patient's susceptibility to other co-morbidities. For example, patients with central obesity (predominantly abdominal) have an increased cardiovascular risk when compared to those with gluteo-femoral obesity (Ibrahim, 2010). Central obesity is due to an increase in intra-abdominal VAT deposits, which in itself can have numerous adverse effects on health. The distribution of adiposity, and therefore the type of obesity, is likely to be due to a number of factors including age, sex, environmental factors and genetic susceptibility.

1.4.3 Environmental and genetic factors involved in obesity

The aetiology of obesity is complex and is a result of environmental factors such as excess calorie intake, a lack of physical activity and genetic factors. Modern lifestyle plays a massive role in obesity as people live more sedentary lifestyle compared to past generations. Also, a "normal" diet has become higher in calories than previously. The combination of a less active lifestyle and a diet of refined sugars and foods high in fat have contributed to the global increase in obesity. Studies have found that increased energy expenditure through exercise of 500kcal/week can significantly reduce the risk of obesity and related risk of T2DM (Helmrich *et al*, 1991).

Even though there are genetic factors that can cause an individual to become obese such as the monogenic condition that causes leptin deficiency or resistance, genetic causes of obesity are not entirely understood, despite a family history often being present. To date, no significant progress has been made in identifying causative genes. Other monogenic conditions such as Prader-Willi syndrome and Lawrence-Moon-Biedl syndrome also can cause obesity (Farooqi and O'Rahilly, 2005). An increase in body fat has been closely associated with an increase in morbidity and mortality and obesity is associated with other co-morbidities such as hypertension, dyslipidaemia, CVD and T2DM (Poirier *et al*, 2006). Obesity is associated with the appearance of a chronic, low grade inflammatory state due to changes in function of adipocytes and macrophage within AT (Ross, 1999). During adipocyte dysfunction there is an increase in secretion of pro-inflammatory and pro-diabetic

adipocytokines, accompanied by a decreased production of adiponectin. As adipocytes enlarge, increased levels of adipocyte-derived free fatty acids (FFA) are released which can stimulate the local macrophages to produce tumour necrosis factor alpha (TNFα). Saturated FFA bind to the toll-like receptor-4 (TLR-4) which is expressed on macrophages resulting in nuclear factor kappa-light-chain-enhancer of activated B cells (NF-kB) activation. Macrophage-derived TNFα activates human adipocytes thereby enhancing the expression of various genes (e.g. *IL-6*). Macrophages are more prevalent in AT of obese subjects and increased macrophages are associated with increased insulin resistance (Hajer *et al*, 2008). Increased weight has also been associated with an increase in ROS production and systemic markers of oxidative stress (Keany, 2003). This increase in systemic oxidative stress plays a role in the dysregulation of adipokine production in AT (Furukawa, 2013). Differences in adipokine production can contribute to insulin resistance in obesity (Hotamisligil, 1993) and therefore may contribute to the development of T2DM.

1.5 Diabetes Mellitus

Diabetes Mellitus (DM) is a common complex carbohydrate metabolic disorder that is caused by genetic and environmental factors (Andrulionyte *et al*, 2004). Patients with diabetes have abnormally high levels of blood glucose due to insufficient insulin levels or activity. The two most common classes of diabetes are Type 1 Diabetes Mellitus (T1DM) and T2DM.

1.5.1 Blood glucose and insulin

In healthy individuals, insulin produced by β-cells of the pancreas, stimulates glucose uptake from the bloodstream to be utilised for energy production and storage as glycogen in the liver, skeletal muscle and AT to be utilised later as an energy source. In patients with diabetes, the cell is unable to take up blood glucose due to abnormally low or absent insulin levels as seen in T1DM, or due to insulin resistance, seen in T2DM, leading to elevated blood glucose levels and associated complications.

1.5.2 Type 2 diabetes

Approximately 90% of people with diabetes have T2DM (Zimmet *et al*, 2001). It is a multi-factorial disease that usually occurs in older and/or obese people (Zimmet *et al*, 2001). Lifestyle factors such as physical inactivity and obesity have been associated with the development of the disease. T2DM is characterised by hyperglycaemia however, unlike T1DM ketoacidosis (high levels of ketone bodies in the blood) is typically absent. In the early stages of T2DM the disease can be managed by increased exercise and dietary modification, however as the duration of the disease increases, oral medication and/or insulin may be necessary. T2DM is caused by a combination of aetiologies: (i) insulin resistance, where insulin is present at normal or elevated levels but the individual is resistant to its action; (ii) β-cell dysfunction, where the processing of proinsulin to insulin is impaired; and (iii) β-cell destruction.

1.5.3 Insulin resistance

IR occurs when insulin is produced but is unable to be utilised effectively. IR leads to an increased requirement of insulin as muscle, fat and liver cells are unable to respond to insulin present at physiological levels and therefore are unable to take up glucose from the blood stream. As a result of this higher demand for insulin, pancreatic β-cells increase insulin production allowing blood glucose to be maintained at a healthy level. Over prolonged periods of IR, β-cells become unable to maintain the production of insulin to meet the demand leading to the onset of T2DM (Capurso and Capurso, 2012). This occurs due to excess levels of blood glucose building up as insulin levels are reduced. IR has been associated with an increased BMI and a lack of physical activity, with studies showing that weight loss reduces IR, preventing or delaying the onset of T2DM (Poirier *et al*, 2006).

1.5.4 β-cell dysfunction and destruction

β-cell dysfunction results in impaired insulin secretion and is considered to play a secondary role in the pathogenesis of T2DM after obesity and IR, although more recent studies suggest that it is associated with the development of obesity and IR (Shoelson *et al*, 2007). During β-cell destruction islets fail to secrete insulin although they do secrete other markers, for example, the levels of pro-insulin secreted by β-cells is increased along with the secretion of amyloid fibrils, which are normally secreted alongside insulin and have a toxic effect on islet cells. This leads to apoptotic cell death of the β-cells and the replacement of the islet by amyloid and ultimately diabetes. β-cell dysfunction, destruction and IR are a result of

hyperglycaemic conditions, which in turn results in further hyperglycaemia leading to the pathogenesis of T2DM (Figure 1.4).

Figure 1.4 Hyperglycemic induction of IR, β-cell dysfunction and T2DM

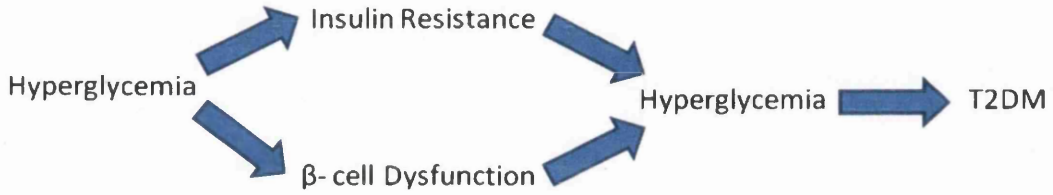

Multi-factorial metabolic changes predominantly related to hyperglycaemia lead to damage and functional impairment of both large (macrovascular) and small (microvascular) blood vessels within the body resulting in concomitant conditions.

1.5.5 Co-morbidities

As previously mentioned T2DM is a heterogenous disease characterised by abnormal glucose tolerance, insulin dysregulation, dislipidaemia and inflammation which combined lead to further complications.

Macrovascular complications occur due to damage of blood vessels. CHD, peripheral vascular disease and stroke occur when there is hypoperfusion to the heart, periphery and brain respectively, due to atherosclerosis. Diabetes is considered a major risk factor for CHD (Flekac *et al*, 2008), which can ultimately lead to angina (chest pains), cardiac failure (shortness of breath), and in worse cases

myocardial infarction (heart attack). CHD is a multi-factorial disease that is the main cause of premature mortality and is associated with a 2-4 times greater morbidity in patients with T2DM compared to those without diabetes (Kawalska *et al*, 2007). This is due to mechanisms involved in the pathogenesis of the disease being induced by hyperglycaemia and resulting oxidative stress. High levels of oxidative stress have been observed in patients with CHD (Stephens *et al*, 2007), and ROS have been found to activate a number of biomolecular pathways that are associated with the pathogenesis of vascular disorders (Flekac *et al*, 2008).

Microvascular complications include retinopathy, nephropathy and neuropathy (Armstrong and al-Awadi, 1991), which affect the small vessels of the eye, kidney and nervous system respectively. Increased oxidative stress induced by hyperglycaemia plays a critical role in the pathogenesis of these diabetes complications (Mehta *et al*, 2006; Dronavalli *et al*, 2008). Diabetic retinopathy results in damage to the retina of the eye causing loss of sight and it is the most common cause of blindness within patients with diabetes. The development of retinopathy is highly dependent on duration and severity of hyperglycaemia in T2DM and has also been associated with the presence of hypertension and oxidative stress (van Reyk *et al*, 2003). Diabetic nephropathy is diabetes associated kidney disease effecting approximately 40% of patients with T2DM (Gross *et al*, 2005). It is the single most common condition in patients with end stage renal failure, particularly in westernised countries (Ritz, 2006) and is characterised initially by microalbuminuria and proteinuria. The main risk factors for nephropathy, similar

to other microvascular conditions are prolonged hyperglycaemia, untreated hypertension and genetic susceptibility (Gross *et al*, 2005). Diabetic neuropathy is the dysfunction of peripheral nerves. As seen in other microvascular complications, longevity of hyperglycaemia increases the risk of developing neuropathy as well as genetic susceptibility but to a lesser extent (van Dam, 2002). Oxidative stress has been surmised to play a role in peripheral nerve damage, which occurs in hyperglycaemia due to increased ROS, decreased nitric oxide and glutathione, and damage from advanced glycation end products (AGEs) (Boulton *et al*, 2005).

1.5.6 Oxidative stress in diabetes

Diabetes is associated with high levels of ROS due to hyperglycaemia (Kiritoshi *et al*, 2003; Blasiak et al, 2004; Salpea et al, 2009) and is evident in subjects with poor glycaemic control (Shin *et al*, 2001). The oxidants produced by hyperglycaemia are pathogenic as they alter the structure of proteins and lipids causing deleterious vascular effects (Flekac *et al,* 2008). Pancreatic β-cells have been found to be particularly susceptible to ROS damage, suggesting that excessive ROS produced due to ongoing hyperglycaemia and/or obesity can cause β-cells to lose function and impaired insulin signalling resulting in the onset of T2DM (Stephens *et al*, 2009). Endogenous anti-oxidative enzymes attempt to control ROS levels by removing excessive oxidants (Lee *et al*, 2006). However, in DM these scavenger enzymes are less effective as their defensive role is hampered by excessive oxidative stress (Flekac *et al,* 2008). In addition, exogenous antioxidants, such as vitamins, can decrease ROS levels; however these may have little effect if there is excessive

oxidative stress. Alterations in the genetic code of these anti-oxidant enzymes may reduce the overall expression, activity and efficiency of the enzymes to maintain levels of excess ROS.

1.6 Nucleic acids

Deoxyribonucleic acid (DNA) and ribonucleic acid (RNA) encode genetic information required for the development and functioning of all living organisms. Damage to these nucleic acid sequences, such as that induced by oxidative stress, may result in the increased or decreased expression of genes and overall dysfunction of cellular mechanisms. To understand the damage caused in an environment of oxidative stress understanding the structure and function of DNA and RNA is important.

DNA is a double stranded polymer made up of anti-parallel chains of nucleotide monomers in a double helix structure. Each nucleotide is made up of a sugar, base and phosphate group. There are four different types of base that make up DNA; adenine (A), guanine (G), cytosine (C) and thymine (T). These bases form the inside of the DNA double helix structure via hydrogen bonding of paired purine (A and G) and pyrimidine (C and T) bases, therefore an A base will only pair with T and G will only pair with C. The sequence of the bases within the nucleic acids determines the resulting proteins they code for. In the coding regions of these sequences, every three bases makes up a codon that is transcribed via RNA into amino acids, which are the building blocks for protein synthesis. Any alterations in the DNA sequence

may lead to a change in the resulting amino acid sequence effecting the overall function of the final protein.

RNA is single stranded structure, similar to DNA, with the main difference being an uracil (U) in RNA in place of the thymine (T) in DNA. Alterations in the sequence of DNA may not only occur due to oxidative damage but also in the process of DNA replication, resulting in an altered RNA sequence.

1.6.1 DNA replication

DNA replication allows biological inheritance of genetic material. Prior to dividing it is necessary for a cell to make copies of its DNA, which is carried out in a 5'-3' direction by a highly accurate DNA polymerase to ensure all daughter cells receive complete genetic information. This process is semi-conservative, meaning that each resulting cell will contain one copy of the parent strand of DNA and one copy of a new replicated strand.

DNA polymerase must have a template strand of DNA or RNA to replicate, along with a primer of complementary bases to the template. DNA polymerases are also able to proof-read the new DNA strand to ensure the correct bases have been inserted, in order to reduce the chance of error that may result in lost information within the daughter cells. Reverse exonuclease activity identifies incorrect bases, which are removed and replaced with the correct base. Errors formed during DNA replication that are not corrected lead to DNA damage within the daughter cells. A

naturally occurring form of DNA damage associated with DNA replication is the shortening of telomere sequences to prevent the loss of coding sequences.

1.7 Telomeres

Telomeres are DNA repeat sequences found at the end of chromosomes that have a protective role against chromosomal deterioration and chromosomal fusion. These single stranded telomeric regions shorten during replication, which is a natural process to prevent the shortening of the genes located at the chromosome ends. If chromosome ends contained genes, their coding sequences would erode with each cell division causing mutations. Cells have developed a protective strategy by placing noncoding DNA repeat sequences, telomeric repeats, at the ends of chromosomes. The human non-coding repeat sequence is TTAGGG. During each cell division, the telomeric repeat sequence shortens and can therefore be representative of the cell's biological age (Astrup *et al*, 2010).

Within adult human somatic cells there is no active telomerase enzyme present to protect against the loss of repeat sequences, so approximately 100 base pairs of shortening occurs with every cell division. Due to the fact that in adult cells there is no replenishment of telomeric sequence the telomere acts as a time delay until the eventual loss of genetic code, resulting in the cessation of cell division. This replicative senescence appears to be a mechanism to ensure genomic stability by enforcing a limit to the number of divisions a cell can undertake before it becomes unstable and increases the likelihood of anomalies within the sequence (Houben *et*

al, 2008). Telomere shortening has been associated with poor health and disease in conditions such as diabetes (Salpea *et al*, 2009). An estimated loss of approximately 20bp is expected during replication but in reality 50-100bp have been found to be lost, which has been explained by shortening due to presence of free radicals.

1.8 DNA damage

DNA damage is a physical abnormality seen in DNA, including single-stranded and double-stranded breaks. If DNA damage is left uncorrected it can result in either the initiation of apoptosis or the prevention of further transcription. Oxidative stress causes DNA damage and although low level ROS are present at all times due to natural metabolic processes, in times of excess oxidative stress the cell is unable to repair background levels of damage. This may ultimately resulti in apoptosis or in very severe cases bypassing controlled cell death to the destruction of the cell. Endogenously produced ROS and replication errors result in different types of DNA damage, which are summarised in Table 1.3. Exogenous sources of damage include radiation (UV, x-rays, etc), hydrolysis, mutagenic chemicals and viruses (Helton & Chen, 2007). If damaged DNA is replicated, the sequence containing the error will be inherited by the daughter cell. Once errors are inherited the DNA modification cannot be corrected, except in rare cases of 'back mutation' (gene conversion). The majority of damage caused to DNA is localised to the primary structure in the form of base modification. Modifications can affect the structure of DNA in the form of adducts or incorrect bonds.

As previously mentioned, oxidative stress has numerous associations with a variety of disease including diabetes, CVD and inflammatory diseases as well as aging (Rossner & Sram, 2012).

Table 1.3 Examples of endogenous types of DNA damage

Source	Modification
Oxidation of bases	8-oxo-7,8-dihydroguanine (8-oxoG)
Alkylation of bases	Methylation
Hydrolysis of bases	deamination, depurination and depyrimidination
Adduct formation	benzo[a]pyrene diolepoxide-dG adduct, aristolactam I-dA adduct
Mismatch of bases	Caused by errors in DNA replication, when a base is skipped or incorrectly inserted into the new DNA strand

An environment of high oxidative stress, such as that brought on by hyperglycaemia, is a major source of DNA damage such as the oxidation of bases and sugar phosphate binding sites (Blasiak *et al*, 2004). Alterations such as these are associated with cancer development in patients with diabetes due to their mutagenic effects and resulting DNA replication arrest (Palazzo *et al*, 2012). Lymphocytes are ideal markers of DNA damage and mutation as they circulate for many years through various organs accumulating DNA damage (Palazzo *et al*, 2012).

1.9 Mutation types

A mutation is an inherited alteration within the genome or a result of un-repaired DNA damage. A mutation differs from DNA damage as a mutation is a change in the base sequence of the DNA and it is unable to be recognised by potential repair enzymes once a mutation becomes part of the sequence, and therefore cannot be repaired. Although there is a clear underlying difference between DNA damage and mutation, DNA damage often is the cause of DNA synthesis errors during replication or repair, which may ultimately cause mutation. There are a number of mutation types ranging from single base pair alterations to massive chromosomal abnormalities, all of which have the ability to alter the function of the gene product. If a mutation arises only in a somatic cell the mutant characteristics will affect only the individual in which the mutation occurs and will not be inherited by the next generation, known as a somatic mutation. A germ-line mutation is where the mutation is within a germ line cell and can be passed on to the next generation producing an individual with the mutation in both its somatic and germ-line cells. Diaz-Llera and colleagues (2000) noted that DNA mutation induced by ROS are commonly on a smaller scale such as point mutations, particularly base pair substitutions, insertions and deletions (Table 1.4).

Table 1.4 Summary of point mutations caused by ROS

Mutation	Description	Example
Base pair substitution	One base pair replaced by another. Transition mutation – purine/pyrimidine replaces same type. Transversion mutation - a purine replaces a pyrimidine or vice versa	A:T → G:C or A:T → T:A
Missense mutation	A base pair substitution causing a change in mRNA codon, resulting in amino acid change in final protein. May or may not result phenotypic alteration	Insertion of different amino acid
Nonsense mutation	A base pair substitution causing a change in mRNA codon from one amino acid to a stop codon, resulting in premature chain termination and incomplete protein	Amino acid → ATG (stop codon)
Base pair insertion/ deletion	Base pair inserted into or deleted from sequence resulting in a base pair shift. May result in an alteration to amino acid codon sequence	

If DNA damage occurs cells utilise multiple DNA repair pathways to correct damaged DNA including nucleotide excision repair, mismatch repair, base excision repair, homologous recombination, and non-homologous end joining pathways (Helton and Chen, 2007). Impairment of these pathways results in unreliable repair of DNA damage that may lead to increased mutagenesis (Zhang et al, 2007).

1.10 Aims

Although 80% of patients with T2DM are obese, less than 10% of obese people have diabetes (Beck-Nielsen and Hother-Niesen, 1996). The aim of this thesis was to explore the role that AT plays in T2DM and obesity using hVAT obtained from subjects undergoing abdominal surgery that were categorised as lean (L), obese (O)

and obese with T2DM (ODM). This cross-sectional study attempted to examine markers of oxidative stress and identify particular genes that may play a role in T2DM in obese subjects. The study was undertaken with the following objectives:-

1. Examine adipose markers of oxidative stress in subjects to determine the extent of oxidative burden within this sample set that may be attributed to obesity and/or diabetes.
2. Investigate differences in basal gene expression of genes involved in oxidative stress and inflammation between the three sample groups, using a commercial PCR array, to determine the effects of oxidative burden on genes within this population.
3. Investigate differences in gene expression between the three sample groups, focusing on genes whose expression were found to be altered in aim **2** in more detail, using RT-PCR analysis.
4. To culture mouse adipose cells (3T3-L1) to examine candidate gene expression in response to a 'biochemical stress'.
5. An additional aim was included to sequence the gene of interest found as a result of aims **2** and **3** for polymorphisms/mutations that may account for the change in gene expression observed.

CHAPTER TWO

MATERIALS AND METHODS

2.1 Human samples

2.1.1 Recruitment of subjects

The Welsh Institute of Metabolic and Obesity Surgery (WIMOS) provides bariatric services for all of Wales and is based at Morriston Hospital, Swansea. It was established in June 2011 and is a multi-disciplinary service offering weight loss surgery to approximately 70 patients a year. Prior to this, obesity surgery was carried out in an ad-hoc manner, with around 11 patients a year being funded for bariatric surgery on the National Health Service (NHS). The service comprises of two bariatric surgeons, physician, psychologist, dietician, physician and a specialist nurse. WIMOS is closely linked with Swansea University's College of Medicine where there is on-going research related to diabetes treatment, insulin resistance, exercise physiology and health care economics.

Participants were recruited from the bariatric-obesity clinic (Professor John Baxter/ Mr Jonathan Barry/ Mr Scott Caplin/ Professor Jeffrey Stephens) and general surgical clinics at Morriston Hospital, Swansea. Surgical procedures were carried out every Wednesday and private cases on occasional Sundays at the Princess of Wales Hospital, Bridgend. Liaison with the WIMOS Specialist Clinical Nurse Nia Eyre was maintained in regards to surgical lists and patient information to ensure patients met inclusion criteria for the study. Participants were included in the study if they were aged between 18 and 80 years of age, were undergoing an abdominal surgical procedure and were medically fit enough for surgery. Participants were excluded if

they were unable to give informed consent or had a confirmed underlying malignancy.

2.1.2 Collection of visceral adipose samples

Human visceral adipose tissue (hVAT) samples were collected from subjects that were categorised as being lean (L), where BMI<30; obese (O), where BMI≥30 and obese with T2DM (ODM). Ethical approval (REC ref no.:08/WMW0/68) was obtained for sample collection and informed consent was obtained prior to surgery. Sample collections were carried out by myself every Wednesday at Morriston Hospital, Swansea and the occasional Sunday for private surgery at the Princess of Wales Hospital, Bridgend, over a 32 month period between October 2009 and May 2012. Collections began at 8.30am on the day of the surgery, when informed consent was obtained from subjects prior to any procedures. The order of subjects was defined by the surgical list, which was decided before the day of surgery.

During the procedures, theatre staff would allocate an area within the theatre for the collection apparatus to be set up. Samples were collected towards the end of the planned abdominal surgery and consisted of a 3x3cm cut of hVAT removed via laproscopic surgical scissors from the greater omentum. No additional incision was required and there was no risk associated with the collection. As the samples were removed they were cut into small pieces and placed in a 2ml centrifuge tube with 1.5ml RNAlater® (Ambion Inc, UK) to preserve tissue. Tubes were then stored in a sample box until transportation to the Institute of Life Science, Swansea University

where they were kept overnight at 4°C before storage at -20°C until required. At time of collection samples were anonymised with a sample number and no further contact was made with the participant. Problems during recruitment are described in detail in Chapter 7. Consent was given to collect additional clinical information. BMI was calculated by dividing the weight (in kilograms) of the patient by their height (in meters) squared and categorised as L, O and ODM. Blood pressure was measured during the patient's pre-operative check-up and individuals with a systolic BP ≥140 and/or a diastolic BP ≥90 mmHg or on antihypertensive medications were considered hypertensive.

2.2 Nucleic acid extractions

2.2.1 RNA

Total RNA was extracted from hVAT using RNeasy Lipid Tissue Mini Kit (Qiagen, UK) and was carried out following the manufacturer's protocol detailed below. All extractions were carried out within the Diabetes Research Laboratory in the Institute of Life Science, Swansea University under sterile conditions. Prior to every extraction all pipettes were cleaned with 70% ethanol, all micro-centrifuge tubes were sterilised by autoclaving and sterile RNase free filter tips were used to prevent RNA contamination. As RNA is known to be less stable than DNA at room temperature all work was carried out promptly and all samples were kept on ice when necessary. All buffers and spin columns were provided in the kit unless otherwise stated.

Sample disruption and homogenisation

Human VAT samples weighing 100mg were added to 1ml QIAzol lysis buffer in a 2ml ceramic matrix tube (MP Biomedicals, USA) on ice then homogenised for 20 seconds in a FastPrep® Homogeniser (MP Biomedicals, USA). The samples were left on ice for 1 minute then homogenised for a further 20 seconds. Lysate was then transferred to a clean 1.5ml tube and left to incubate at room temperature (rtp) for 5 minutes.

Separation of aqueous and organic phases

Chloroform (200µl) was added to the lysate, shaken for 15 seconds, left to incubate at rtp for 3 minutes then centrifuged for 15 minutes at 12,000rpm (13,400xg) at 4°C. The upper aqueous phase was transferred to a clean 1.5ml tube, 500µl 70% ethanol added and mixed by vortex.

Total RNA purification

The sample was transferred to an RNeasy mini spin column and centrifuged for 15 seconds at 13,000rpm (15,700xg), and the flow-through discarded. 700µl Buffer RW1 was added to the spin column and centrifuged for 15 seconds at 13,000rpm (15,700xg) and the flow-through discarded. 500µl Buffer RPE was added to the spin column and centrifuged for 15 seconds at 13,000rpm (15,700xg) and the flow-through discarded. A further 500µl of Buffer RPE was added and centrifuged for 2 minutes at 13,000rpm (15,700xg). The spin column was transferred to a clean 1.5ml tube and 30µl RNase free water added and centrifuged for 1 minute at 13,000rpm

(15,700xg). This elution step was then repeated and the final volume of total RNA divided into 20µl aliquots and stored at -80°C.

RNA quantification

Total RNA concentration was quantified using a NanoDrop 8000 UV-Vis Spectrophotometer (Thermo Scientific, UK). Total RNA concentration was measured at an absorbance of 260nm. The purity of the RNA had to be such that absorbance levels between 260nm-230nm were between 1.8-2.2ng/µl to be free of protein contamination and 260nm-280nm between 1.8-2.0ng/µl to be free of DNA contamination as per manufacturer's instruction. All readings were blanked with RNase free water.

2.2.2 DNA

Total DNA was extracted from hVAT using QIAamp DNA Mini Kit (Qiagen, UK) and was carried out following the manufacturer's protocol detailed below. All extractions were carried out under sterile conditions. Prior to every extraction all pipettes were cleaned with 70% ethanol, all micro-centrifuge tubes were sterilised by autoclaving and sterile RNase free filter tips were used to prevent RNA contamination. All buffers and spin columns were provided in the mini kit unless otherwise stated.

Sample disruption and homogenisation

In a 2ml centrifuge tube, hVAT samples weighing 25mg were broken up using a sterile scalpel and added to 180µl Buffer ATL and 20µl proteinase K and mixed by vortex. The samples were incubated at 56°C as per manufacturer's protocol until the tissue was completely lysed.

Total DNA purification

Tubes were briefly centrifuged before adding 4µl RNase A (100mg/ml), mixed by pulse vortexing for 15 seconds and incubated at rtp for 2 minutes. 200µl Buffer AL was added to the tubes and mixed by pulse vortexing for 15 seconds before incubation at 70°C for 10 minutes. Lysate was then transferred into a clean 1.5ml tube and left to incubate at rtp for 5 minutes. Tubes were briefly centrifuged before adding 200µl 100% ethanol and mixed by vortexing before being transferred to the QIAamp mini spin column, centrifuged at 8,000rpm (5,900xg) for 1 minute and the flow-through discarded. 500µl Buffer AW1 was added to the spin column and centrifuged at 8,000rpm (5,900xg) for 1 minute. The QIAamp spin column was then transferred to a clean collections tube, discarding the flow-through and 500µl Buffer AW2 added before centrifugation at 13,200rpm (16,100xg) for 3 minutes. This step was then repeated using a clean collection tube and then transferred to a clean 1.5ml centrifuge tube for elution.

Elution of total DNA

Buffer AE (200µl) was added to the column and incubated at room temperature for 5 minutes before centrifugation at 8,000rpm (5,900xg) for 1 minute. This was repeated with a further 200µl Buffer AE and resulting total DNA was aliquoted and stored at -20°C until needed.

DNA quantification

Total DNA concentration was quantified using a NanoDrop 8000 UV-Vis Spectrophotometer (Thermo Scientific, UK). Total DNA concentration was measured at an absorbance of 260nm. All readings were blanked with RNase free water.

2.3 Measures of oxidative damage

2.3.1 Relative change in $ABTS^+$ fluorescence

Plasma Total Antioxidant Status (TAOS), previously described by Sampson *et al* (2002) and Stephens *et al* (2009) is a method to measure the antioxidant capacity in a plasma sample. TAOS is a photometric microassay that determines a sample's capacity to inhibit the peroxidase-mediated formation of the 2, 2-azino-bis-3-ethylbensthiazoline-6-sulphonic acid ($ABTS^+$) radical. The inhibition of $ABTS^+$ formation is proportional to the sample's antioxidant capacity, therefore, if a sample has high levels of oxidative stress, the resultant TAOS will be low. The assay is split into two arms, a control and a test arm. In the control arm saline is incubated with hydrogen peroxide and ABTS. The hydrogen peroxide acts as a free radical donor causing the formation of the $ABTS^+$ radical, producing a colourmetric change

which can be measured at 405nm. As saline contains no antioxidant molecules the reaction goes to completion. In the test arm, the hydrogen peroxide and ABTS are instead incubated with the test plasma sample (which will contain antioxidant molecules) therefore preventing the reaction going to completion by varying degrees depending on the antioxidant content. It is then possible to calculate the percentage of inhibition of the reaction for the test sample relative to saline:

TAOS % = (Control absorbance - Test absorbance)/ Control absorbance X 100)

This method (followed as per Stephens *et al,* 2009) has not been used to measure TAOS in tissue homogenates. I conducted this protocol in 61 hVAT homogenates and the assay was not conclusive on four separate occasions. Therefore, in order to test oxidative capacity in hVAT homogenates this method was modified to measure the change in $ABTS^{+}$ formation ($\Delta ABTS^{+}$) within a sample relative to a saline control. The assay was carried out using the protocol method to determine $\Delta ABTS^{+}$ as described below:

$\Delta ABTS^{+}$= Sample absorbance/Control absorbance

The intra-assay coefficient of variation (CV) was 0.9 – 1.6%, while the inter-assay CV were 6.2 – 9.4% (raw data in appendix 1).

Sample disruption and homogenisation

hVAT samples weighing 25mg were added to 250µl RIPA buffer and 1.3µl protease inhibitor cocktail (Sigma, UK) in a 2ml centrifuge tube. Samples were sonicated using a Sonics Vibra Cell VCX 130 ultrasonic processor (Sonics, USA) for 15 seconds, then centrifuged for 10 minutes at 4,200rpm (1,600xg) at 4°C. The supernatant was then transferred into a clean 2ml tube and stored at -80°C. Tissue homogenates were stable for 1 month.

Measurement of change in $ABTS^+$

2.5µl phosphate buffered saline (PBS) for the control and 2.5µl hVAT homogenate samples were placed in a 96-well ELISA plate in triplicate. To each well was added 20µl ABTS (20mmol/L), 20µl horse radish peroxidase (HRP) (30mU/ml) and 40µl PBS (pH7.4) (all Sigma, UK). To initiate the reaction 20µl H_2O_2 (0.1mmol/L) was added to each well and the plate was incubate at 37°C for 12 minutes.

Analysis of data

After incubation, absorbance was read for each well using a Polarstar Omega plate reader (BMG Labtech, Germany) at a wavelength of 405nm. The increase in absorbance due to the accumulation of $ABTS^+$ in each sample was read along with the absorbance of the PBS control. The relative change in $ABTS^+$ was calculated as previously described.

2.3.2 Thiobarbituric acid reactive substances assay

Lipid peroxidation as a measure of oxidative stress was investigated in hVAT homogenates using a thiobarbituric acid reactive substances (TBARS) assay (Cayman Chemical c/o Cambridge Bioscience, UK) (Armstrong *et al,* 1994; Yagi, 1998) and was carried out following the manufacturer's fluorometric protocol detailed below. All assays were carried out under sterile conditions. Prior to every assay all pipettes were cleaned with 70% ethanol, all micro-centrifuge tubes and tips were sterilised by autoclaving. hVAT samples were homogenised as described in section 2.3.1. The intra-assay CVs ranged from 5.2-7.1%, while the inter-assay CVs range from 16.2-19.6% (raw data in appendix 2).

Preparation of standards

25µl malondialdahyde (MDA) standard was diluted with 975µl double distilled water to obtain a stock standard solution of 12.5µM. Sterile 2ml centrifuge tubes were labelled A-H and the volume of MDA stock solution and water were added to each tube according to Table 2.1.

Table 2.1: MDA fluorometric standards

Tube	MDA (µl)	Water (µl)	MDA concentration (µM)
A	0	1000	0
B	5	995	0.0625
C	10	990	0.125
D	20	980	0.25
E	40	960	0.5
F	80	920	1.0
G	200	800	2.5
H	400	600	5.0

TBARS assay

100µl of standard or sample were added to a labelled 15ml centrifuge tube containing 100µl SDS solution and mixed by inversion. 4ml colour reagent was added to each tube and boiled for 1 hour. The tubes were cooled on ice for 10 minutes and centrifuged for 10 minutes at 4,200rpm (1,600xg) at 4°C. As the reagent becomes unstable after 30 minutes immediate use is necessary. 150µl from each tube was plated in duplicate into a black 96 well plate and read fluorometrically using a Polarstar Omega plate reader (BMG Labtech, Germany) at an excitation wavelength of 530nm and an emission wavelength of 550nm.

2.3.3 Measure of telomere length

As described in detail in section 1.7, telomeres are DNA repeat sequences found at the end of chromosomes that shorten during replication and are representative of the cell's biological age. Telomere length was measured according to the method described by Cawthon *et al* (2002), which comprises of a 2-step PCR protocol. A period of 5 days was spent at the Centre for Cardiovascular Genetics, University College London with Professor Steve Humphries's research group learning this method on human DNA. The technique compares the number of telomere DNA repeat sequences against a single copy gene (SCG) (acidic ribosomal phosphoprotein PO [36B4]) for each sample, producing a ratio value (T/S ratio) that can be compared between sample groups as a relative measure of telomere length. This technique has been previously used within DNA obtained from whole blood (Salpea *et al*, 2008), but has previously not been used with hVAT. The intra-assay CVs ranged from 0.3-3.2%, while the inter-assay CVs range from 2.1-3.7% (raw data in appendix 3).

Primer design and optimisation

Primers were previously designed and optimised for the human telomere sequence and for the SCG (acidic ribosomal phosphoprotein PO [36B4]) by members of the Centre for Cardiovascular Genetics, University College London. Primers were purchased from Eurofins MWG Operon (Germany) using the primer sequences shown in Table 2.2 and diluted using RNase free water as shown in Table 2.3.

Performing telomere length assay

DNA extracted from hVAT (see section 2.2.2) was diluted with RNase free water to a 5ng/µl concentration as described by Salpea *et al* (2008). Each sample and control was run in triplicate. For each sample 6µl diluted DNA (or water for control) was added to 12.5µl 2xSensimix SYBR No-ROX master mix (Bioline, UK), 1µl telomere forward primer, 1µl telomere reverse primer and 4.5µl PCR H_2O. Using a Rotor-Gene 6000 Real-Time PCR Detection System (Corbett c/o Qiagen, UK) samples were run on the telomere program for an incubation of 10 minutes at 95°C followed by 22 cycles of 15 seconds at 95°C and 120 seconds at 58°C. The method was repeated from the start using the SCG forward and reverse primers instead and run on the SCG program with an incubation of 10 minutes at 95°C followed by 30 cycles of 15 seconds at 95°C and 60 seconds 58°C.

Telomere length data analysis

Raw data was analysed using the comparative quantification software (Rotor-Gene 6000, Corbett Research Ltd, UK), which calculated the reaction 'take-off' point for each sample. The take-off point is 80% of the peak exponential amplification level. Using the take-off point and overall amplification for each reaction, the software calculated a relative number of repeats for telomere and SCG copies, termed the 'rep conc'. These values allowed the T/S ratio to be calculated for each sample which is then used as a relative telomere length and can be compared between samples:

T/S ratio= Telomere rep conc/SCG rep conc

Table 2.2: Telomere and SCG primer sequences

Name	Sequence (5'-3')	Length (bases)
Telo F'	GGTTTTTGAGGGTGAGGGTGAGGGTGAGGGTGAGGGT	37
Telo R'	TCCCGACTATCCCTATCCCTATCCCTATCCCTATCCCTA	39
SCG F'	CAGCAAGTGGGAAGGTGTAATCC	23
SCG R'	CCCATTCTATCATCAACGGGTACAA	25

Table 2.3: Telomere and SCG primer dilutions

Name	Primer volume (µl)	H_2O volume (µl)	Working Concentration (nM)
Telo F'	6.75	193.25	135
Telo R'	45.00	155.00	900
SCG F'	15.00	185.00	300
SCG R'	25.00	175.00	500

2.3.4 Comet assay

Comet is a single cell gel electrophoresis assay used for measuring DNA damage in individual cells. Damaged DNA containing fragments and strand breaks are separated using electrophoresis resulting in a characteristic "comet tail" shape and then visualised microscopically with Vista Green DNA dye.

An attempt was made at measuring DNA damage within hVAT homogenates using a methodology previously described by Cerda *et al* (1997). This method required strict laboratory conditions which were not feasible, and time restraints on optimising the method meant that an alternative commercial assay was required to gather reliable results. DNA damage was measured in hVAT homogenates using the commercially available Oxiselect™ 96-well Comet assay kit (Cell Biolabs Inc, UK) and carried out following the manufacturer's protocol detailed below. All assays were carried out under sterile conditions. Prior to every assay all pipettes were cleaned with 70% ethanol, all micro-centrifuge tubes and tips were sterilised by autoclaving. All samples were run in duplicate. The intra-assay CVs ranged from 5.5-7.6% while the inter-assay CVs range between 5.1-5.9%.

Sample preparation

hVAT samples were broken up using a sterile scalpel and added to 2ml ice cold cell dissociation buffer (PBS, 20mM EDTA without Mg_2^+ and Ca_2^+) (Invitrogen, UK) in a 2ml centrifuge tube. Samples were left to stand for 5 minutes on ice before the supernatant was then transferred to a clean 2ml tube avoiding any transfer of debris, centrifuged for 15 minutes at 13,000 rpm (15,700xg) and the resulting supernatant discarded. The remaining pellet of cells was re-suspended in 1ml ice cold PBS (without Mg^{2+} and Ca^{2+}). Cell number was assessed using a Scepter™ handheld automated cell counter (Millipore, UK). Cells were diluted to give a cell count of $1X10^5$. The cell suspensions were stored at 4°C until required.

Preparation of reagents

Oxiselect™ Comet agarose was dissolved at 95°C for 20 minutes before being transferred to a 37°C waterbath until needed. Vista Green DNA dye was diluted 1:10000 in TE Buffer (10mM Tris, pH7.5, 1mM EDTA) and stored at 4°C protected from light. To prepare 1xLysis buffer, 14.6g NaCl was added to 20ml EDTA solution and 10ml 10xLysis solution. The solution was adjusted to 90ml total volume using de-ionised water, mixed thoroughly until all NaCl had dissolved and adjusted to pH 10 using 10M NaOH. The total solution was then made up to be 100ml using deionised water and stored at 4°C before use.

To prepare alkaline solution, 1.2g NaOH was added to 0.2ml EDTA solution and made up to a total volume of 100ml using deionised water. The solution was mixed thoroughly to dissolve NaOH and stored at 4°C before use. To prepare alkaline electrophoresis solution, 12g NaOH was added to 2ml EDTA solution and adjusted to 1L total volume using deionised water. The solution was mixed thoroughly to dissolve NaOH and stored at 4°C before use.

Comet assay

In a 96 well plate, maintained at 37°C using a heat block, 10µl cell suspension for each sample was added to 90µl pre-heated Oxiselect™ Comet agarose. All samples were pipetted to mix and 20µl immediately transferred onto the pre-heated (37°C) Oxiselect™ 96-well Comet slide using a multichannel pipette ensuring complete coverage of each well (Figure 2.1a). Maintaining a horizontal position the slide was

incubated at 4°C for 15 minutes in the dark to allow the cell/agarose mixture to embed onto the slide. The slide was then immersed in 100ml 1xLysis buffer for 1 hour at 4°C in the dark to denature DNA. The 1xLysis buffer was gently aspirated off and the slide immersed in 100ml pre-chilled alkaline solution for 30 minutes at 4°C in the dark.

Alkaline electrophoresis

Maintaining a horizontal position the slide was transferred from the alkaline solution to a horizontal electrophoresis chamber (Figure 2.1b). The chamber was filled with pre-chilled alkaline electrophoresis solution until the slide was covered. A current of 300mA at 24 volts was applied for 25 minutes as per manufacturer's protocol. This electric current results in migration of the damaged DNA fragments away from the intact DNA. Following electrophoresis the slide was transferred to a clean container and immersed in 100ml pre-chilled deionised water for 2 minutes. The water was then gently aspirated and the wash repeated a further two times, followed by a final wash with pre-chilled 70% ethanol for 5 minutes. The slide was carefully removed from the ethanol and allowed to air dry at rtp.

DNA staining and visualisation

50µl diluted Vista Green DNA dye was added to each well and incubated for 15 minutes at room temperature. Using an Axio imager fluorescence microscope (Zeiss, Germany) the DNA migration could be visualised and photographed using a fitted Axiocam with FITC filter for measurement and further analysis (Figure 2.1c).

Figure 2.1: Flowchart representation of Comet assay methodology

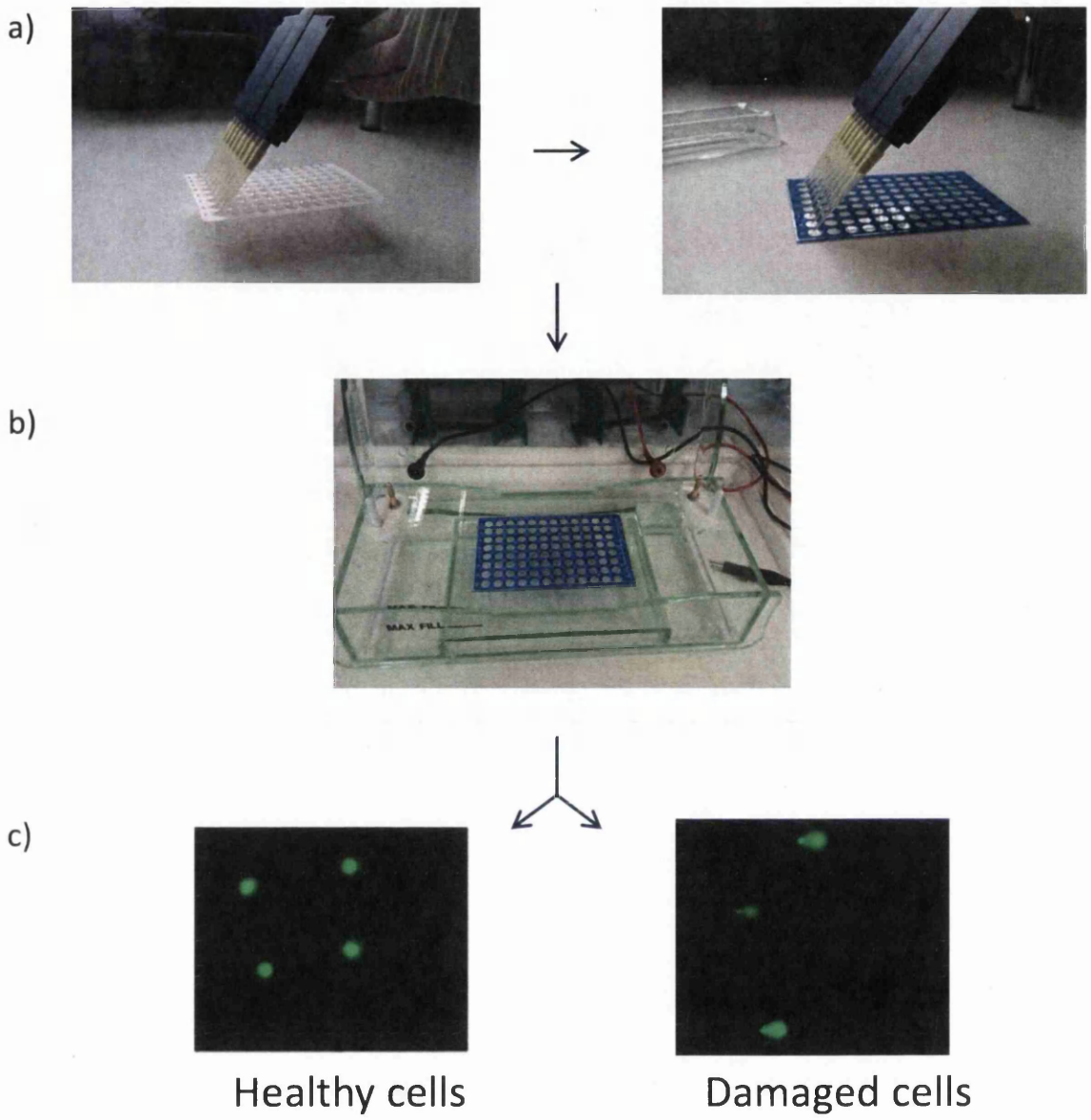

a) 10µl sample suspension added to 90µl Oxiselect™ Comet agarose in a 96 well plate and transferred onto Oxiselect™ 96-well Comet slide. b) Comet slide transferred to horizontal electrophoresis chamber with 24 volts applied for 25 minutes. c) DNA migration visualised and photographed for measurement and analysis.

Analysis of results

Analysis of the Comet assay utilises 2 main parameters to measure cellular DNA damage, (i) Tail DNA% and (i) Tail Moment. Tail DNA% is the relative amount of DNA in the tail compared to the total DNA of the cell (Figure 2.2) and is quantified by measuring DNA intensity using the following calculation:

Tail DNA% = (Tail DNA intensity / Cell DNA intensity) x 100

Tail Moment is a measure of the displacement between intact genetic material in the nucleus, known as the 'Comet Head' and the resulting 'Tail'. There are two commonly used methods of calculating Tail Moment (Figure 2.2):

(i) ***Olive Tail Moment = Tail DNA% x Tail Moment Length***

(ii) ***Extent Tail Moment = Tail DNA% x Length of Tail***

Figure 2.2: Structure of a resulting 'Comet'

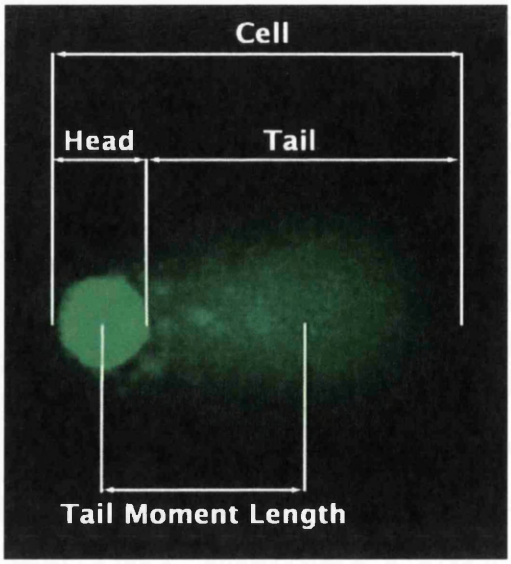

(www.cellbiolabs.com, accessed 10th September '12)

For each sample, 50 cells were photographed using an Axio imager fluorescence microscope with Axiovision camera and a FITC filter. Cells were measured using the commercially available Comet assay specific software CometScore™ which allows automatic calculation of all parameters from the captured images, along with other measures to verify calculations manually. Measures calculated are defined in Appendix 4.

2.4 Gene expression analysis in hVAT using PCR arrays

Commercially available PCR arrays were utilised to analyse gene expression in RNA extracted from hVAT samples (section 2.2.1). All PCR arrays were carried out in a sterile, UV irradiated PCR hood. All pipettes were cleaned with 70% ethanol, all micro-centrifuge tubes were sterilised by autoclaving and sterile RNase free filter tips were used. Gene expression profiling was carried out using the RT^2 Profiler PCR Oxidative Stress Arrays (Qiagen, UK) and was carried out following the manufacturer's protocol. These arrays allow the expression profile of 84 genes related to oxidative stress including peroxidises, peroxiredoxins, genes involved in ROS metabolism and superoxide metabolism, 5 housekeeping genes, controls for genomic DNA contamination, RNA quality and general PCR performance for quality control of the arrays as shown on the plate layout (Appendix 5).

Genomic elimination

RNA concentration for each sample was calculated to determine the required volume. 2µl Genomic Elimination buffer was added to each finalised sample and RNase free water was added to give a total volume of 10µl, mixed via pipette and incubated for 5 minutes at 4°C then put on ice for 1 minute.

cDNA synthesis

mRNA contained within the total RNA was reverse transcribed in order to make cDNA. Reverse transcription master mix containing 4µl BC3 (5XRTbuffer3), 1µl P2 (primer + control mix), 2µl RE3 (RT enzyme mix 3) and 3µl RNase free water was added to 10µl of the RNA from the genomic elimination step. The mix was incubated for 15 minutes at 42°C, then 5 minutes at 95°C. The resulting cDNA reaction was diluted by adding 91µl RNase free water, vortexed and put on ice.

Real-Time PCR

A RT-PCR master mix sufficient for a 96-well plate was prepared containing 1275µl RT^2 SYBR green qPCR mastermix, 102µl diluted cDNA reaction and 1173µl RNase free water. 25µl of master mix was pipetted into each well of the 96 well PCR array plate and sealed with a PCR plate film. The plate was centrifuged and transferred to a MyIQ thermocycler (Biorad, Germany) and run for 1 cycle of 10 minutes at 95°C followed by 40 cycles of 95°C for 15 seconds and 60°C for 1 minute (Figure 2.4).

PCR array data analysis

Analysis of the RT-PCR array was performed using a specific validated online program (www.SABiosciences.com/pcrarraydataanalysis.php). The software shows comparisons between the groups, which allows the identification of significantly up or down regulated genes ($p \leq 0.05$).

Figure 2.3: Flowchart representation of the RT-PCR array methodology

Reverse transcribe RNA to cDNA

Add cDNA to RT^{2}qPCR Master mix and aliquot into 96 well array plate

Run on Biorad MyIQ thermocycler

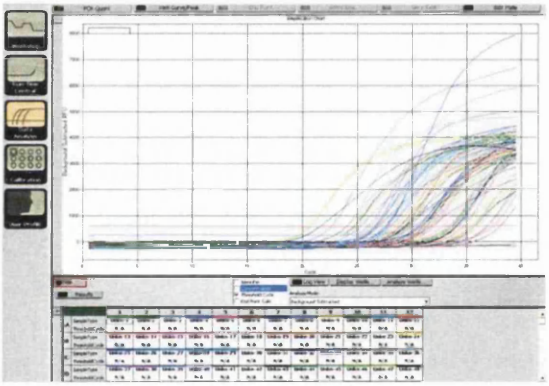

Data analysis

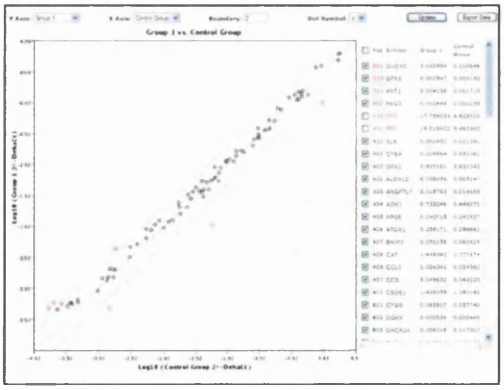

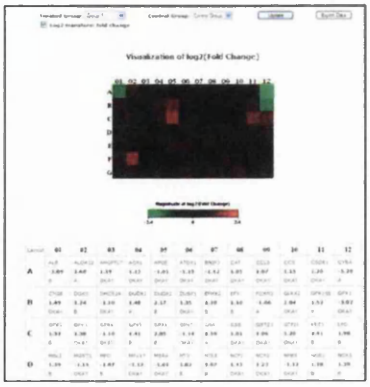

Reverse transcription of RNA to cDNA, which is then mixed with the RT^{2}qPCR Master mix, aliquoted in the 96 well plate and run on the RT thermocycler before data analysis.

2.5 Real Time-Polymerase Chain Reaction of genes of interest from PCR arrays

Genes that were found to be significantly up or down regulated in hVAT by the PCR array analysis were selected for further expression analysis using Real Time-Polymerase Chain Reaction (RT-PCR). RT-PCR is a sensitive technique for gene expression quantification of a target gene in a sample (Hruz *et al*, 2011) particularly in samples low in mRNA concentration such as fatty tissues (Pfaffl *et al*, 2002). Firstly, it requires the mRNA transcripts to be copied into complementary DNA (cDNA) via reverse transcription, which is then amplified and coupled to a PCR reaction. Fluorescence is used to follow the rate of amplification during the PCR reaction. During the exponential stage of the PCR reaction the fluorescence will meet a certain threshold when the number of PCR cycles to reach this threshold is measured (Ct value) and the concentration is directly proportional to the initial starting quantity of mRNA, therefore allowing the measurement of gene expression.

In a standard PCR, the reaction depends upon *Taq* polymerase, which is unable to use RNA as a template. Therefore, the initial step of RT-PCR is to convert mRNA into cDNA using an RNA-dependant DNA polymerase enzyme, reverse transcriptase, which uses the mRNA as a template to generate cDNA in the presence of oligo-dT or random decamer primers.

Internal standards are required during RT-PCR to ensure reverse transcription efficiency and to act as an internal control for sample to sample biases such as differences in RNA template quantities, stability of RNA and sample loading

variation (Hruz *et al*, 2011). These standards are cellular RNA that undergo RT-PCR along with the target genes simultaneously, and is then used as a reference to normalise target genes expression (Karge *et al*, 1998). The standard or housekeeping gene is chosen as it is expressed at a constant level in all tissue types. A reliable housekeeping gene is β-actin as it is a highly expressed gene and is frequently used as an internal standard for RT-PCR.

During RT-PCR, the detection of a fluorescent reporter which accumulates during the PCR reaction allows the quantification of an amplified product as the fluorescence is directly proportional to the amplified product. There are four main fluorophores used for RT-PCR (i) hybridisation probes, (ii) molecular beacons, (iii) Taqman probes (iv) SYBR Green 1. In this study the use of SYBR Green 1 dye is utilised to quantify gene expression as it requires a more simple approach and does not require the use of complex probes. SYBR Green 1 is an intercalating dye that binds directly to the minor grooves of DNA and on binding produces a fluorescent signal. The disadvantage of this method is that it is more susceptible to errors. There is a risk of non-specific binding to any double stranded DNA so the reaction requires full optimisation to minimise formation of primer dimers.

Primer design

RT-PCR primers were designed using gene sequence information from NCBI (http://www.ncbi.nlm.nih.gov/) or sequences that had been previously published (GPX1 primers, Boutet *et* al (2009); GSR primers, Corrales *et al* (2011)) and

synthesised by Eurofins MWG Operon (Germany). For primer design, the final intron-exon boundary was located using the mRNA sequence and primers of approximately 20 nucleotides in length identified spanning this region, with an annealing temperature of approximately 60°C. Self-complementary sequences were avoided in order to prevent secondary structure formations. These primers were designed to amplify fragments of cDNA of 100-150 bp in size from GPx1, GSR, PPARγ and IL-6 as target genes, and β-actin as a housekeeping gene. The resulting primer sequences are shown in Table 2.4. On arrival, all primers were re-hydrated using PCR H_2O to a concentration of 100μM. 100μl of stock primer was transferred to a clean 1.5ml microcentrifuge tube and diluted with 567μl PCR H_2O, aliquoted into 50μl measures and stored at -20°C.

Primer efficiency calculations

PCR efficiency calculations allow the determination of efficiency of each primer set. A dilution series of pooled cDNA from hVAT samples were run in triplicate for each primer set, allowing the best PCR efficiency estimation (Pfaffl *et al*, 2002). The percentage efficiency of the reactions was calculated using the following equation:

$$\%Efficiency = (10^{(-1/slope)})-1) \times 100$$

cDNA synthesis

All reactions were carried out in a sterile, UV irradiated PCR hood with specially designated pipettes, sterile filter tips and micro-centrifuge tubes to reduce risk of contamination.

Table 2.4 RT-PCR Primer sequences for human samples

Name	Sequence (5'-3')	Length (bases)
GPx1 F'	GACTACACCCAGATGAACGAGC	22
GPx1 R'	CCCACCAGGAACTTCTCAAAG	21
GSR F'	ATCCCCGGTGCCAGCTTAGG	20
GSR R'	AGCAATGTAACCTGCACCAACAA	21
PPARγ F'	ACAGCGACTTGGCAATATTTATTG	24
PPARγ R'	AGCTCCAGGGCTTGTAGCA	19
IL-6 F'	CCTGATCCAGTTCCTGCAGAA	21
IL-6 R'	TCCTGCAGCCACTGGTTCT	19
ACTB F'	GATGGCCACGGCTGCTTC	18
ACTB R'	TGCCTCAGGGCAGCGGAA	18

mRNA contained within total RNA extracted from the hVAT (section 2.2.1) was reverse transcribed to make cDNA using a RETROscript kit (Ambion Inc, UK) according to the manufacturer's protocol. A master mix for the desired amount of reactions was prepared containing 1µl oligo-dT primers, 1µl random decamer primers, 2µl RT buffer, 4µl dNTP mix and 1µl MMLV reverse transcriptase enzyme (100U) per reaction. The master mix was vortexed and centrifuged to ensure total mixing and 9µl aliquoted into 0.2ml micro-centrifuge tubes. 100ng of total RNA was added and brought to a total volume of 20µl with the addition of RNase free water. The tubes were vortexed and incubated at 44°C for 1 hour and 90°C for 10 minutes in order to denature the enzyme. The resultant cDNA was stored at -20°C until required.

RT- PCR

Each reaction contained 12.5µl iQ SYBR Green Supermix (Biorad, UK), 1µl forward primer (15pmol), 1µl reverse primer (15pmol), 7.5µl PCR H_2O and 3µl cDNA. A master mix for the desired amount of reactions was made containing all of the above reagents except the cDNA. The master mix was vortexed, centrifuged and aliquoted into micro-centrifuge tubes containing 3 reactions, as every sample was run in triplicate. 9µl of sample cDNA (3µl per reaction) was added to each tube and mixed. 25µl of the final mix was aliquoted into the wells of a sterile 96-well PCR plate in triplicate. When samples were loaded the plate was sealed using an optical quality sealing tape sheet (Biorad, UK) and centrifuged.

Using a CFX Connect Real-Time PCR Detection System (Biorad, UK) samples were run for 1 cycle of 95°C for 3 minutes then 40 cycles of 94°C for 30 seconds, 60°C for 30 seconds and 72°C for 30 seconds; 1 cycle of 55°C for 30 seconds; 1 cycle of 95°C for 30 seconds then 40 cycles of 55°C for 10 seconds.

Relative quantification

The $2^{-\Delta\Delta CT}$ method was used to quantify the level of gene expression changes between groups in a relative fashion (Livak *et* al, 2001). The formula to calculate this was:

$$X=2^{-\Delta\Delta CT}$$

Where in this study:

X = Fold change in gene expression

$\Delta\Delta C_T = \Delta C_{T\,(\text{sample group})} - \Delta C_{T\,(\text{control sample group})}$

$\Delta C_T = C_{T(\text{test sample})} - C_{T\,(\text{internal housekeeping gene})}$

2.6 Gene sequencing

After analysis of the PCR array and RT-PCR gene expression results in hVAT, one particular gene stood out as having differing levels of expression across the L, O and ODM sample groups. GSR codes an antioxidant enzyme involved in the maintenance of glutathione levels in environments of high oxidative burden. Alterations to the genetic code for the GSR gene may explain changes in expression. To investigate

further, the GSR gene was selected for sequencing to identify any mutations or polymorphisms that may account for the expression difference observed in this cohort.

Primer design

GSR gene sequencing primers were designed using gene sequence information from NCBI (www.ncbi.nlm.nih.gov/) and synthesised by Eurofins MWG Operon (Germany). For primer design, the complete mRNA sequence for the GSR gene was used divided into 5 fragments of approximately 700bp each. Primers of approximately 20 nucleotides in length were identified spanning the different sections, with each primer set designed to overlap both the previous and following gene fragment to ensure none of the sequence was lost (Figure 2.4). Primers were designed with an approx annealing temperature of 60°C and self-complementary sequences were avoided in order to prevent secondary structure formations. The resulting primer sequences are shown in Table 2.5.

Figure 2.4 Diagram of overlapping primers spanning mRNA sequence

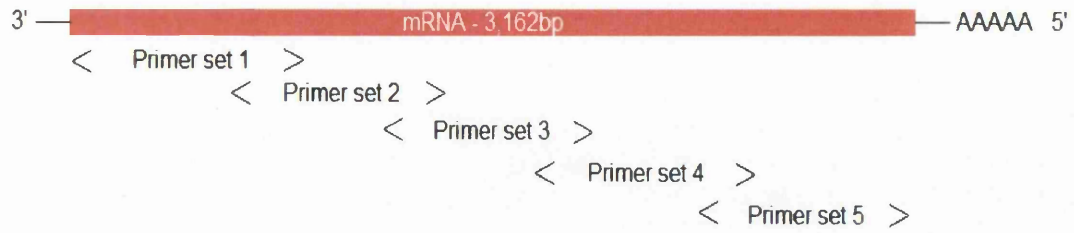

Polymerase chain reaction

hVAT RNA for 61 samples was reverse transcribed to cDNA (section 2.5). However, due to the position of the various primer sets compared to the polyA tail differing amounts of oligo-dT and random decamer primers were used:

- primer sets 1 and 2 - 2µl random decamer
- primer set 3 - 1µl random decamer and 1µl oligo-dT
- primer sets 4 and 5 - 2µl oligo-dT

2µl cDNA for each sample was added to PCR reactions for each primer set, which consisted of 10µl Buffer, 3µl $MgCl_2$, 1µl dNTP mix, 1µl forward primer, 1µl reverse primer, 0.5µl *Taq* polymerase enzyme and 31.5µl PCR H_2O. Samples were vortexed and centrifuged and transferred to MJ Research Thermal Cycler and run on the corresponding optimised program for each primer set (Table 2.6).

Table 2.5 GSR gene sequencing primer sequences

Name	Sequence (5'-3')	Length (bases)
GSR 1 F'	GCGCATGCTTAGTCACCGTG	20
GSR 1 R'	GATCCCAAGCCCACAATAGAG	21
GSR 2 F'	CAATCTCACCAAGTCCCATATAG	23
GSR 2 R'	GTGGCTGAAGACCACAGTTGG	21
GSR 3 F'	GAAAAGCTCTTCTTACTCCAG	21
GSR 3 R'	GCTTTATATTTGGGATGAGGC	21
GSR 4 F'	GTACATAATAGAACTTATTTATGG	24
GSR 4 R'	CGGCTTCTCACATTACATGC	20
GSR 5 F'	GCTGCTTCAAGGATGAGACC	20
GSR 5 R'	TATAAGAAGAAAAGGCTGTAATTTT	25

Table 2.6 Programs for GSR sequencing primers

Primer set	Program
GSR 1	94°C for 2mins 33 cycles of: 94°C for 30secs 56°C for 30secs 72°C for 25secs 15°C forever
GSR 2	94°C for 2mins 25 cycles of: 94°C for 10secs 56°C for 10secs 72°C for 15secs 15°C forever
GSR 3	94°C for 2mins 30 cycles of: 94°C for 30secs 62°C for 30secs 72°C for 25secs 15°C forever
GSR 4	94°C for 2mins 30 cycles of: 94°C for 30secs 56.7°C for 30secs 72°C for 25secs 15°C forever
GSR 5	94°C for 2mins 30 cycles of: 94°C for 30secs 57.8°C for 30secs 72°C for 25secs 15°C forever

PCR purification

PCR products were purified using QIAquick PCR purification kit (Qiagen, UK) following the manufacturers protocol. 45µl PCR product for each sample was added to 225µl Buffer PB and vortexed. Mixture was transferred to QIAquick spin column and centrifuged at 13,000rpm (15,700xg) for 1 minute, the flow through was

discarded and repeated for a further 1 minute. The QIAquick spin column was transferred into a clean 1.5ml tube, 50µl water added to the centre of the column membrane and centrifuged at 13,000rpm (15,700xg) for 1 minute. The resulting purified PCR products were labelled and stored at -20°C until sent for sequencing.

Sanger sequencing

Purified PCR products were sequenced by a commercial sequencing company (Source Bioscience, UK), which adopts the Sanger sequencing methodology. This method elongates complementary DNA sequences with a mix of dideoxynucleotides (ddNTPs) labelled with coloured fluorescent dye, each emitting light at different wavelengths. The resulting DNA sequence is fragmented and passed through a laser field and fluorescence detection device, which stimulate the fluorochromes and identifies bases in sequence order, displaying them in the form of a chromatograph.

Sequencing analysis

Resulting chromatographs were analysed and compared between samples by visualising the sequence using specific software (Chromas Lite Version 2.1.1) that allows the conversion of the chromatograph sequence into a format that can be exported into Mutation Surveyor® software. Mutation Surveyor® allows the comparison of each sample's sequence against a wildtype sequence, obtained from NCBI database, and hence the identification of any mutations between sample sequences. Any mutations observed are finally verified by re-sequencing.

2.7 Mouse 3T3-L1 cell line

3T3 is a mouse (*Mus musculus*) fibroblast cell line. The L1 generation is a continuous sub-strain of 3T3, which has been developed through clonal isolation. The cells have a complete cell cycle of 14 hours and require medium renewal every 2-3 days. The cell line contains insulin receptors, which in the presence of insulin and other factors, can induce differentiation from pre-adipocyte to adipocyte. This line has been widely used in *in vitro* association studies involving obesity and type 2 diabetes (D'Esposito *et al,* 2012).

2.7.1 Cell Culture

All cell culture and experiments were carried out within the sterile environment of a unidirectional laminar flow hood that was pre-cleaned with 70% ethanol and UV irradiated to reduce the risk of contamination. Prior to use, all media were pre-warmed in a water bath at 37°C.

3T3-L1 cells were grown in 75cm^2 flasks containing 30ml Dulbecco's Modified Eagle Medium media (DMEM) (either DMEM high glucose [4.5g/L] or DMEM low glucose [1g/L]), fetal bovine serum (FBS) (10%), penicillin-streptomycin (2%) and sodium bicarbonate (1%) and incubated in a 5% CO_2 environment at 37°C. When sub-culturing, cells were washed with PBS, trypsinised and re-suspended in 30ml of pre-warmed medium. Cells were split 1 in 3 10ml of re-suspended cells and medium were transferred into 2 x clean 75cm^2 flasks and 10ml remaining in the original

flask. Each flask had an additional 20ml of pre-warmed media added and incubated in a 5% CO_2 environment at 37°C.

2.7.2 Pro-oxidant treatment of 3T3-L1 cells

Lipopolysaccharide (LPS) are found in the cell wall of Gram-negative bacteria, and act as an endotoxin, inducing strong responses in mammalian immune systems, so was used as a pro-oxidant biochemical stressor treatment. The LPS (Sigma, UK) used in the study was sourced from *Escherichia coli* and purified by phenol extraction. This LPS serotype has been used to stimulate B-cells and induce nitric oxide synthase (NOS) in human hepatocytes. A working concentration of 1μg/ml for treatment was taken from previous studies conducted by Kizaki *et al*, (2002), with all experiments being conducted in triplicate. LPS was administered after 3 days of culturing to allow for healthy growth and confluency. Cells were left for a full 14 hour cell cycle post treatment before being re-suspended in PBS for extraction of RNA.

2.7.3 RNA extraction from 3T3-L1 cells

Total RNA was extracted from cells using RNeasy Mini Kit (Qiagen, UK) following the manufacturer's protocol. Prior to every extraction the hood and all pipettes were cleaned and UV irradiated, all micro-centrifuge tubes and RNA free water were sterilised by autoclaving and sterile RNase free filter tips were used.

Before extraction, cells were suspended in 10ml PBS, centrifuged and supernatant discarded. Homogenisation was carried out by re-suspending the pellet in 600µl Buffer RLT mix (10µl β-mecaptoethanol + 1ml Buffer RLT) and passing the lysate through a 20-gauge needle 5 times. Homogenised lysate was transferred to a RNeasy mini column and collection tube, centrifuged for 15 seconds at 10,000rpm (9,300xg) and flow through discarded. 700µl Buffer RW1 was added, centrifuged for 15 seconds at 10,000rpm (9,300xg) and flow through discarded. 500µl Buffer RPE was added, centrifuged for 15 seconds at 10,000rpm (9,300xg) and flow through discarded, with the Buffer RPE step being repeated for a second time. The RNeasy column was placed in a clean centrifuge tube and the RNA was eluted by the addition of 50µl of RNase free water directly onto the column membrane and centrifuged for 1 minute at 10,000rpm (9,300xg). The elution step was repeated with a further 50µl of RNase free water and the final volume of total RNA was aliquoted into 20µl measures and stored at -80°C.

2.7.4 Mouse RT-PCR primer design

RT-PCR primers were designed using gene sequence information from the NCBI sequence database (www.ncbi.nlm.nih.gov/) and supplied by Eurofins MWG Operon (UK). For primer design, the final intron-exon boundary was located using the mRNA sequence and primers of approximately 20 nucleotides in length identified spanning this region, with an annealing temperature of approximately 60°C. Self-complementary sequences were avoided in order to prevent secondary structure formations. These primers were designed to amplify fragments of cDNA of

100-150 bp in size from mouse GPx1 and GSR as target genes; and mouse β-actin as a housekeeping gene. The resulting primer sequences are shown in Table 2.7. On arrival, all primers were re-hydrated using PCR H_2O to a concentration of 100µM. 100µl of stock primer was transferred to a clean 1.5ml microcentrifuge tube and diluted with 567µl PCR H_2O, aliquoted into 50µl measures and stored at -20°C.

Table 2.7 Mouse RT-PCR primer sequences

Name	Sequence (5'-3')	Length (bases)
M GPx1 F'	CAATGTAAAATTGGGCTCGAA	21
M GPx1 R'	GTTTCCCGTGCAATCAGTTC	20
M GSR F'	ATCGTGCATGAATTCCGAGT	20
M GSR R'	GGTGGTGGAGAGTCACAAGC	20
M ACTB F'	ATGGAGGGGAATACAGCCC	19
M ACTB R'	TTCTTTGCAGCTCCTTCGTT	20

All RT-PCR reactions were conducted as per the hVAT samples described earlier (section 2.5).

2.8 Statistical analysis

Statistical analysis was performed using SPSS (Version 19). Data are reported for those individuals within the L, O and ODM groups. Results are presented as mean

and standard deviation. For data that was normally distributed after log transformation, the geometric mean and approximate standard deviation are shown. For data that could not be transformed to a normal distribution the median and interquartile range are given. Analysis of variance (ANOVA) was used to assess the association between group and baseline characteristics for data that was normally distributed after log transformation. For data that could not be transformed to a normal distribution analysis was carried out using the Kruskal-Wallis and Mann-Whitney tests. Chi-squared tests were used to compare differences in categorical variables by group. In all cases a P-value of < 0.05 was considered statistically significant. Two sided statistical testing was performed. Any further specific statistical analysis is detailed in each chapter.

CHAPTER THREE

BIOMARKERS OF OXIDATIVE STRESS AND DNA DAMAGE IN VISCERAL ADIPOSE TISSUE

3.1 Introduction

Oxidative stress is free radical-mediated damage caused by excess levels of ROS, as previously described (Section 1.1). In the case of increased levels of ROS, cells have defensive antioxidant systems that scavenge ROS and repair oxidative damage (Section 1.1.2). Increased oxidative stress is associated with obesity and T2DM (Codoner-Franch *et al,* 2011; Rehman *et al*, 1999), and can result in increased DNA damage within these populations (Apelt *et al*, 2009; Tatsch *et al*, 2012).

3.1.1 Measures of oxidative stress

During this chapter, experiments were undertaken to satisfy aim **1** as laid out in Chapter 1 (Section 1.10). In order to measure oxidative stress in hVAT in the three different subject groups (L, O and ODM) four methods were selected as markers to provide a "global" view of oxidative burden. Over recent years a number of measurements of oxidative stress have been developed, although few hold the reliability and specificity that is required for their use in a more clinical setting. To measure ROS directly is considered unfeasible due to their highly reactive state and short half-life (Brandes *et al*, 2005), therefore, common practice has adopted measures of ROS induced damage that result from high levels of oxidative stress. Meeting the objective of this study required the consideration of techniques that would gather the global oxidative status of the subjects and measure levels of resulting oxidative damage.

3.1.2 Total antioxidant capacity

Antioxidant activity may be measured by the overall capacity of antioxidants, measurement of specific enzymes (SOD, catalase or GPx) or the resistance of a sample to an external oxidant. A marker of total antioxidant capacity was chosen, in the form of the TAOS assay. TAOS is a method, described by Sampson *et al* (2002), to measure global antioxidant levels in a sample relative to a saline control. It was chosen to allow the relative active antioxidant levels within the samples to be compared between subject groups; L, O and ODM. This method was the ideal choice as it was an established technique within the research group and was easily accessible and has been used widely within clinical studies (Dandana *et al*, 2011).

Although TAOS has become more widely used in studies examining oxidative stress it does have its limitations as do other measures of its kind. These methods work on the basis of a sample's ability to quench free radicals that are present such as 1,1-diphenyl-2-picrylhydrazl or, in the case of TAOS, $ABTS^{+}$ radicals. Drawbacks observed in measures of this type were inconsistencies in results between methods therefore showing no association or correlation. Also, variation within results have been observed during prolonged storage of samples proving concerns about the overall stability of the markers (Codoner-Franch *et al*, 2011). Measures of antioxidant capacity, such as those mentioned are predominantly measured within plasma samples. Therefore analysing this in hVAT samples was basic and experimental. Our review of the available literature has shown that the TAOS assay and other measures of total antioxidant capacity have not been used to measure antioxidant levels in AT homogenates. Therefore, this was novel basic work.

3.1.3 Measures of lipid peroxidation

Increased levels of oxidative stress lead to the initiation of lipid peroxidation, which is the degradation of lipids (Section 1.1.3). TBARS was chosen as a method of measuring products of lipid peroxidation related to oxidative stress. The measurement of products of lipid peroxidation, such as aldehydes, have been widely used as a quantitative measure of oxidative stress in plasma samples in a number of studies. Increased levels of F_2-isoprostanes have been observed in obesity and T2DM (Keaney *et al*, 2003; Helmersson *et al,* 2004). The measurement of plasma and urinary F_2-isoprostanes have become the gold standard measures of lipid peroxidation *in vivo*, although, the techniques involves a complex protocol involving gas chromatography–mass spectrometry (GC-MS) analysis (Yin *et al*, 2009).

Alternatively, TBARS assays quantify the concentration of MDA in samples as a marker of oxidative stress. MDA is the most widely studied peroxidation product, and as well as its use as a marker of oxidative stress it also has a mutagenic effect on DNA (Del-Rio *et al*, 2005). TBARS was chosen for this study due to its more basic methodology, without the requirement of mass spectrometry. It does however have its limitations as this spectrophotometric assay is not entirely specific to the measurement of MDA, as other aldehydes similar to MDA may also be detected. Previous studies using TBARS observed increased MDA concentration in plasma samples from obese subjects (Lima *et al*, 2004; Furukawa *et al,* 2013). This method, according to the literature, has not be used in hVAT samples.

3.1.4 Markers of oxidative DNA damage

Excessive ROS causes oxidative damage to DNA that may cause premature cell senescence, often a result of telomere shortening (Section 1.7) or damage in the form of strand breaks. Two markers of DNA damage were chosen to compare the extent of oxidative damage in subjects with obesity and T2DM. These were (i) a PCR-based method to measure telomere length and (ii) a Comet assay to quantify DNA damage, such as double strand breaks, associated with oxidative stress.

A method for the measurement of telomere length was chosen with the rationale that telomeres have been observed to shorten at a faster rate in environments of oxidative stress, such as in obesity and T2DM (Zglinicki, 2002). Telomere length is an established measure that we and collaborators at UCL have used (Salpea *et al*, 2009). This made it accessible for me to visit the research group at UCL to learn the technique and adapt it for the laboratory in Swansea. Previous studies have examined telomere lengths in a number of different tissues (but not AT) and found that overall there was little difference in telomere length between tissue types (Friedrich *et al,* 2000), but did show that leukocytes may serve as a surrogate for an individual's telomere length; as a result since then most studies have focused on using leukocytes for this technique. This does not mean that the method is not successful in other tissues, although no literature has been described examining telomere lengths with AT.

As another method of measuring oxidative DNA damage a commercial Comet assay was chosen. Initially an in-house assay protocol was attempted following a method

described by Cerda *et al* (1997) although optimisation was unsuccessful due to very strict conditions that were unable to be met. For this reason a commercially available alternative was utilised. The Comet assay was chosen as it is widely used as a quick and reliable way to analyse DNA damage in individual cells. In the past it has been used to investigate oxidative damage in relation to various conditions, including diabetes (Ibarra-costill *et al,* 2010) and to study the effects of prescription drugs on cells (Sliwinska *et al*, 2008). Previous studies using the Comet assay to investigate DNA damage in obesity found a positive association between DNA damage, BMI, antioxidant status and MDA concentration (Bukhari *et al*, 2010). No literature was found using the Comet assay to examine DNA damage in AT samples, as the majority of studies used blood plasma for analysis.

3.2 Aims

The purpose of the work described in this chapter was firstly to attempt to measure two different biomarkers of oxidative stress ($\Delta ABTS^{+}$ and TBARS) and two markers of DNA damage (telomere length and Comet) in hVAT. The second aim was to examine these biomarkers in samples obtained from lean, obese and obese patients with T2DM in order to get an overview of the difference in oxidative burden between the groups in this population that may be associated with obesity and/or diabetes.

3.3 Methods

Biomarkers of oxidative stress ($\Delta ABTS^+$ and TBARS) and DNA damage (telomere length and Comet) were measured in 61 hVAT samples. Samples were categorised as L, which have a BMI <30; O, which have a BMI>30 and ODM with a BMI>30 and have T2DM.

3.3.1 Biomarkers of oxidative stress in visceral adipose tissue

3.3.1.1 $\Delta ABTS^+$ within hVAT homogenate samples relative to saline control

Relative change in $ABTS^+$ ($\Delta ABTS^+$), as described in detail in Chapter 2 (Section 2.3.1) is a protocol modified from a previously described method that measured total antioxidant status (TAOS) in plasma (Sampson *et al*, 2002; Stephens *et al,* 2009). This protocol was developed to allow use of tissue homogenates instead of blood plasma samples. $\Delta ABTS^+$ was successfully measured in hVAT homogenates of 61 subjects. Higher levels of $ABTS^+$ formation is indicative of increased levels of oxidative stress in the hVAT samples.

3.3.1.2 Thiobarbituric acid reactive substances

Thiobarbituric acid reactive substances (TBARS) is a marker of lipid peroxidation (Section 1.1.3), a mechanism of cellular injury and an indicator of oxidative stress. The assay measures malondialdehyde (MDA) concentration, as a natural product of lipid peroxidation, which readily reacts with 2-thiobarbituric acid (TBA) to form a red fluorescent adduct that is measured fluorometrically. TBARS can be used to assay lipid peroxidation in plasma, serum, urine, tissue homogenates and cell lysates. Tissue homogenates from hVAT (Section 2.3.1) were successfully assayed in

61 subjects (Section 2.3.2). Using an MDA standard curve the concentration of MDA in the homogenates was calculated. Higher concentration of MDA is indicative of a higher level of lipid peroxidation, and therefore, higher oxidative stress within the hVAT.

3.3.2 Biomarkers of DNA damage in visceral adipose tissue

3.3.2.1 Telomere length

As described in Chapter 1 (Section 1.7), telomeres are DNA repeat sequences found at the end of chromosomes that shorten during replication and are therefore representative of the cell's biological age. As discussed, environments of high oxidative stress potentially lead to accelerated telomere shortening and have been implicated in the pathogenesis of T2DM. Telomere length was successfully measured in DNA extracted from 61 hVAT samples (Sections 2.2.2 and 2.3.3). Relative telomere length was calculated as the ratio of telomere repeats to single-copy gene copies, termed the T/S ratio, using a validated quantitative PCR-based method.

3.3.2.2 Comet assay

The Comet assay was utilised as a marker of DNA damage. It is a method to visualise DNA damage within a cell by the use of electrophoresis resulting in 'comet-like' tails that can be measured microscopically. The longer the comet tail the higher degree of damage. Comet assay was successfully carried out on hVAT homogenates from 61 samples in duplicate (Section 2.3.4).

3.3.3 Statistical analysis

I chose to analyse the differences between all groups (L v O v ODM), as well as subcategorising by L v O+ODM, which groups lean v all obese subjects together; and L+O v ODM, grouping subjects with no diabetes against those with diabetes.

Data was analysed as described in Chapter 2 (Section 2.8). For samples run in triplicate, average values were used for analysis. TBARS and TAOS data were normally distributed after log transformation, so geometric mean and approximate standard deviation are shown. T/S ratio data could not be transformed to a normal distribution so the median and interquartile ranges are given. All data from the Comet assay were normally distributed and presented as mean and standard deviation for all measures, with exception of 'Tail mean intensity' which could not be transformed to a normal distribution and is displayed as median and interquartile range. Data were analysed using the Kruskal-Wallis test for non-parametric data.

3.4 Results

3.4.1 Baseline characteristics

3.4.1.1 L v O v ODM

hVAT samples were collected from 61 subjects, grouped as L, O and ODM (L/O/ODM: 20/20/21), to investigate the association between oxidative stress and baseline characteristics. As shown in Table 3.1, age was significantly different across groups (P=0.028). The L group was approximately 5 years older than the O group and approximately 11 years older than ODM group, with a significant linear

relationship across groups from L, O to ODM (P=0.006). As expected a significant difference was seen in the weight and BMI (P=<0.001 for both), being greatest in the ODM group. There was no significant difference in blood pressure (SBP or DBP) between groups, however as expected blood glucose levels were significantly higher in the ODM group (P=0.015). Plasma levels of creatinine (P=0.016) and albumin (P=0.046) were significantly lower in the ODM group.

DNA and RNA concentration was quantified to ensure required concentration and purity for examination. DNA concentration showed no different between groups but of interest the RNA concentration was 20% lower in the ODM group compared to L and O, however this did not reach significance (P=0.422). Although not significantly different there was a higher proportion of males in the L group and there was no difference in smoking status between groups. Significant co-morbidities seen in the ODM group were hypertension (P=0.009) and obstructive sleep apnoea (OSA) (P=0.001). A significantly higher proportion of subjects in the ODM group were on statin (P=0.020) and ACE inhibitor (P=0.043) therapies.

Table 3.1 Baseline characteristics compared between groups

	Lean (n=20)	Obese (n=20)	Obese/T2DM (n=21)	P
Age (years)	55.3 (17.4)	49.7 (10.8)	44.3 (8.6)	**0.028**
Weight (kg)	73.5 (13.1)	119.6 (36.1)	136.9 (26.5)	**<0.001**
BMI (kg/m^2)	25 (2.8)	41 (10.8)	50 (10.7)	**<0.001**
SBP (mmHg)	139 (23.4)	130 (17.0)	144 (19.7)	0.130
DBP (mmHg)	80 (13.2)	79 (11.9)	76 (14.3)	0.604
Glucose (mmol/L)*	5.7 (0.6)	5.6 (0.3)	8.1 (1.6)	**0.015**
Cholesterol (mmol/L)	5.3 (1.4)	5.5 (1.7)	4.8 (1.2)	0.501
HDL-C (mmol/L)	1.5 (0.3)	1.2 (0.3)	1.1 (0.3)	0.053
LDL-C (mmol/L)	3.3 (1.1)	3.5 (1.6)	2.6 (0.9)	0.229
Triglycerides (mmol/L)	1.2 (0.2)	1.6 (0.8)	2.7 (1.4)	0.057
Creatinine (µmol/L)	78.2 (17.5)	78.7 (12.6)	66.3 (14.4)	**0.016**
Albumin (mmol/L)	46.7 (8.1)	43.4 (2.4)	42.2 (4.5)	**0.042**
DNA (ng/µl)	15.6 (6.3)	15.1 (6.7)	15.2 (12.1)	0.980
RNA (ng/µl)	98.0 (61.4)	96.7 (51.7)	77.0 (55.1)	0.422
Males % (n)	55.0 (11)	40.0 (8)	35.0 (7)	0.359
Current smoker % (n)	25.0 (5)	25 0 (5)	14.3 (3)	0.648
Hypertension % (n)	20.0 (4)	25.0 (5)	61.9 (13)	**0.009**
OSA % (n)	0 (0)	15.0 (3)	47.6 (10)	**0.001**
Statins % (n)	5.0 (1)	30.0 (6)	42.9 (9)	**0.020**
ACE inhibitor % (n)	20.0 (4)	10.0 (2)	42.9 (9)	**0.043**

Baseline characteristics of hVAT samples in L, O and ODM groups. *Log transformed data. Mean and standard deviation shown or geometric mean and approximate standard deviation for log transformed data. Analysis performed by ANOVA after appropriate transformation. χ^2-test was used to compare groups. P-value shows significance where P<0.05

3.4.1.2 L v O+ODM

Prior to analysis, I chose to examine baseline characteristics between L v O+ODM to look at the effects of obesity between groups. The results are detailed in Table 3.2. Age (P=0.020), weight (P<0.001) and BMI (P<0.001) were significantly different between groups. Blood pressure and cholesterol levels were not significantly different between the two groups and although not significant, glucose levels were higher in the O+ODM subjects. HDL-C (P=0.031) and albumin (P=0.014) were significantly lower in the O+ODM group, and there was no significant difference in gender. There were more than four times the number of subjects with hypertension in the O+ODM group but this was not statistically significant. All subjects with OSA fell into the O+ODM group, therefore making it significant (P=0.005); and there was a significantly higher proportion of subjects on statin treatment in the obese subjects (P=0.008).

Table 3.2 Baseline characteristics between lean and obese groups (O+ODM)

	Lean (n=20)	Obese+Obese T2DM (n=41)	P
Age (years)	55.3 (17.4)	46.9 (10.0)	**0.020**
Weight (kg)	73.5 (13.1)	128.7 (32.2)	**<0.001**
BMI (kg/m^2)	25 (2.8)	46 (11.6)	**<0.001**
SBP (mmHg)	139 (23.4)	137 (19.5)	0.799
DBP (mmHg)	80 (13.2)	77 (13.0)	0.441
Glucose (mmol/L)*	5.7 (0.6)	7.1 (0.7)	0.162
Cholesterol (mmol/L)	5.3 (1.4)	5.0 (1.3)	0.659
HDL-C (mmol/L)	1.5 (0.3)	1.1 (0.3)	**0.021**
LDL-C (mmol/L)	3.3 (1.1)	2.8 (1.2)	0.448
Triglycerides (mmol/L)	1.2 (0.2)	2.4 (1.4)	0.094
Creatinine (µmol/L)	78.2 (17.5)	72.2 (14.8)	0.173
Albumin (mmol/L)	46.7 (8.1)	42.7 (3.7)	**0.014**
DNA (ng/µl)	15.6 (6.3)	15.1 (9.6)	0.841
RNA (ng/µl)	98.0 (61.4)	86.9 (53.6)	0.472
Males % (n)	55.0 (11)	36.6 (15)	0.172
Current smoker % (n)	25.0 (5)	19.5 (8)	0.331
Hypertension % (n)	20.0 (4)	43.9 (18)	0.068
OSA % (n)	0 (0)	31.7 (13)	**0.005**
Statins % (n)	5.0 (1)	36.6 (15)	**0.008**
ACE inhibitor % (n)	20.0 (4)	26.8 (11)	0.561

Baseline characteristics between lean and obese (O+ODM) groups to look at effects of obesity between groups. *Log transformed data. Mean and standard deviation shown or geometric mean and approximate standard deviation for log transformed data. Analysis performed by ANOVA after appropriate transformation. χ^2-test was used to compare groups. P-value shows significance where $P<0.05$

3.4.1.3 L+O v ODM

I chose to examine baseline characteristics between L+O v ODM to look at the effects of non-diabetes (n=40) and diabetes (n=21). The results are shown in Table 3.3. Age (P=0.022), weight (P<0.001) and BMI (P<0.001) were significantly different between groups. There was no significant difference in blood pressure, cholesterol, lipoprotein and albumin levels. Levels of plasma glucose (P=0.004) and triglycerides (P=0.019) were significantly higher in the group with diabetes. There was a higher proportion of males in the non-diabetes group although this was not significant. RNA concentration was lower in the diabetes group compared to non-diabetes although this difference was not significant. The co-morbidity hypertension (P=0.002) and OSA (P<0.001) were significantly more prevalent in the subjects with diabetes and more subjects in the diabetes group were on statin (P=0.032) and ACE inhibitor treatments (P= 0.016).

Table 3.3 Baseline characteristics between no-diabetes (L+O) and diabetes groups

	No Diabetes (n=40)	Diabetes (n=21)	P
Age (years)	52.5 (14.5)	44.3 (8.6)	**0.022**
Weight (kg)	96.0 (35.3)	136.9 (26.5)	**<0.001**
BMI (kg/m^2)	33 (10.9)	50 (10.7)	**<0.001**
SBP (mmHg)	135 (20.9)	144 (19.7)	0.116
DBP (mmHg)	79 (12.5)	76 (14.3)	0.339
Glucose (mmol/L)*	5.6 (0.4)	8.1 (1.6)	**0.004**
Cholesterol (mmol/L)	5.4 (1.5)	4.8 (1.2)	0.244
HDL-C (mmol/L)	1.3 (0.3)	1.1 (0.3)	0.060
LDL-C (mmol/L)	3.4 (1.3)	2.6 (0.9)	0.084
Triglycerides (mmol/L)	1.4 (0.6)	2.7 (1.4)	**0.019**
Creatinine (µmol/L)	78.4 (15.1)	66.3 (14.4)	**0.004**
Albumin (mmol/L)	45.2 (6.4)	42.2 (4.5)	0.065
DNA (ng/µl)	15.4 (6.4)	15.2 (12.1)	0.927
RNA (ng/µl)	97.4 (56.0)	77.0 (55.1)	0.188
Males % (n)	47.5 (19)	35.0 (7)	0.288
Current smoker % (n)	25.0 (10)	14.3 (3)	0.606
Hypertension % (n)	22.5 (9)	61.9 (13)	**0.002**
OSA % (n)	7.5 (3)	47.6 (10)	**<0.001**
Statins % (n)	17.5 (7)	42.9 (9)	**0.032**
ACE inhibitor % (n)	15.0 (6)	42.9 (9)	**0.016**

Baseline characteristics between non-diabetes (L+O) and diabetes groups to look at the effect of diabetes between groups *Log transformed data. Mean and standard deviation shown or geometric mean and approximate standard deviation for log transformed data. Analysis performed by ANOVA after appropriate transformation. χ^2-test was used to compare groups. P-value shows significance where P<0.05

3.4.2 Biomarkers of oxidative stress in visceral adipose tissue

3.4.2.1 ΔABTS^{+} within hVAT homogenate samples relative to saline control

ΔABTS^{+} data analysis was carried out using a modified calculation from previously described TAOS assay (Sampson *et al*, 2002; Stephens *et al*, 2009); in order to give a change in ABTS^{+} formation per sample relative to saline control results. There was no overall difference in ΔABTS^{+} between groups (Figure 3.1) (L v O v ODM: 2.0 (0.1) v 2.0 (0.3) v 1.9 (0.01), P=0.813). Additionally, no difference was observed when L group was compared to combined O+ODM group (L v O+ODM: 2.0 (0.1) v 2.0 (0.2), P=0.752) (Figure 3.2); or when combined L+O group was compared to ODM group (L+O v ODM: 2.0 (0.2) v 1.9 (0.1), P=0.518) (Figure 3.3).

Figure 3.1 ΔABTS^{+} between groups relative to saline

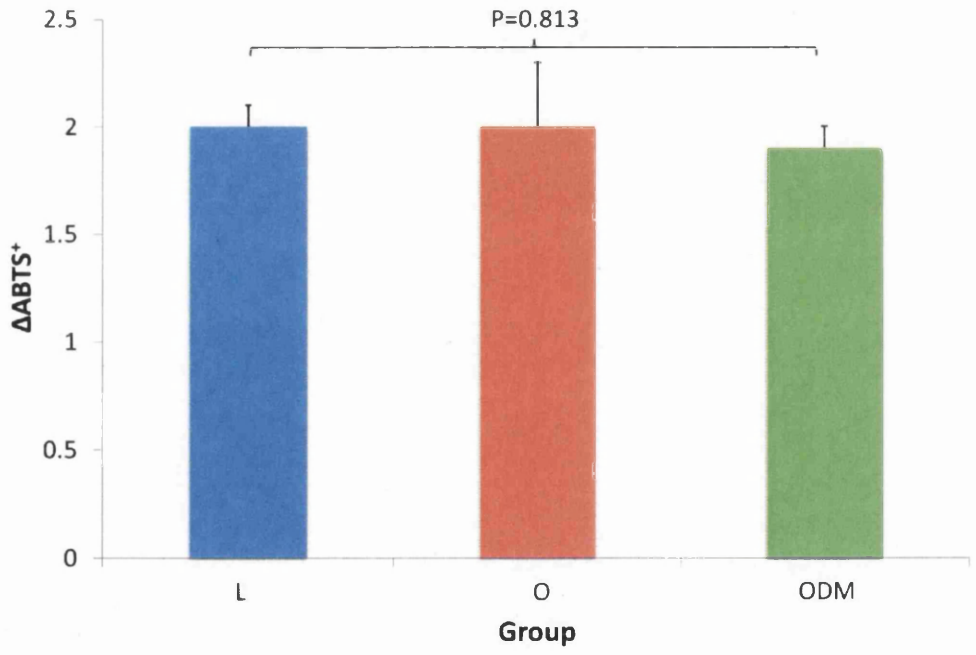

Relative ΔABTS^{+} between groups. Geometric mean and approximate standard deviation shown

Figure 3.2 $\Delta ABTS^{+}$ between lean and obese groups (O+ODM) relative to saline

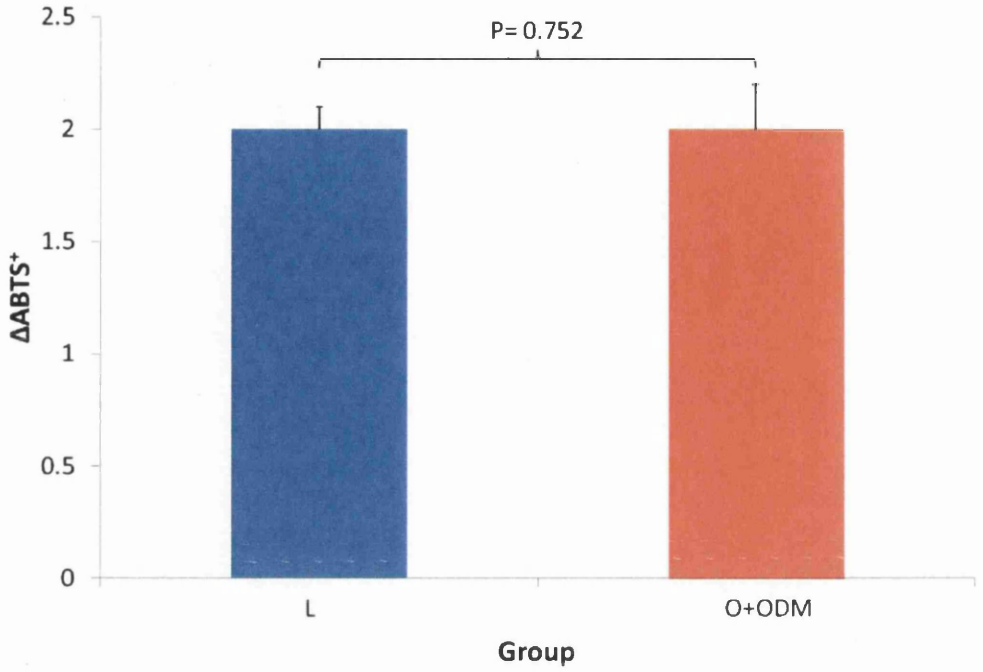

Relative $\Delta ABTS^{+}$ between lean and obese (O+ODM) groups to look at effects of obesity. Geometric mean and approximate standard deviation shown

Figure 3.3: $\Delta ABTS^{+}$ between no-diabetes (L+O) and diabetes groups relative to saline

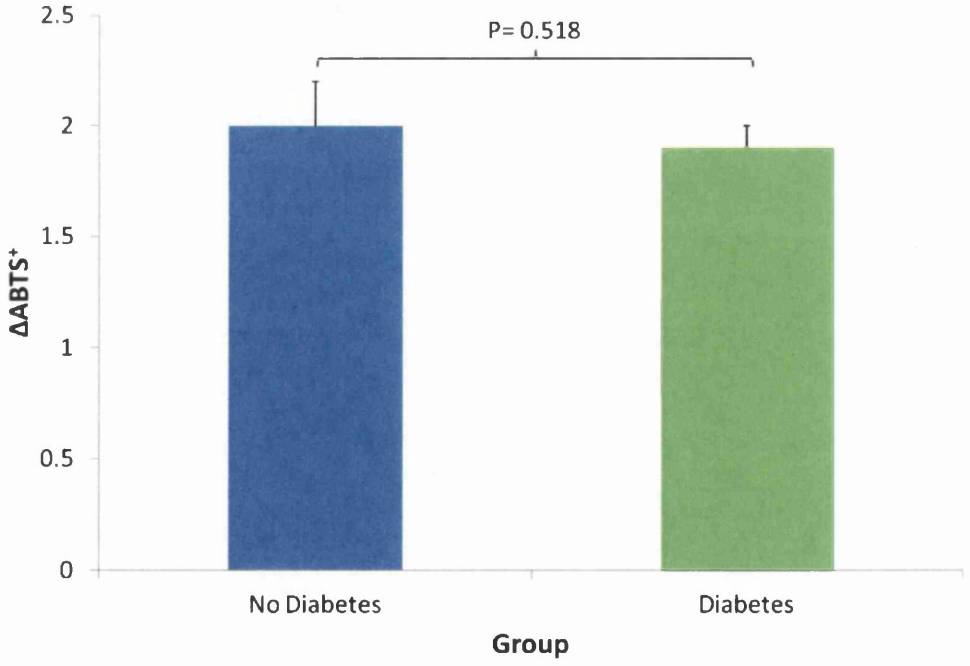

Relative $\Delta ABTS^{+}$ between no-diabetes (L+O) and diabetes groups to look at effects of diabetes. Geometric mean and approximate standard deviation shown

3.4.2.2 Thiobarbituric acid reactive substances (TBARS)

TBARS were measured as an indicator of oxidative stress in 61 hVAT homogenates using an MDA standard curve to calculate the concentration of MDA within each sample. As shown in Figure 3.4, there was no significant change in MDA concentration between groups (L v O v ODM (μM): 19.6 (8.4) v 18.4 (11.4) v 9.8 (3.8), P=0.110). A higher MDA concentration was observed in the L group when compared to combined O+ODM group although not significant (L v O+ODM (μM): 19.6 (8.4) v 13.5 (7.1), P=0.238) (Figure 3.5). A significantly lower MDA concentration was observed in the ODM group when compared to the combined L+O (L+O v ODM (μM): 19.0 (10.0) v 9.8 (3.8), P=0.036) (Figure 3.6).

Figure 3.4 MDA concentration between groups

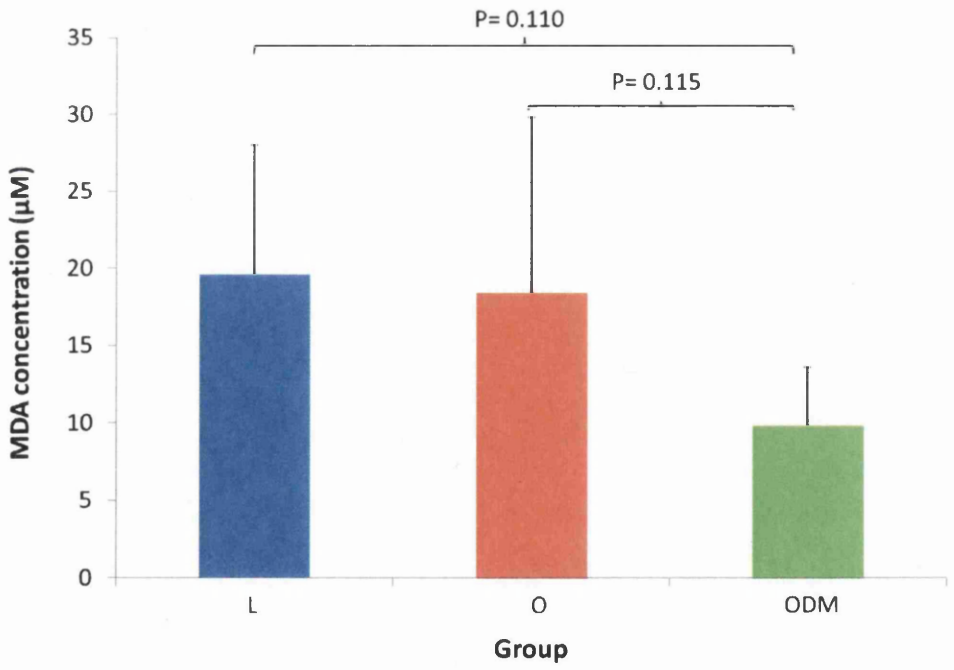

MDA concentration between groups. Geometric mean and approximate standard deviation shown

Figure 3.5 MDA concentration between lean and obese groups (O+ODM)

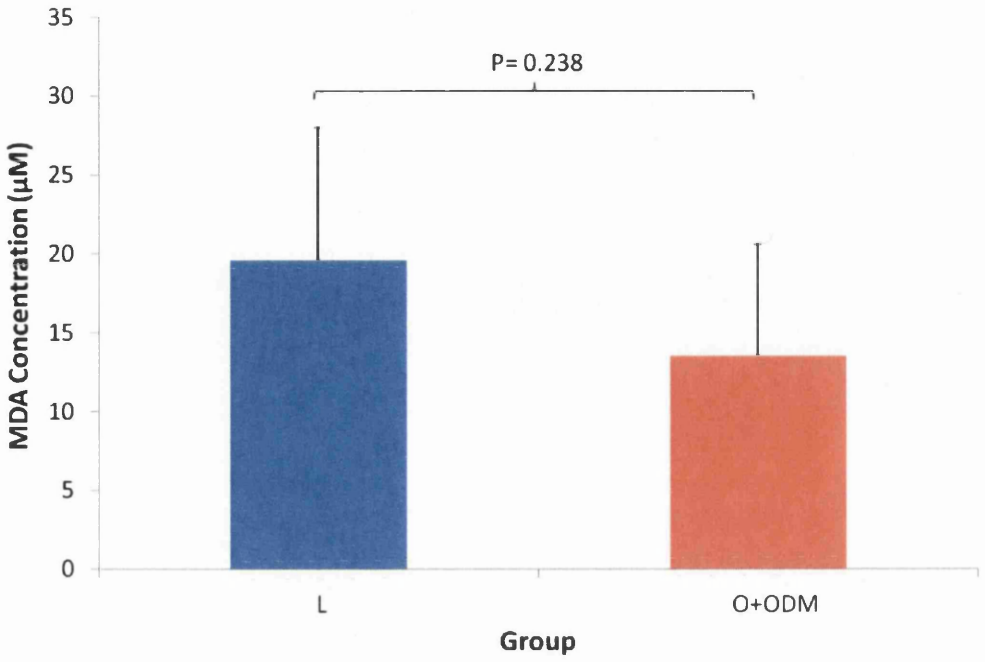

MDA concentration between lean and obese (O+ODM) groups to look at effects of obesity. Geometric mean and approximate standard deviation shown

Figure 3.6 MDA concentration between no-diabetes (L+O) and diabetes groups

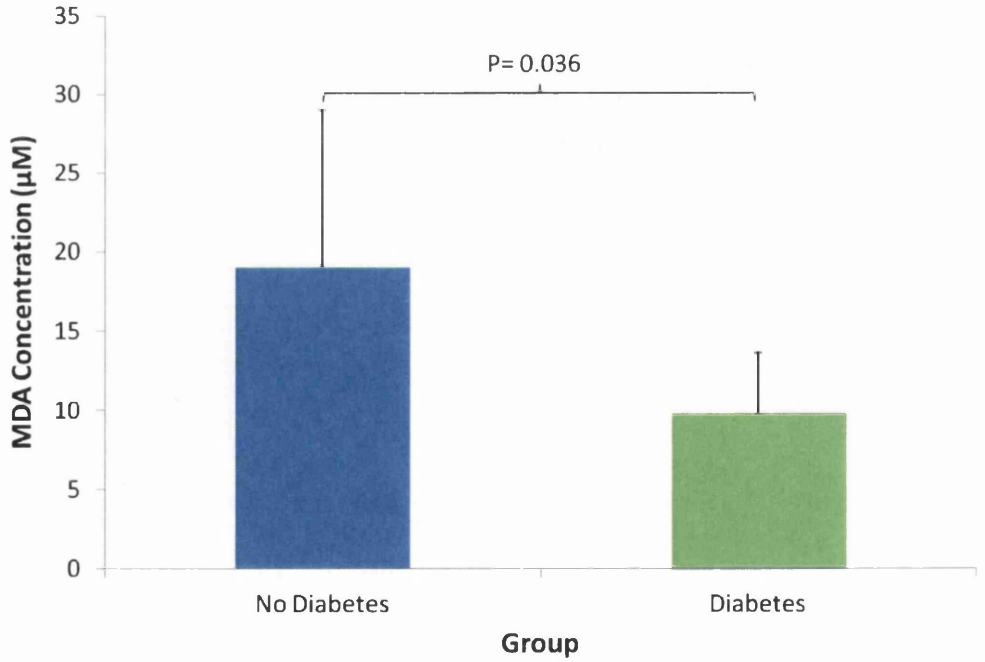

MDA concentration between no-diabetes (L+O) and diabetes groups to look at effects of diabetes. Geometric mean and approximate standard deviation shown

3.4.3 Biomarkers of DNA damage in visceral adipose tissue

3.4.3.1 Telomere length

Relative telomere length was calculated as the ratio of telomere repeats to single-copy gene copies (T/S ratio) in 60 DNA samples. As shown in the box plot (Figure 3.7), T/S ratio was four times higher in ODM subjects when compared to L and O groups (L v O v ODM: 1.0 [0.8 - 4.3] v 1.0 [0.9 - 4.2] v 4.4 [2.1 - 4.8], P=0.064) with a significant difference between O and ODM groups (P=0.048). There was no significant difference observed in the T/S ratio between the L group and combined O+ODM group (L v O+ODM: 1.0 [0.8 - 4.3] v 3.8 [0.9 - 4.8], P=0.221) (Figure 3.8); however this was significantly higher for diabetes group compared to no-diabetes group (L+O v ODM: 1.0 [0.9 - 4.2] v 4.4 [2.1 – 4.8], P=0.019) (Figure 3.9).

Figure 3.7 Median telomere length (T/S ratio) between groups

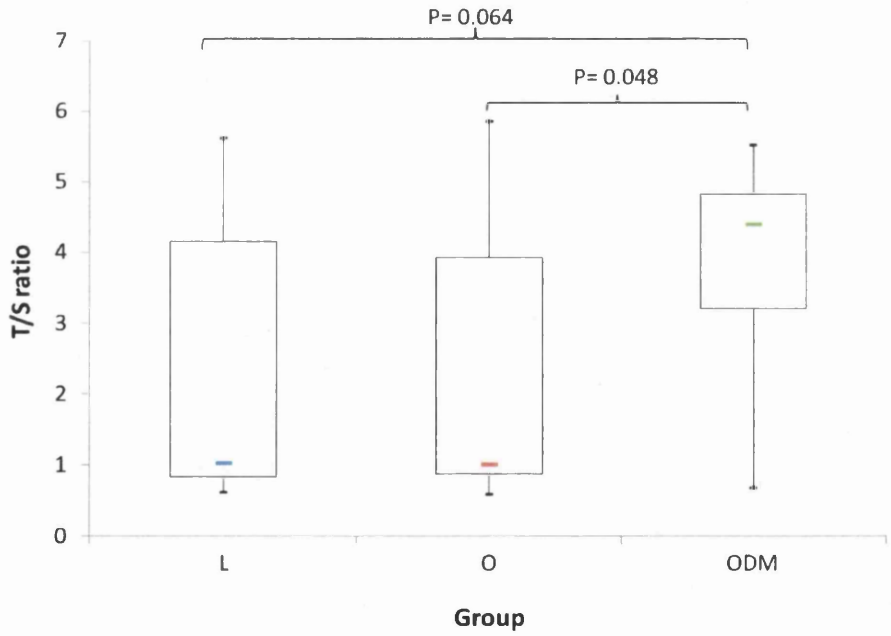

T/S ratios between groups. Median and interquartile range shown. Coloured marker shows median, 'box' shows quartile range and outer markers show minimum and maximum values

Figure 3.8: Median telomere length (T/S ratio) between lean and obese (O+ODM) groups

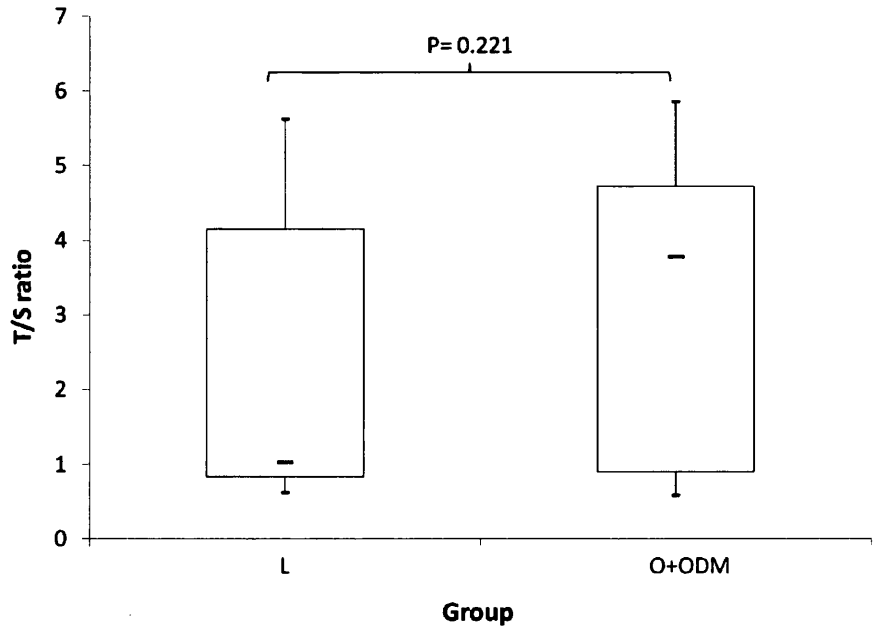

T/S ratio between lean and obese (O+ODM) groups to look at effects of obesity. Median and interquartile range shown. Coloured marker shows median, 'box' shows quartile range and outer markers show minimum and maximum values

Figure 3.9: Median telomere length (T/S ratio) between no-diabetes (L+O) and diabetes groups

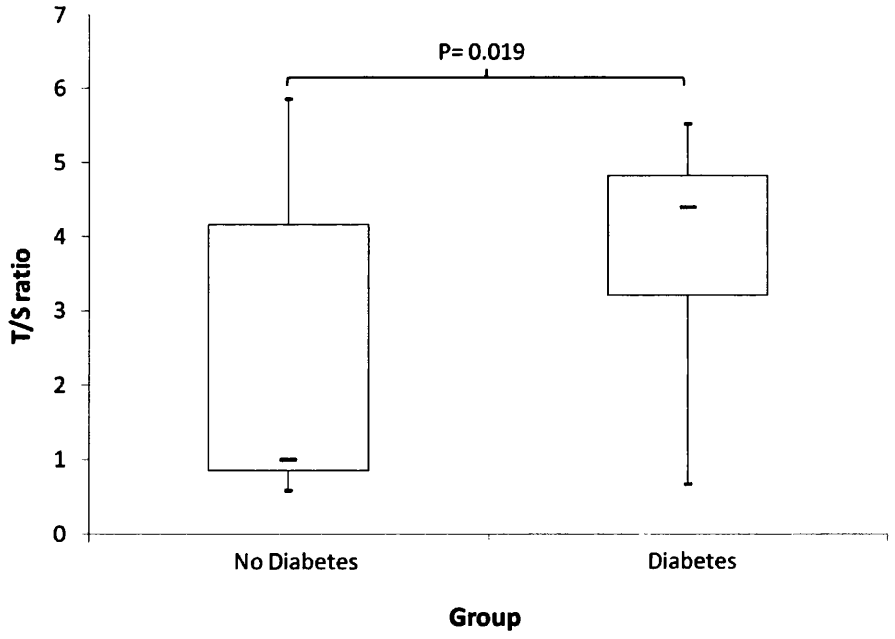

T/S ratio between no-diabetes (L+O) and diabetes groups to look at effect of diabetes between groups. Median and interquartile range shown. Coloured marker shows median, 'box' shows quartile range and outer markers show minimum and maximum values

3.4.3.2 Comet assay

The Comet assay was utilized to calculate several previously described comet parameters (Section 2.3.4, Appendix 4) as a measure of DNA damage in 61 hVAT samples. Examples of comets analysed for each group are shown in Figure 3.10. As shown in Table 3.4, there was no significant difference between the groups for any comet measures. No significant difference in parameters was seen between L and O groups. When comparing O and ODM groups there was a significant difference found in Comet intensity (1.1×10^5 [33403.4] v 1.4×10^5 [38356.4], P=0.023), Head intensity (3.3×10^4 [8276.1] v 3.9×10^4 [11731.0], P=0.048) and Tail intensity (7.9×10^4 [28272.3] v 9.9×10^4 [28799.1], P=0.030).

There was no significant difference observed in comet parameters between the L group and combined O+ODM group so results have not been tabulated. When comparing the non-diabetes subjects to the diabetes groups (L+O v ODM) the Head intensity for ODM group was significantly higher (3.3×10^4 [8856.4] v 3.9×10^4 [11731.0], P=0.033) (Table 3.5).

Figure 3: Examples of comets from each group

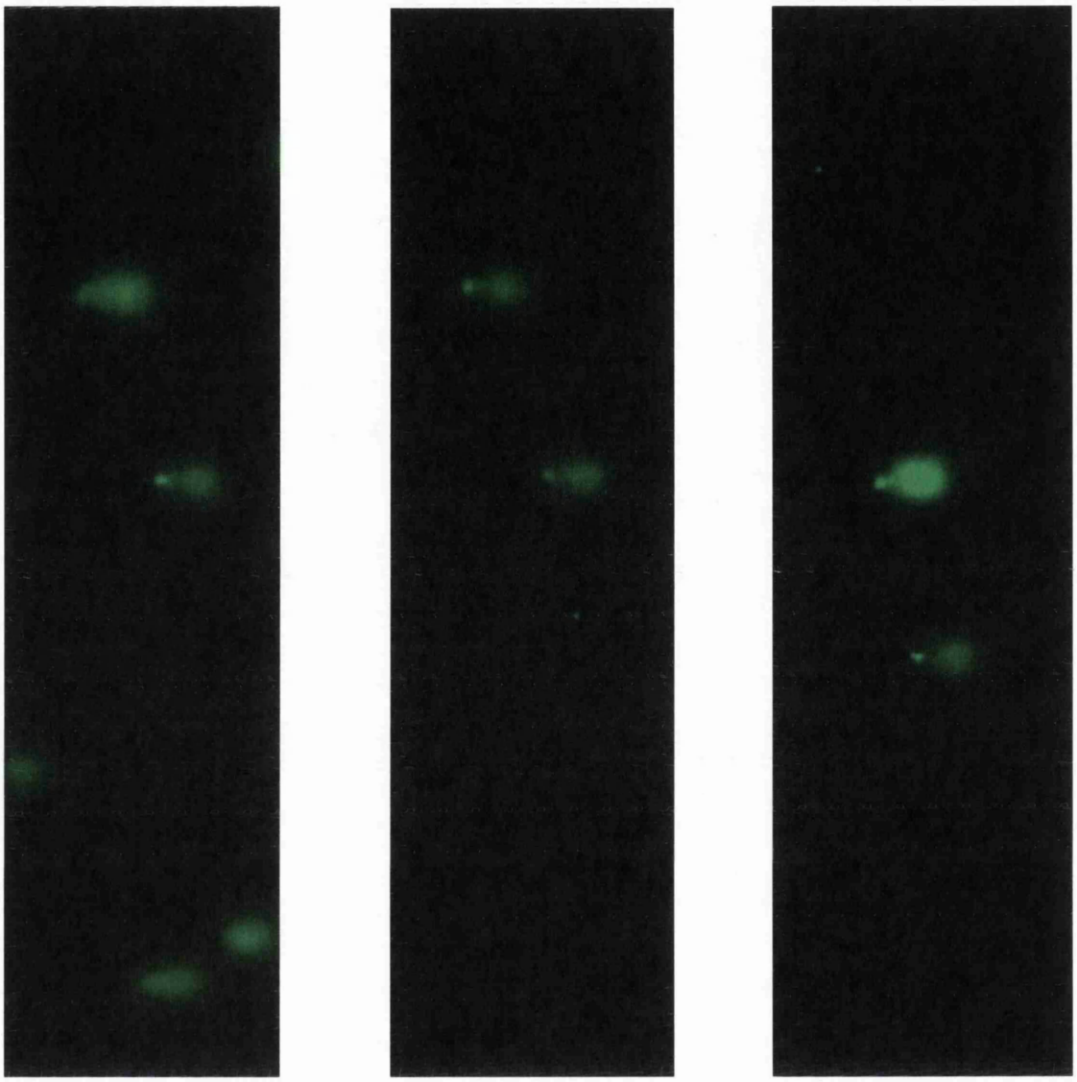

Table 3.4 Comet measures compared between groups

	Lean (n=20)	Obese (n=20)	Obese/T2DM (n=21)	P
Comet length (μm)	77.45 (12.0)	76.99 (8.1)	79.00 (6.9)	0.764
Comet height (μm)	59.88 (5.4)	60.00 (9.5)	62.28 (5.9)	0.476
Comet area (μm^2)	3.7×10^3 (906.6)	3.7×10^3 (805.3)	4.0×10^3 (674.0)	0.418
Comet intensity (cd x 1000)	1.2×10^5 (44980.1)	1.1×10^5 (33403.4)	1.4×10^5 (38356.4)	0.102
Comet mean intensity (cd x 1000)	27.35 (10.1)	26.65 (5.7)	30.39 (7.9)	0.293
Head diameter (μm)	36.81 (4.0)	36.90 (4.8)	38.75 (3.7)	0.245
Head area (μm^2)	2.1×10^3 (639.7)	2.2×10^3 (463.9)	2.3×10^3 (554.7)	0.307
Head intensity (cd x 1000)	3.4×10^4 (9567.3)	3.3×10^4 (8276.1)	3.9×10^4 (11731.0)	0.096
Head mean intensity (cd x 1000)	17.98 (6.2)	15.88 (4.6)	17.18 (4.9)	0.448
Head DNA (%)	30.04 (7.5)	31.25 (8.3)	29.30 (3.8)	0.652
Tail length (μm)	40.65 (10.1)	40.09 (5.7)	40.25 (4.6)	0.969
Tail area (μm^2)	1.6×10^3 (468.3)	1.5×10^3 (445.5)	1.6×10^3 (347.8)	0.746
Tail intensity (cd x 1000)	8.9×10^4 (37579.9)	7.9×10^4 (28272.3)	9.9×10^4 (28799.1)	0.139
Tail mean intensity[#] (cd x 1000)	82.43 [57.5-313.3]	64.43 [53.9-632.7]	77.97 [55.3-150.1]	0.897
Tail DNA (%)	69.96 (7.5)	68.75 (8.3)	70.70 (3.8)	0.652
Tail moment	29.40 (8.6)	28.67 (6.4)	29.20 (3.9)	0.936
Olive moment	16.24 (3.3)	16.09 (2.9)	16.53 (1.9)	0.870

Comet parameters between groups. Mean and standard deviation shown. [#] Data not normalised after log transformation shown as median and interquartile range

Table 3.5 Comet measures between no-diabetes (L+O) and diabetes groups

	Lean+Obese (n=40)	Obese/T2DM (n=21)	P
Comet length (μm)	77.22 (10.1)	79.00 (6.9)	0.472
Comet height (μm)	59.92 (7.6)	62.28 (5.9)	0.221
Comet area (μm^2)	3.7×10^3 (846.46)	4.0×10^3 (674.0)	0.186
Comet intensity (cd x 1000)	1.2×10^5 (39564.7)	1.4×10^5 (38356.4)	0.055
Comet mean intensity (cd x 1000)	27.00 (8.1)	30.39 (7.9)	0.121
Head diameter (μm)	36.85 (4.3)	38.75 (3.7)	0.093
Head area (μm^2)	2.1×10^3 (553.4)	2.3×10^3 (554.7)	0.145
Head intensity (cd x 1000)	3.3×10^4 (8856.4)	3.9×10^4 (11731.0)	**0.033**
Head mean intensity (cd x 1000)	16.93 (5.5)	17.18 (4.9)	0.863
Head DNA (%)	30.64 (7.8)	29.30 (3.8)	0.461
Tail length (μm)	40.37 (8.1)	40.25 (4.6)	0.951
Tail area (μm^2)	1.6×10^3 (452.5)	1.6×10^3 (347.8)	0.565
Tail intensity (cd x 1000)	8.4×10^4 (33252.7)	9.9×10^4 (28799.1)	0.089
Tail mean intensity[#] (cd x 1000)	69.15 [57.4-319.2]	77.97 [55.3-150.1]	0.773
Tail DNA (%)	69.36 (7.8)	70.70 (3.8)	0.461
Tail moment	29.04 (7.5)	29.20 (3.9)	0.927
Olive moment	16.16 (3.1)	16.53 (1.9)	0.616

Comet parameters between non-diabetes (L+O) and diabetes groups to look at the effect of diabetes. Mean and standard deviation shown. [#] Data not normalised after log transformation shown as median and interquartile range

3.5 Discussion

The aim of the work in this chapter was to examine two markers of oxidative stress and two markers of DNA damage in hVAT and examine the differences in samples from L, O and ODM patients. Four different markers were chosen to get an overall understanding of the extent of oxidative burden within this sample set. TAOS was chosen to measure global oxidative stress within the samples and examine any differences in overall antioxidant levels between the three groups. As a measure of oxidative stress-induced lipid peroxidation the TBARS assay was used. DNA damage was measured using two different markers of oxidative damage. Firstly, a measure of telomere length, to observe any damage present at chromosomal level, and a commercial Comet assay to assess DNA fragmentation due to damage such as strand breaks which has been shown to be more common in oxidative stress.

Overall, no differences were observed between groups for both $\Delta ABTS^{+}$ and MDA concentration in the hVAT samples. Sampson *et al* (2002) measured plasma TAOS and F_2-isoprostanes in a sample of patients with T2DM and without T2DM. They observed no significant difference in TAOS between subjects with and without T2DM, but did observe differences in plasma F_2-isoprostanes. This may have been related to the fact that plasma TAOS assay is a less sensitive assay than the F_2-isoprostanes measure. However, more recent studies using the TAOS assay to measure oxidative capacity found that the plasma TAOS assay has good correlations with plasma F_2-isoprostanes and associated with prospective CHD risk (Stephens *et al*, 2006). Previous studies have not examined the measurement of TAOS in tissue homogenates. I chose to examine the use of TAOS in tissue homogenates but as the

assay did not work (see Chapter 2) it was modified to measure $\Delta ABTS^{+}$ formation. As the use of tissue homogenates was experimental in the case of the $\Delta ABTS^{+}$ assay it was to be expected that the results obtained may have been limited. These results were not different between groups. Further work is required to examine the use of total antioxidant measures in tissue homogenates. Although adipose would be suspected to be a site of high oxidative stress it may not necessarily be a site of high antioxidant production.

With respect to TBARS there was no significant change in MDA concentration between groups. A higher MDA concentration was observed in the L group when compared to combined O+ODM group but this was not significant, although a significantly lower MDA concentration was observed in the ODM group compared to the L+O group. This result was not expected, as I would expect to see an increased oxidative state within the ODM group due to the double burden of diabetes and obesity, therefore resulting in increased levels of lipid peroxidation. The paradoxical lower MDA level observed in patients with T2DM compared to the other groups may be a result of acute oxidative cellular damage leading to the initiation of apoptotic and antioxidant pathways. Sturgeon *et al* (2010) found a significantly lower MDA concentration in subjects of a lower aged group when compared to a group of middle-aged to older subjects and an increased concentration in overweight middle-aged to older participants compared to those of a normal weight. This suggests that age, as well as weight, was associated with increased lipid peroxidation in that study. TBARS have not been measured in hVAT previously as they are routinely measured using blood plasma. Another possible

explanation for the results observed for $\Delta ABTS^{+}$ and TBARS may be due to the assays being carried out on hVAT homogenates, which may be low in oxidants/antioxidants compared to other tissue types.

With respect to markers of DNA damage, telomere length (T/S ratio) was four times higher in ODM subjects when compared to L and O groups. A significant difference was seen between O and ODM groups, with the T/S ratio being higher in the ODM group. There was no significant difference when comparing groups by obesity (L v O+ODM), but was four times greater in the diabetes group, when comparing by diabetes status (L+O v ODM). It would have been expected that telomeres would shorten at a quicker rate in conditions of increased oxidative burden, such as diabetes and obesity. The surprisingly higher T/S ratio seen in the group with T2DM suggests that telomere shortening was not a fundamental factor within this population. The paradoxically higher T/S ratio in obese patients with diabetes has not been seen in past studies, for example, Salpea *et* al (2010) found telomere length to be significantly shorter in patients with T2DM compared to controls, but this study was not conducted in patients who were morbidly obese. The lower T/S ratios observed in the L+O group may be due to the significantly higher mean age of this group. Previous studies have shown that telomere length shortens with age (Houben *et al,* 2008; Astrup *et al*, 2010). The difficulty in comparing these studies is that historically telomere length is measured in leukocyte DNA, whereas the experimental use of hVAT DNA may not show the same relationship between telomere senescence and diabetes, primarily due to cell turnaround time and antioxidant capacity. The novel part of this study was the use of hVAT in this

otherwise commonly used method. A study by Friedrich and colleagues (2000) looked at telomere length in different tissue types including leukocytes, skin and synovial tissue. The results determined that overall telomere length differs between tissue types dependent on the proliferation rates of the tissue, although, when comparing two types of tissue from one donor there is linear correlation between the two. This suggests that the rate at which a telomere shortens is tissue independent as far as genetically determined regulation was considered. So the measurement of telomere length in one tissue may be used as a determinant of relative telomere length in other tissues from the same individual. The results in this chapter may also be due to sample size as numbers in this sample set are far lower compared to past studies, which may account for the difference in results (Salpea *et al*, 2010).

There was a significant difference found in Comet intensity, head intensity and tail intensity in the ODM group. This suggests a greater overall DNA content detected within the cells although not necessarily high percentage of reported DNA damage as a high amount of DNA remained within the nucleus of the cells. There was no significant difference observed between the L and O+ODM groups. The head intensity for diabetes group was significantly higher than the group with no diabetes. This suggests a lower amount of damaged DNA fragments migrating from the nucleus, which is what would be expected in the samples with diabetes and therefore, expected to have increased oxidative stress. In previous studies, comet assay results are described using the parameters 'Tail moment' and 'Olive moment', which are calculated as described in Chapter 2 (Section 2.3.4). Neither of these

measures proved significant showing no overall difference in DNA damage between the groups.

Previous studies looking at DNA damage in lymphocytes of patients with T2DM found that levels of basal endogenous and oxidative DNA damage using a measure of mean tail DNA were significantly higher compared to patients without T2DM (Blasiak et al, 2004). Their results agree with other studies showing an increased extent of DNA damage in peripheral blood lymphocytes in patients with diabetes (Collins *et al*, 1998; Dincer *et al*, 2002a; Rehman *et al*, 2004). However, similar to my results, some studies show no association between diabetes and increased DNA damage (Anderson *et al*, 1998).

Thakkar and Jain (2010) describe the use of the Comet assay to visualise the extent of active cell death or apoptosis within the cells. They found that cells undergoing apoptosis show particularly high levels of fragmented DNA in each cell due to the increased formation of double strand breaks. This results in a very small percentage of DNA remaining within the 'head' of the comet. With respect to my results taking this into account, it may show that the cells from the ODM samples are undergoing a higher rate of apoptosis. My results showed, though not significant, a lower percentage of DNA in the head and a higher percentage DNA in the tail of cells from the ODM samples compared to samples in the L and O groups. This may suggest that the cells have reached a threshold of oxidative stress that can no longer be recovered and have therefore initiated programmed cell death or apoptosis.

It has been considered that age of onset of T2DM may play a role in the subject's susceptibility to DNA damage and impairment of repair mechanisms (Blasiak, 2004), with subjects over the age of 50 often having co-existing pathophysiological conditions that may contribute to further impairment of DNA repair pathways. Previous studies have also highlighted the importance of glycaemic control and its role in DNA damage and repair (Collins *et al*, 1998; Dincer *et al*, 2002; Blasiak *et al*, 2004). Within this sample set there were significantly higher blood glucose levels in the ODM group, which suggests that due to poor glycaemic control these subjects should, in fact, show a higher level of DNA damage. This, however, was not observed. There may be other confounding factors such as an individual's medication, as statins (particularly Simvastatin) for example, have been found to have protective properties against oxidative stress induced DNA damage in patients with T2DM (Manfredini *et al,* 2010; Shin *et al*, 2005). A significantly higher percentage of the subjects in the ODM group were receiving statin treatment, which may explain the protective effect against oxidative stress observed in this chapter.

Overall, previous studies showed a higher level of oxidative DNA damage in patients with T2DM compared to those without (Lodovici *et al,* 2008; Collins *et al*, 1998). There is an association between increased levels of oxidative damage products and the development of further complications in patients with diabetes (Collins *et al,* 1998; Dincer *et al,* 2002). As with telomere senescence, the level of DNA damage is expected to be increased in older patients. Kushwaha *et al* (2011) found that there was an increased background level of DNA damage in rats over time, which is

supported by other studies by Hamilton *et al* (2001) and Fraga *et al* (1990). In these studies the products of DNA damage showed increased levels in rodent tissue and were found to be strongly correlated to the age of the specimens. This age related DNA damage was considered to be accumulated due to a combination of increased oxidative stress and a lower level of DNA repair over time.

Previous studies in this area were carried out using plasma leukocytes and not AT. It may be that the defining reason for the lack of conclusive results is due to the use of hVAT instead of leukocytes.

There were limitations and problems encountered with the experiments within this chapter. Firstly, my studies were conducted in hVAT as no blood was collected for parallel studies in plasma, as the original focus was on fat. This would have been useful to determine if the results gathered in this work are a reliable representation of the samples' oxidative burden or, in fact, restricted by the use of hVAT instead of leukocytes. Secondly, the in-house Comet assay could not be successfully optimised so a commercial kit was used in its place. Finally, from the outset, the work in hVAT homogenates was novel, with a lack of reports in the scientific literature on the methods employed. This makes the outcome of this work important as careful consideration is required for future work in this area.

When the results from these four assays are combined it is possible to get an overall view of the level of oxidative damage in the hVAT of this population. To analyse oxidative stress at a global level $\Delta ABTS^{+}$ and TBARS were used as markers resulting

in no significant difference between the groups suggesting that T2DM was not associated with an environment of high oxidative stress within these samples. To follow on from this, the samples were analysed at a chromosomal/DNA level using telomere length and Comet as measures of DNA damage, again showing no significant differences to suggest that DNA damage was the trigger factor for T2DM in these subjects.

According to previous literature I expected to see a progressive increase in oxidative stress in the O and ODM subjects examined here. This, however, was not seen. Instead a protective effect was seen in the ODM subjects with lower levels of lipid peroxidation and less DNA damage observed. There may be changes in gene expression levels in antioxidant genes within the AT that may result in a protective effect against oxidative stress. In order to examine this, gene expression studies were carried out focusing on genes involved in oxidative stress and inflammation to determine any changes may explain the results seen in the chapter.

CHAPTER 4

GENE EXPRESSION DIFFERENCES IN OBESITY AND DIABETES

4.1 Introduction

Changes in DNA, such as base alterations, can affect an individual's risk of disease or response to medication. DNA alterations not only are observed within the actual DNA sequence in the form of mutations or polymorphisms, but also can occur as an alteration in levels of gene expression. A study by Apelt and colleagues (2009) showed that differences in gene expression may have wider reaching knock-on effects on the expression and activity of other biochemical molecules and influence the overall function of a physiological process. Their investigations focused on the expression of erythrocyte acid phosphatase (*ACP1*), a cell cycle regulation factor, and the resulting biological effects on glutathione reductase (GSR) activity, finding that increased expression of *ACP1* had a significant negative effect on GSR activity. This decreased GSR activity was found to be associated with hypertension, especially in patients with T2DM (Apelt *et al,* 2009).

In this chapter the focus is on gene expression levels in hVAT samples in obesity and T2DM. The previous chapter showed a surprisingly low level of oxidative stress in subjects with T2DM. It may be hypothesised that a difference in gene expression of antioxidant genes in defence against the high level of oxidation was observed in these samples, therefore, reducing the overall oxidative burden. In order to examine this, a gene expression study was carried out focusing particularly on genes involved in oxidative stress pathways in AT, in an attempt to determine any differences that may occur between obesity and T2DM. A similar study was carried out in mice by Nadler and colleagues (2000) looking at a high number of gene transcripts in adipose tissue from lean, obese and obese mice with diabetes. They

identified differences in expression of genes involved in adipocyte differentiation in obese mice and genes involved in signal transduction and energy transduction in mice with varying degrees of hyperglycaemia. The study utilised DNA microarrays, which analyse high numbers of gene transcripts simultaneously. An alternative method of gene expression analysis is RT-PCR, which allows the examination of selected candidate genes of interest using specific primers. To satisfy the requirement in this part of the study the use of DNA microarrays is too large scale and too high in cost. Therefore the use of RT-PCR arrays was chosen as the most suitable method of analysis, both in terms of scale and price.

RT-PCR arrays allow the gene expression profiles of 84 genes to be analysed in a sample simultaneously, including built in quality control measures. Arrays may be designed to look at particular individual genes of interest, although to get a general overview of any changes that may be occurring in particular pathways, for example those involved in oxidative stress, commercially available arrays are designed with a focused panel of genes from each area of scientific interest. As mentioned, in this chapter the focus was on oxidative stress so a PCR array containing a panel of genes involved in oxidative stress and antioxidant defence was used. This panel includes genes involved in ROS metabolism, such as superoxide dismutase (*SOD*) and NADPH oxidase (*NOX*); oxidative response genes, such as glutathione peroxidase (*GPX*) and apolipoprotein E (*APOE*); and antioxidant genes, including *GPX* genes and catalase (*CAT*).

Previous studies have found oxidative stress-induced gene expression changes in obesity and T2DM. Peroxiredoxin (PRDX), an antioxidant which is highly expressed in AT, was found to have significantly reduced expression within obese mice and in human subjects with a BMI>25 (Huh *et al*, 2012). According to Sadi and colleagues (2009), rats with induced diabetes displayed decreased expression in SOD and CAT but showed no difference in GPX expression (Sadi *et al*, 2009).

4.2 Aim

The purpose of the work described in this chapter was to examine the expression profiles of 84 genes involved in pathways of oxidative stress in 30 hVAT samples using commercially available PCR arrays and examine any gene expression differences seen between samples classified as L, O and ODM. It was hypothesised that genes involved in defence against oxidative stress would show increased expression in the samples with increased oxidative stress. In the previous chapter, results from the complete sample population showed that oxidative stress markers were increased in the O group and then significantly decreased in the ODM group. For this reason, genes involved in antioxidant pathways are expected to show differing expression accordingly, although a smaller sample set is studied in this chapter.

4.3 Methods

4.3.1 PCR array

PCR array data were collected for 30 samples chosen from consecutive patients undergoing surgery, with blinding as to the nature of the samples (L/O/ODM:

11/9/10). RNA was extracted from the hVAT as previously described (Section 2.2.1) and reverse transcribed to cDNA (Section 2.4). Using the SABiosciences Human Oxidative Stress and Antioxidant Defense RT^2 Profiler PCR Array (Section 2.4), the expression profile of 84 genes (detailed in Figure 2.3) related to oxidative stress including peroxidises, peroxiredoxins, genes involved in ROS metabolism and superoxide metabolism were analysed. The 96 well plates included 5 housekeeping genes, plus integrated controls for genomic DNA contamination, RNA quality and PCR performance for quality control of the arrays. cDNA samples were combined with the provided RT-PCR master mix, aliquoted into the PCR arrays and run on a Biorad MyIQ thermocycler.

4.3.2 Data analysis

Analysis of the array data was carried out using the specific online program (www.SABiosciences.com/pcrarraydataanalysis.php). The program utilises the $2^{-\Delta\Delta CT}$ quantification method to calculate the level of gene expression change in the samples. The formula to calculate this was:

$$X=2^{-\Delta\Delta CT}$$

Where in this study:

X = Fold change in gene expression

$\mathbf{\Delta\Delta C_T}$ = $\Delta C_{T\,(\text{sample group})} - \Delta C_{T\,(\text{Control sample group})}$

$\mathbf{\Delta C_T}$ = $C_{T(\text{test sample})} - C_{T\,(\text{Internal housekeeping gene})}$

When comparing groups of samples mean C_T values were used. The software shows differences in fold change between the groups in different visual formats allowing identification of up or down regulated genes. Any genes with a fold-change of more than 2-fold, as described by manufacturer, were flagged to be further investigated and any genes that differed between groups $P<0.05$ were considered significant.

4.4 Results

4.4.1 Baseline characteristics

4.4.1.1 L v O v ODM

hVAT samples from 30 subjects, which were grouped as L, O and ODM, were selected while blinded to their classification (L/O/ODM: 11/9/10). Baseline characteristics of subjects were analysed for differences between groups as this sample set differed from the previous chapter. As shown in Table 4.1, the only significant differences between the groups were understandably weight and BMI, with both being significantly higher in the ODM group ($P<0.001$ for both weight and BMI); and hypertension, which was significantly higher in the ODM group compared to others ($P=0.033$).

Table 4.1 Baseline characteristics compared between groups

	Lean (n=11)	Obese (n=9)	Obese/T2DM (n=10)	P
Age (years)	54.8 (17.9)	52.3 (9.0)	42.6 (11.4)	0.120
Weight (kg)	71.0 (13.6)	108.7 (30.8)	144.2 (28.2)	**<0.001**
BMI (kg/m^2)	25 (2.2)	37 (9.0)	51 (12.3)	**<0.001**
SBP (mmHg)	138 (26.1)	130 (17.9)	142 (18.0)	0.455
DBP (mmHg)	81 (14.4)	81 (11.0)	76 (9.7)	0.558
Glucose (mmol/L)*	5.2 (0.3)	6.1 (0.4)	8.7 (1.8)	0.058
Cholesterol (mmol/L)	5.9 (1.8)	5.7 (2.4)	5.2 (1.2)	0.761
HDL-C (mmol/L)	1.5 (0.4)	1.0 (0.2)	1.1 (0.2)	0.082
LDL-C (mmol/L)	3.9 (1.5)	3.8 (2.1)	2.9 (0.8)	0.419
Triglycerides (mmol/L)	1.3 (0.2)	2.1 (0.5)	2.6 (1.5)	0.437
Creatinine (µmol/L)	76.8 (20.6)	79.5 (9.4)	68.9 (18.2)	0.401
Albumin (mmol/L)	47.9 (10.8	42.8 (2.9)	41.4 (5.6)	0.166
RNA (ng/µl)	93.8 (60.3)	73.0 (38.5)	59.2 (46.2)	0.294
Males % (n)	45.5 (5)	44.4 (4)	40.0 (4)	0.966
Current smoker % (n)	36.4 (4)	33.3 (3)	20.0 (2)	0.682
Hypertension % (n)	9.1 (1)	22.2 (2)	60.0 (6)	**0.033**
OSA % (n)	0 (0)	11.1 (1)	30.0 (3)	0.127
Statins % (n)	9.1 (1)	11.1 (1)	50.0 (5)	0.050
ACE inhibitor % (n)	27.3 (3)	11.1 (1)	50.0 (5)	0.176

Baseline characteristics of hVAT samples in L, O and ODM groups. *Log transformed data. Mean and standard deviation shown or geometric mean and approximate standard deviation for log transformed data. Analysis performed by ANOVA after appropriate transformation. χ^2-test was used to compare groups. P-value shows significance where P<0.05

4.4.1.2 L v O+ODM

Prior to analysis, I chose to examine baseline characteristics between L v O+ODM to look at the effects of obesity between groups. Results are detailed in Table 4.2. Weight and BMI were significantly different between groups (P=<0.001 for both). Although not significant, glucose levels were higher in the O+ODM subjects, whilst HDL-C levels were significantly higher in L group compared to O+ODM (P=0.040). There were higher percentages of subjects with hypertension and OSA in the O+ODM group, although the prevalence for both was not significant. Although there were more patients in the O+ODM group on statin and ACE inhibitor treatment, the percentage difference was not significant.

4.4.1.3 L+O v ODM

I chose to examine baseline characteristics between L+O v ODM to look at the effects of non-diabetes (n=20) and diabetes (n=10), results are shown in Table 4.3. Age, weight and BMI were significantly different between groups (P=0.042, P<0.001 and P<0.001 respectively). Blood glucose was significantly higher in subjects with diabetes (P=0.020). There were a higher proportion of males in the non-diabetes group, though not significant. The co-morbidities hypertension and OSA were more prevalent in the subjects with diabetes, with hypertension being significant (P=0.011); and more subjects in the diabetes group were on statin and ACE inhibitor treatment, with statin use being significant (P=0.015).

Table 4.2 Baseline characteristics between lean and obese groups (O+ODM)

	Lean (n=11)	Obese + Obese T2DM (n=19)	P
Age (years)	54.8 (17.9)	47.2 (11.2)	0.161
Weight (kg)	71.0 (13.6)	127.4 (33.9)	**<0.001**
BMI (kg/m^2)	25 (2.2)	45 (12.8)	**<0.001**
SBP (mmHg)	138 (26.1)	136 (18.5)	0.836
DBP (mmHg)	81 (14.4)	78 (10.4)	0.611
Glucose (mmol/L)*	5.2 (0.3)	7.7 (1.4)	0.066
Cholesterol (mmol/L)	5.9 (1.8)	5.3 (1.5)	0.614
HDL-C (mmol/L)	1.5 (0.4)	1.1 (0.2)	**0.040**
LDL-C (mmol/L)	3.9 (1.5)	3.1 (1.3)	0.472
Triglycerides (mmol/L)	1.3 (0.2)	2.5 (1.3)	0.226
Creatinine (µmol/L)	76.8 (20.6)	73.6 (15.5)	0.637
Albumin (mmol/L)	47.9 (10.8)	41.9 (4.7)	0.060
RNA (ng/µl)	93.8 (60.3)	65.7 (42.2)	0.145
Males % (n)	45.5 (5)	42.1 (8)	0.858
Current smoker % (n)	36.4 (4)	26.3 (5)	0.789
Hypertension % (n)	9.1 (1)	42.1 (8)	0.057
OSA % (n)	0 (0)	21.1 (4)	0.102
Statins % (n)	9.1 (1)	31.6 (6)	0.161
ACE inhibitor % (n)	27.3 (3)	31.6 (6)	0.804

Baseline characteristics between lean and obese (O+ODM) groups to look at effects of obesity between groups. *Log transformed data. Mean and standard deviation shown or geometric mean and approximate standard deviation for log transformed data. Analysis performed by ANOVA after appropriate transformation. χ^2-test was used to compare groups. P-value shows significance where $P<0.05$

Table 4.3 Baseline characteristics between non-diabetes (L+O) and diabetes groups

	No Diabetes (n=20)	Diabetes (n=10)	P
Age (years)	53.7 (14.3)	42.6 (11.4)	**0.042**
Weight (kg)	88.0 (29.5)	144.2 (28.2)	**<0.001**
BMI (kg/m^2)	30 (8.9)	51 (12.3)	**<0.001**
SBP (mmHg)	135 (22.6)	142 (18.0)	0.350
DBP (mmHg)	81 (12.6)	76 (9.7)	0.277
Glucose (mmol/L)*	5.6 (0.4)	8.7 (1.8)	**0.020**
Cholesterol (mmol/L)	5.8 (1.9)	5.2 (1.2)	0.456
HDL-C (mmol/L)	1.2 (0.3)	1.1 (0.2)	0.737
LDL-C (mmol/L)	3.8 (1.7)	2.9 (0.8)	0.176
Triglycerides (mmol/L)	1.8 (0.6)	2.6 (1.5)	0.283
Creatinine (µmol/L)	77.9 (16.5)	68.9 (18.2)	0.186
Albumin (mmol/L)	46.1 (9.0)	41.4 (5.6)	0.150
RNA (ng/µl)	84.4 (51.5)	59.2 (46.2)	0.201
Males % (n)	45.0 (9)	40.0 (4)	0.794
Current smoker % (n)	35.0 (7)	20.0 (2)	0.682
Hypertension % (n)	15.0 (3)	60.0 (6)	**0.011**
OSA % (n)	5.0 (1)	30.0 (3)	0.058
Statins % (n)	10.0 (2)	50.0 (5)	**0.015**
ACE inhibitor % (n)	20.0 (4)	50.0 (5)	0.091

Baseline characteristics between non-diabetes (L+O) and diabetes groups to look at the effect of diabetes between groups *Log transformed data. Mean and standard deviation shown or geometric mean and approximate standard deviation for log transformed data. Analysis performed by ANOVA after appropriate transformation. χ^2-test was used to compare groups. P-value shows significance where P<0.05

4.4.2 PCR arrays

hVAT samples were assayed using the SABiosciences Human Oxidative Stress and Antioxidant Defense RT^2 Profiler PCR Array. Gene expression fold changes for 84 genes between groups, compared to control (L) were assessed (Appendix 4).

4.4.2.1 L v O

The scatter graph in Figure 4.1 shows the fold change in gene expression between controls (L) and O subjects. Each marker symbolises a gene from the array and the genes that lay outside of the 2-fold change boundary are labelled red for increased and green for decreased expression levels. There were two genes that had an increased expression by more than 2-fold; glutathione peroxidase 1 (*GPx1*) and glutathione reductase (*GSR*). Only *GSR* was found to be have a significant difference in expression between L and O subjects of +2.15 (P=0.026). Fold change values for genes found to show increased/decreased expression (according to the adopted 2-fold cut-off) are shown in Table 4.4.

Figure 4.1 Difference in gene expression between lean and obese groups

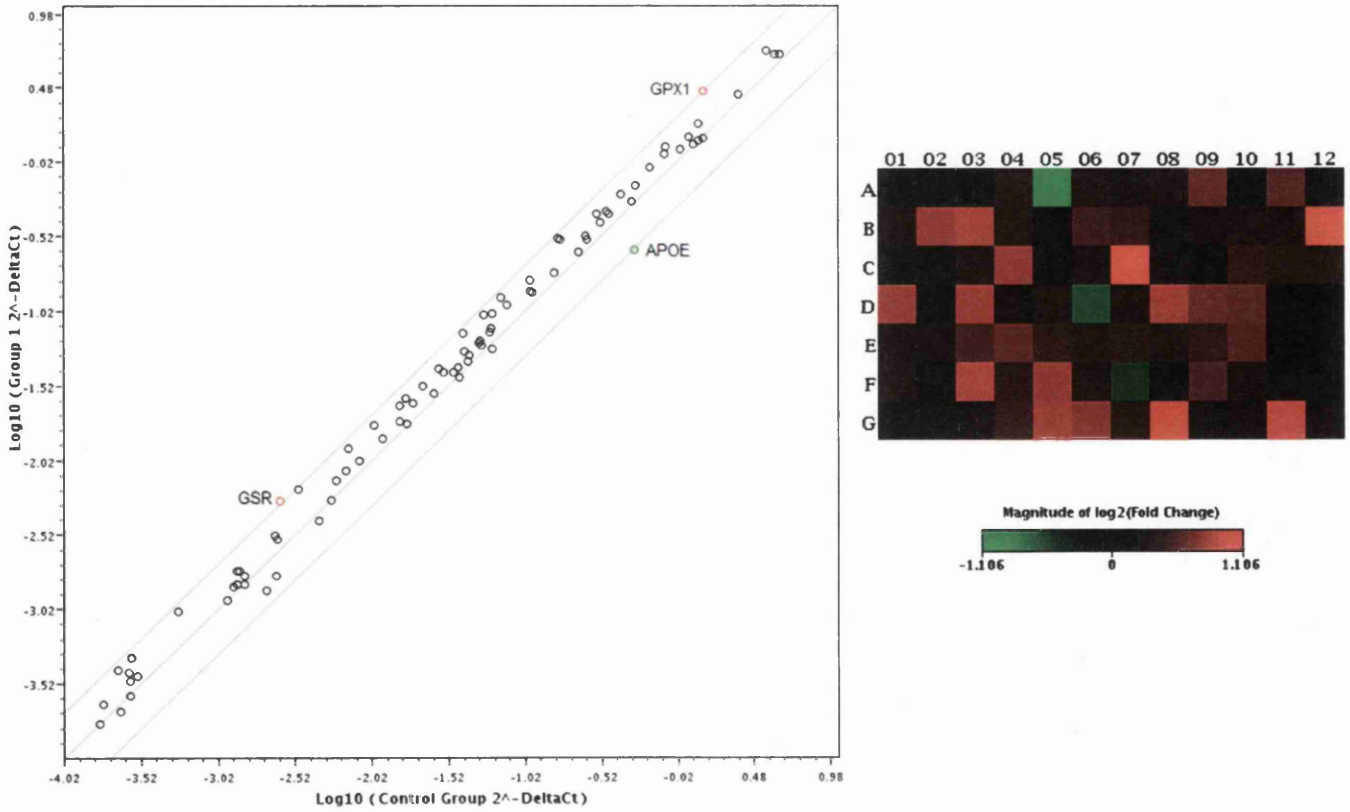

Scatter graph showing gene expression results, where control group is L and group 1 is O. Each marker denotes a gene and band lines define 2-fold change boundary. Heat map represents 96 well array plate, where red pixels show increased and green show decreased expression of genes

Table 4.4 Fold change difference in obese groups compared to lean

Position	Symbol	Name	Fold Change (95%CI)	P
A05	APOE	Apolipoprotein E	0.4976 (0.09, 0.90)	0.23
B12	GPX1	Glutathione peroxidase 1	2.0383 (0.69, 3.38)	0.16
C07	GSR	Glutathione reductase	2.1519 (1.09, 3.21)	**0.03**

Fold change gene expression in O subjects compared to control (L). Red shows genes with increased expression and green shows genes with decreased expression. P-value shows significance where P<0.05

4.4.2.2 L v ODM

The scatter graph in Figure 4.2 shows the fold change gene expression between controls (L) and ODM subjects. There were 15 genes with increased expression in ODM compared to L, including 2 genes from the glutathione peroxidase family, *GSR* and keratin 1 (*KRT1*). Genes with decreased expression were albumin (*ALB*), *APOE* and cytochrome A alpha polypeptide (*CYBA*). *GSR* showed significantly increased expression in the ODM subjects, with a fold-change of +2.56 (P=0.021). Fold change values for genes found to show increased/decreased expression (according to the adopted 2-fold cut-off) are shown in Table 4.5.

Figure 4.2 Difference in gene expression between lean and obese T2DM groups

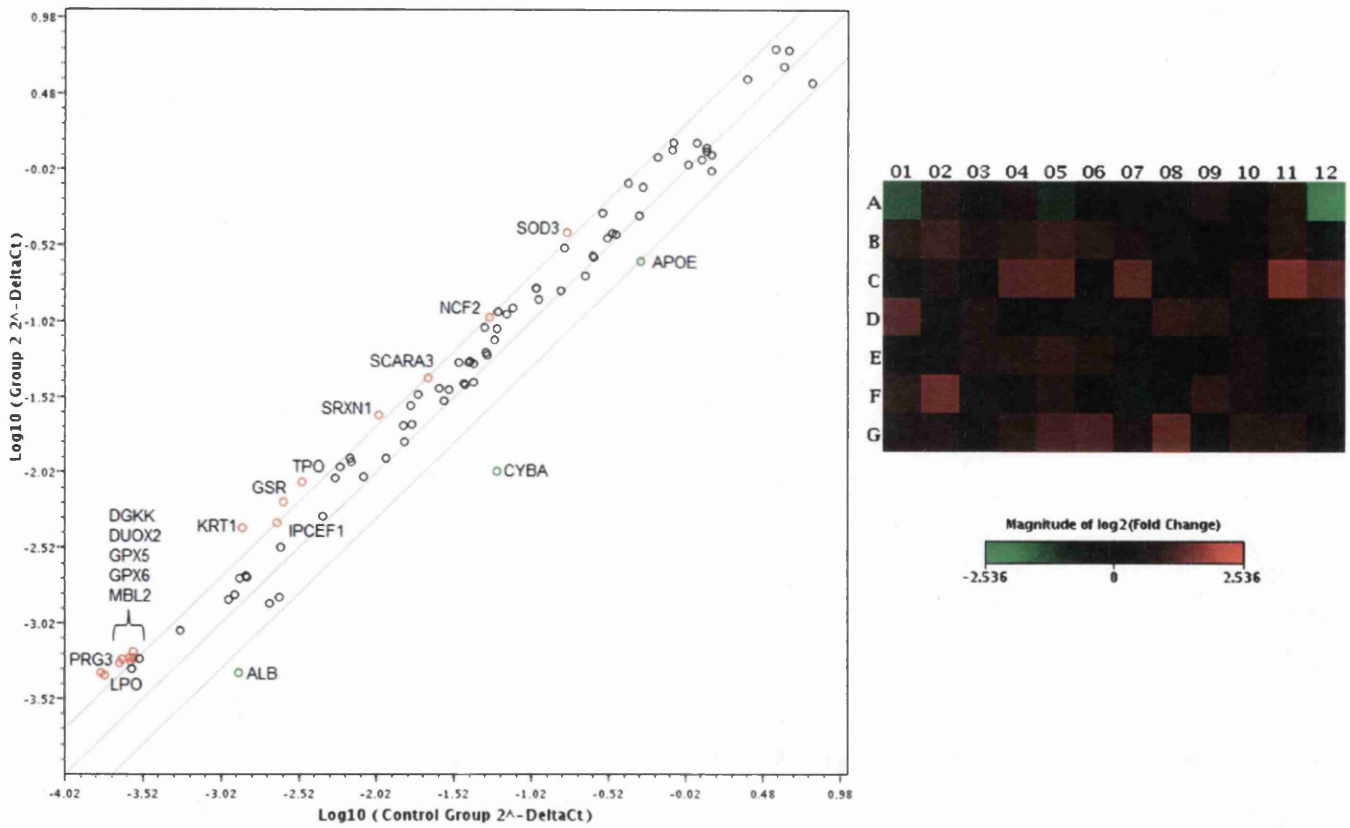

Scatter graph showing gene expression, where control group is L and group 2 is ODM. Each marker denotes a gene and band lines define 2-fold change boundary. Heat map represents 96 well array plate, where red pixels show increased and green show decreased expression of genes

Table 4.5 **Fold change difference in obese T2DM group compared to lean group**

Position	Symbol	Name	Fold Change (95%CI)	P
A01	ALB	Albumin	0.3617 (0.04, 0.68)	0.40
A05	APOE	Apolipoprotein E	0.4933 (0.15, 0.83)	0.13
A12	CYBA	Cytochrome b-245, alpha polypeptide	0.1724 (0.00001, 0.69)	0.99
B02	DGKK	Diacylglycerol kinase, kappa	2.1521 (0.60, 3.70)	0.25
B05	DUOX2	Dual oxidase 2	2.1072 (0.19, 4.03)	0.27
C04	GPX5	Glutathione peroxidase 5 (epididymal androgen-related protein)	2.4415 (0.37, 4.51)	0.25
C05	GPX6	Glutathione peroxidase 6 (olfactory)	2.4817 (0.32, 4.64)	0.19
C07	GSR	Glutathione reductase	2.5617 (1.18, 3.94)	**0.02**
C11	KRT1	Keratin 1	3.1587 (0.08, 6.24)	0.05
C12	LPO	Lactoperoxidase	2.5321 (0.00001, 5.17)	0.31
D01	MBL2	Mannose-binding lectin (protein C) 2, soluble	2.4117 (0.11, 4.71)	0.46
D08	NCF1	Neutrophil cytosolic factor 1	2.0089 (0.77, 3.24)	0.16
E05	IPCEF1	Interaction protein for cytohesin exchange factors 1	2.0201 (0.61, 3.43)	0.22
F02	PRG3	Proteoglycan 3	2.763 (0.07, 5.45)	0.27
F09	SCARA3	Scavenger receptor class A, member 3	2.0141 (0.61, 3.41)	0.15
G05	SOD3	Superoxide dismutase 3, extracellular	2.267 (0.53, 4.00)	0.14
G06	SRXN1	Sulfiredoxin 1	2.3422 (0.61, 4.08)	0.13
G08	TPO	Thyroid peroxidase	2.6356 (0.82, 4.45)	0.06

Fold change gene expression in ODM subjects compared to control (L). Red shows genes with increased expression and green shows genes with decreased expression. P-value shows significance where P<0.05

4.4.2.3 O v ODM

The scatter graph in Figure 4.3 shows the fold change gene expression between controls (O) and ODM subjects. Four genes showed increased expression; *DUOX2, GPX6, KRT1* and proteoglycan 3 (*PRG3*), whilst decreased expression was seen in *ALB, CYBA* and *GPX1*, although none of the changes were significant. Fold change values for genes found to show increased/decreased expression (according to the adopted 2-fold cut-off) are shown in Table 4.6.

Figure 4.3 Difference in gene expression between obese and obese T2DM groups

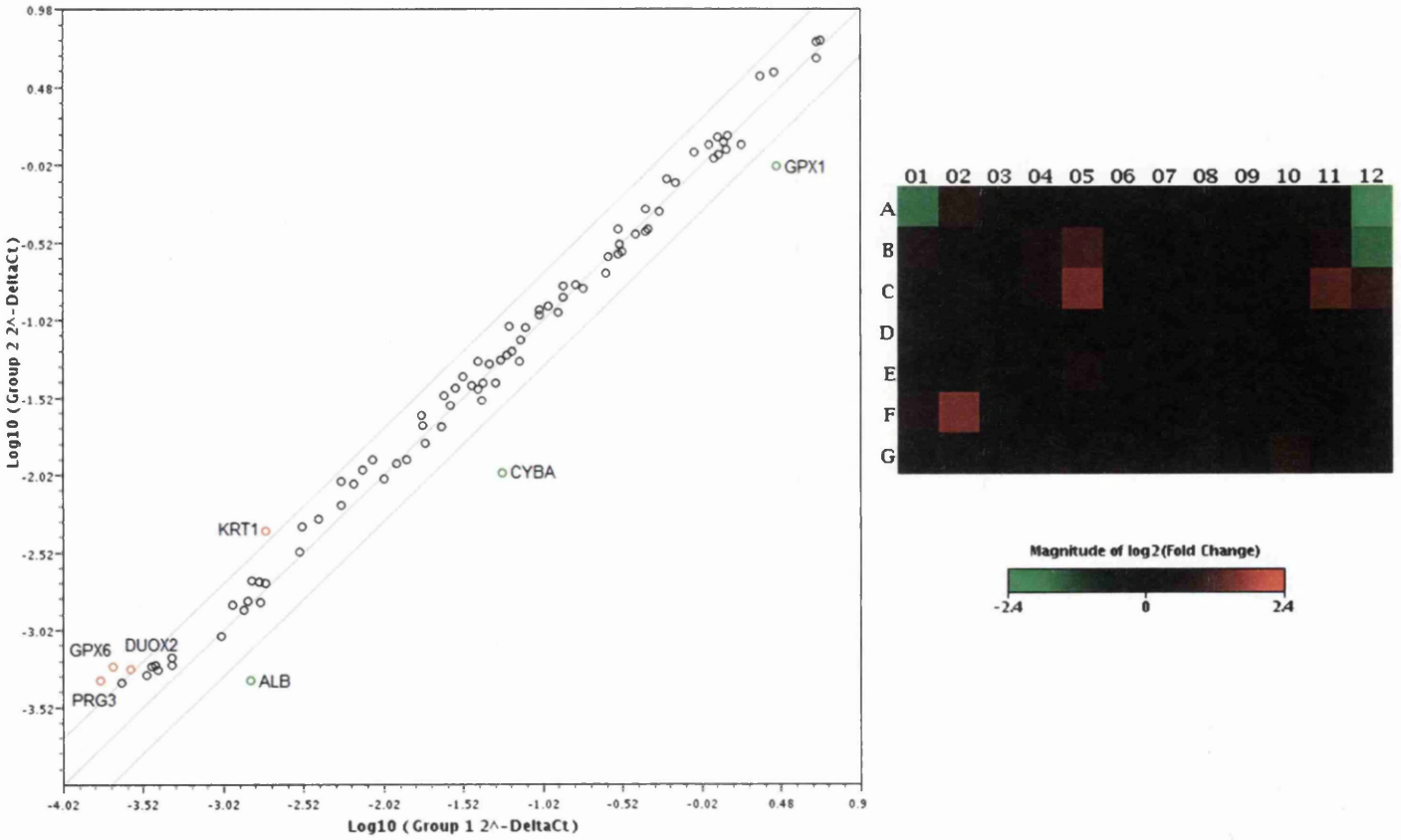

Scatter graph showing gene expression, where group 1 is O and group 2 is ODM. Each marker denotes a gene and band lines define 2-fold change boundary. Heat map represents 96 well array plate, where red pixels show increased and green show decreased expression of genes

Table 4.6 Fold change difference in obese T2DM compared to obese group

Position	Symbol	Name	Fold Change (95% CI)	P
A01	ALB	Albumin	0.32 (0.00001, 0.64)	0.21
A12	CYBA	Cytochrome b-245, alpha polypeptide	0.19 (0.00001, 0.81)	0.62
B05	DUOX2	Dual oxidase 2	2.17 (0.48, 3.86)	0.21
B12	GPX1	Glutathione peroxidase 1	0.33 (0.00001, 0.97)	0.74
C05	GPX6	Glutathione peroxidase 6 (olfactory)	2.85 (0.00001, 5.87	0.21
C11	KRT1	Keratin 1	2.41 (0.00001, 6.19)	0.73
F02	PRG3	Proteoglycan 3	2.81 (0.00001, 5.77)	0.30

Fold change gene expression in O subjects compared to ODM. Red shows genes with increased expression and green shows genes with decreased expression. P-value shows significance where $P<0.05$

4.4.2.4 L v O+ODM

The scatter graph in Figure 4.4 shows the fold change gene expression between controls (L) and O+ODM subjects to look at the effects of obesity. Six genes showed increased expression including *KRT1*, thyroid peroxidase (*TPO*) and *SOD3*, while *CYBA* and *APOE* had decreased expression. The *GSR* gene in particular showed a significant increase in expression of +2.36 (P=0.02). Fold change values for genes found to show increased/decreased expression (according to the adopted 2-fold cut-off) are shown in Table 4.7.

Figure 4.4 Difference in gene expression between lean and obese (O+ODM) groups

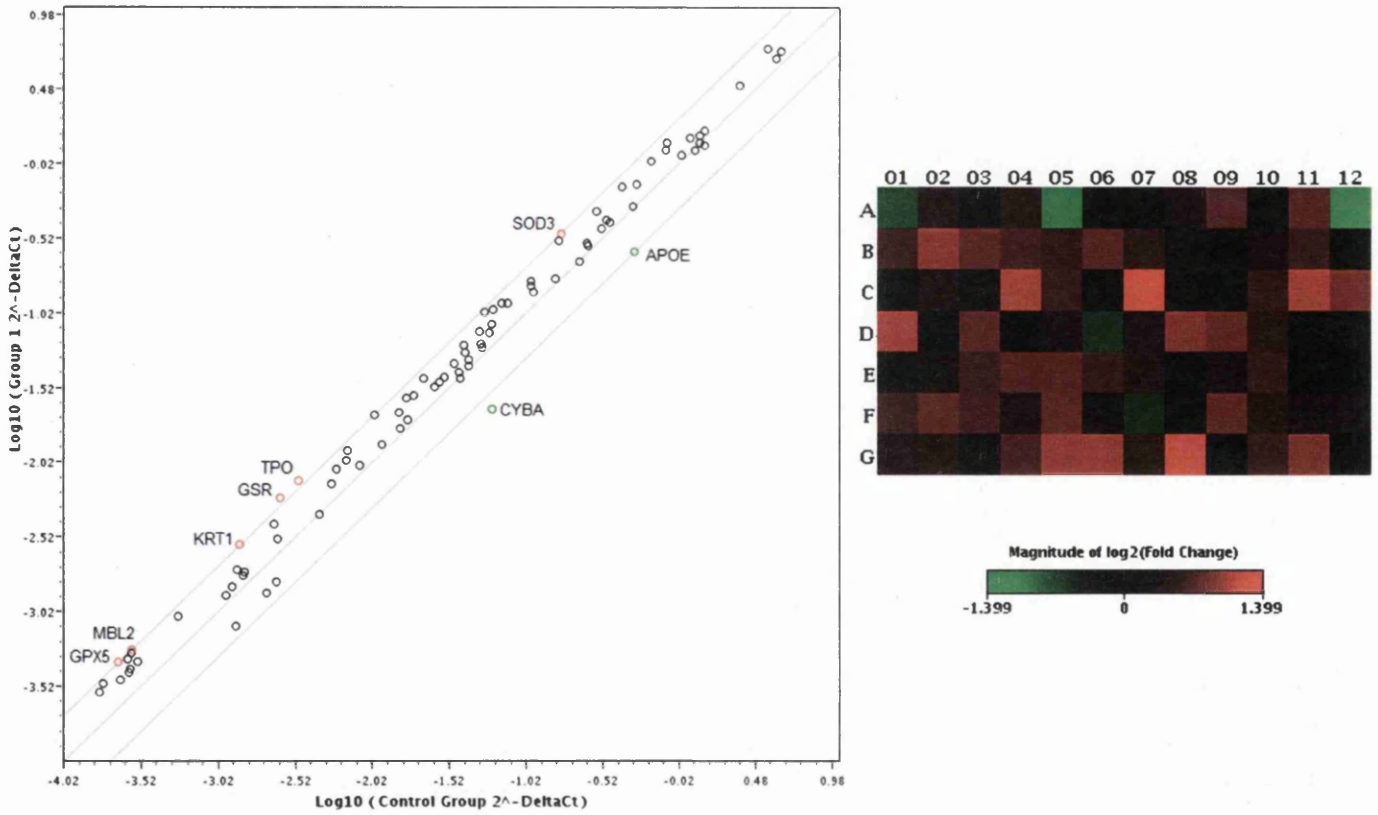

Scatter graph showing gene expression, where control group is L and group 1 is O+ODM. Each marker denotes a gene and band lines define 2-fold change boundary. Heat map represents 96 well array plate, where red pixels show increased and green show decreased expression of genes

Table 4.7 **Fold change difference in obese (O+ODM) groups compared to lean group**

Position	Symbol	Name	Fold Change (95% CI)	P
A05	APOE	Apolipoprotein E	0.4953 (0.18, 0.81)	0.06
A12	CYBA	Cytochrome b-245, alpha polypeptide	0.3793 (0.00001, 1.30)	0.75
C04	GPX5	Glutathione peroxidase 5 (epididymal androgen-related protein)	2.0721 (0.51, 3.63)	0.29
C07	GSR	Glutathione reductase	2.3587 (1.43, 3.28)	**0.02**
C11	KRT1	Keratin 1	2.0817 (0.00001, 4.26)	0.21
D01	MBL2	Mannose-binding lectin (protein C) 2, soluble	2.0599 (0.02, 4.10)	0.35
G05	SOD3	Superoxide dismutase 3, extracellular	2.0044 (0.90, 3.11)	0.16
G08	TPO	Thyroid peroxidase	2.2767 (1.08, 3.48)	0.07

Fold change gene expression in L subjects compared to O+ODM groups. Red shows genes with increased expression and green shows genes with decreased expression. P-value shows significance where P<0.05

4.4.2.5 L+O v ODM

The scatter graph in Figure 4.5 shows the fold change gene expression between controls (L+O) and ODM subjects to look at the effects of diabetes. Five genes showed increased expression including *GPx6, KRT1* and lactoperoxidase (*LPO*), whilst *ALB, CYBA* and *GPx1* showed decreased expression, although none were significant. Fold change values for genes found to show increased/decreased expression (according to the adopted 2-fold cut-off) are shown in Table 4.8.

Figure 4.5 Difference in gene expression between subjects with no diabetes and subjects with diabetes

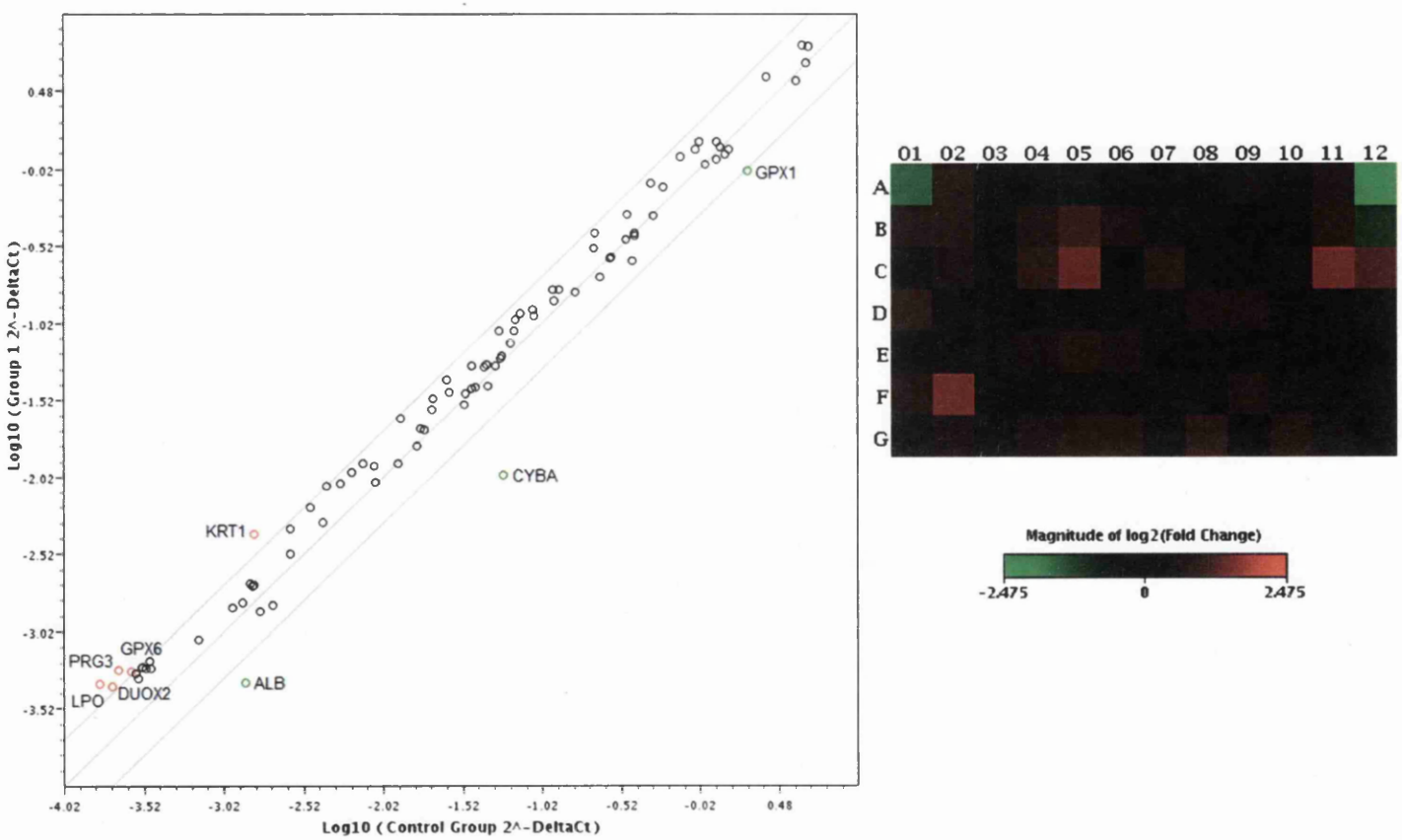

Scatter graph showing gene expression, where control group is L+O and group 1 ODM. Each marker denotes a gene and band lines define 2-fold change boundary. Heat map represents 96 well array plate, where red pixels show increased and green show decreased expression of genes

Table 4.8 Fold change difference in diabetes group compared to no-diabetes (L+O)

Position	Symbol	Name	Fold Change (95%CI)	P
A01	ALB	Albumin	0.344 (0.04, 0.65)	0.21
A12	CYBA	Cytochrome b-245, alpha polypeptide	0.1799 (0.00001, 0.68)	0.75
B05	DUOX2	Dual oxidase 2	2.1348 (0.54, 3.73)	0.10
B12	GPX1	Glutathione peroxidase 1	0.4897 (0.00001, 1.42)	0.75
C05	GPX6	Glutathione peroxidase 6 (olfactory)	2.6401 (0.50, 4.78)	0.07
C11	KRT1	Keratin 1	2.7974 (0.03, 5.56)	0.76
C12	LPO	Lactoperoxidase	2.2659 (0.26, 4.27)	0.19
F02	PRG3	Proteoglycan 3	2.782 (0.47, 5.10)	0.13

Fold change gene expression in diabetes group compared to no-diabetes. Red shows genes with increased expression and green shows genes with decreased expression. P-value shows significance where $P<0.05$

4.4.3 Overview of GSR expression between groups

Throughout analysis the expression levels of *GSR* showed a significant increase in the O group and a further increase in expression in ODM subjects (both compared to L). Due to these significant changes in expression, an overview of *GSR* expression profile between groups observed throughout this chapter is shown in Figure 4.6. A significant difference was observed between subjects in the L and O groups (L v O: 1.00 v 2.15, P= 0.026) and between L and ODM groups (L v ODM: 1.00 v 2.56, P= 0.021). The difference between O and ODM in *GSR* expression increased, although this was not significant (P= 0.565). Difference across all groups was not significant (P= 0.194).

Figure 4.6 Fold change of GSR between groups

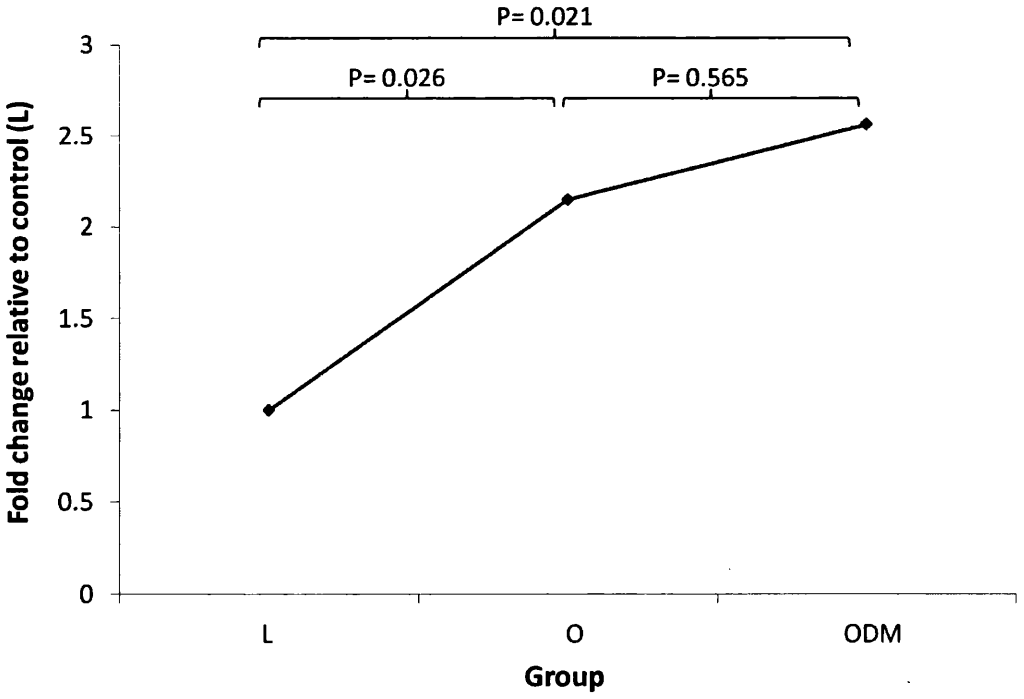

GSR fold change between groups. P-value shows significance where P<0.05

4.5 Discussion

The aim of the work in this chapter was to examine the expression profiles of genes involved in pathways related to inflammation and oxidative stress in hVAT samples and examine any gene expression differences between samples classified as L, O and ODM. 30 samples were obtained consecutively from surgical patients across the 3 categories (L, O, ODM: 11/9/10) and assayed using a commercially available PCR array kit. The resulting data was uploaded into the online analysis program for examination and results were classed as noteworthy if there was a 2-fold change compared to that of the control group and considered significant if $P<0.05$. Of the 84 genes associated with oxidative stress and inflammation examined there was a total of 19 genes that showed a difference in expression of more than 2 fold during group comparisons. However, only one gene, *GSR*, showing significant differences in expression between groups for O, ODM and O+ODM when all compared to controls (L).

GSR is a gene encoding the antioxidant enzyme glutathione reductase, which plays a pivotal role in the maintenance of cellular glutathione by reducing the oxidised form (GSSG) to the antioxidant scavenging reduced form (GSH). Levels of *GSR* expression were observed to increase significantly in obese patients and then continue to increase in obese patients with diabetes. This increased *GSR* expression is not what has been reported in recent literature. Apelt and colleagues (2009) surmised that as the glutathione antioxidant system acts as a ROS scavenger it should be expected that levels of GSR increase with BMI regardless of co-morbidities, although

increased oxidative stress and increased BMI in fact leads to antioxidant systems having an alternative effect and favouring oxidative damage (Apelt *et al*, 2009). In an environment of high oxidative stress, active GSR levels are ultimately decreased due to flavin adenine dinucleotide (FAD) demand by GSR being greater than the availability as dietary riboflavin is insufficient. Calabrese and colleagues (2012) observed significantly decreased levels of systemic reduced GSH and increased oxidised GSSG in patients with T2DM, resulting in a 68% decrease in GSH/GSSG ratio overall (Calabrese *et al*, 2012). It can be assumed that the decreased reduction of GSSG to GSH is due to a decreased level of active GSR or even $NADPH^{+}$, which this redox reaction in dependent on. If $NAPDH^{+}$ levels had been diminished during the polyol pathway; a pathway involved in glucose metabolism, then there may not be adequate levels to assist in GSSG reduction.

Although there are contradictory studies in this area, there are possible explanations for the occurrence of increased GSR in the O and ODM subjects. Studies have shown that patients with diabetes, metabolic syndrome and those at high risk of developing T2DM, such as in obesity, have lower plasma concentrations of reduced GSH (Yoshida et al, 1995; Sharma et al, 2000). It may be assumed that the increased gene expression of GSR observed in this study is to counteract this imbalance. There appear to be two main mechanisms that cause the diminished levels of GSH, which in turn may cause the up regulation of GSR in order to rebalance levels by oxidising cellular GSSG. Firstly, glucose and insulin have direct effects on the synthesis of GSH. Low levels of GSH have been observed in hyperglycaemia due to changes in the rate limiting enzyme of GSH production,

glutamate cysteine ligase (GCL). In environments of chronic high glucose exposure, there are decreased mRNA levels for regulatory subunits of GCL resulting in an overall decrease in cellular GSH (Urata et al, 1996; Catherwood et al, 2002). This may lead to increased expression of GSR to maintain the GSH/GSSG ratio balance. In contrast, high cellular insulin levels have been seen to increase GSH in patients with diabetes by increasing the activity of GCL in GSH synthesis pathway (Bravi et al, 2006). These findings may explain why, in this study, an increase in GSR was seen in O subjects, but also ODM subjects. In the subjects with diabetes there is an environment of high glucose and diminished insulin activity. Increased glucose levels have been shown to decrease systemic GSH and combined with the lack of insulin to increase GSH synthesis there will be a low GSH production overall. It is presumed that this low GSH stimulates the increased expression of GSR to counteract this imbalance of the GSH/GSSG ratio. If this ratio is not regained and maintained then the high glucose/ low insulin levels increase ROS and combined with the low GSH production ultimately result in weakened defences against oxidative stress and increased oxidative damage (Ballatori *et* al, 2009).

Secondly, the lack of required NADPH necessary for GSH regeneration from its oxidised GSSG form via GSR has been observed to cause reduced GSH. NADPH levels may be diminished due to its over consumption within the polyol pathway, responsible for the conversion of glucose to sorbitol via aldose reductase activity. In nomoglyceamic conditions, little glucose enters the polyol pathway but during hyperglycaemia glucose that is not utilised for energy enters for reduction to

sorbitol. During this pathway NADPH levels are diminished resulting in reduced levels available for the glutathione redox reaction.

Additionally, GSR has been identified as having protective effects in diseases associated with oxidative stress such as atherosclerosis (Qiao *et al*, 2007). It may be assumed that the increased expression of *GSR* seen in the obese patients within this study is in fact due to the cells protective mechanism against such conditions.

With respect to albumin, Insenser and colleagues (2012) studied the expression change of circulating proteins, such as albumin, and explained observed differences by the fact that whole adipose samples were used instead of separate adipocytes and stromal vascular fraction as seen in other literature (Insenser *et al*, 2012; Kheterpal *et al,* 2011; Peinado *et al*, 2010). During this study, whole adipose samples were used, which may determine the expression levels of particular circulating proteins that have been seen here.

The genes of particular interest found in this chapter were *GSR* and *GPX1* due to the differences in expression observed across the three subject groups. In order to verify these results and to look at these genes in more detail they were investigated further using a basic RT-PCR method.

CHAPTER 5

GENE EXPRESSION ANALYSIS USING RT-PCR IN HUMAN AND MOUSE SAMPLES

5.1 Introduction

As results from Chapter 4 show, there was a difference in gene expression seen between the three sample groups (L, O and ODM) in 19 genes associated with oxidative stress. In particular, differences were seen in the expression of the *GSR* gene, which was significantly increased in O and ODM subjects when compared to L control samples; and although no significant difference in *GPX1* expression was seen, there was an increase in O subjects and a decrease in ODM subjects. To take these findings further, this chapter aims to further investigate the expression of *GSR* and *GPX1* genes between the three groups and verify the results seen in Chapter 4 via real-time PCR analysis. Alongside these two target genes the expression of *PPARγ* and *IL-6* will also be analysed as two other target genes and *ACTB* as a control housekeeping gene.

5.1.1 GSR

GSR is an antioxidant enzyme that plays a vital role in the glutathione redox cycle, a system for reduced glutathione (GSH) regeneration. This mechanism involves the catalytic conversion of oxidised glutathione (GSSG) to its reduced form, GSH, by NAPDH-dependant GSR (Ahmadpoor *et al,* 2009) (Figure 5.1). It is responsible for the maintenance of circulating GSH levels, making up the primary defence against oxidative stress by scavenging ROS and repairing damage (Pastore *et al*, 2003). The regeneration of GSH through GSR requires NADPH, generated via glucose-6-phosphate dehydrogenase (G6PDH) during the conversion of glucose-6-phosphate into ribulose 5-phosphate in the pentose phosphate pathway. In conditions of increased oxidative stress the *GSR* gene is expected to have increased expression in

order to reduce oxidised glutathione (GSSG) to its GSH form to protect against oxidative stress. This gene was chosen for further investigation due to the significant differences in gene expression observed in the previous chapter.

Figure 5.1. GSH redox cycle

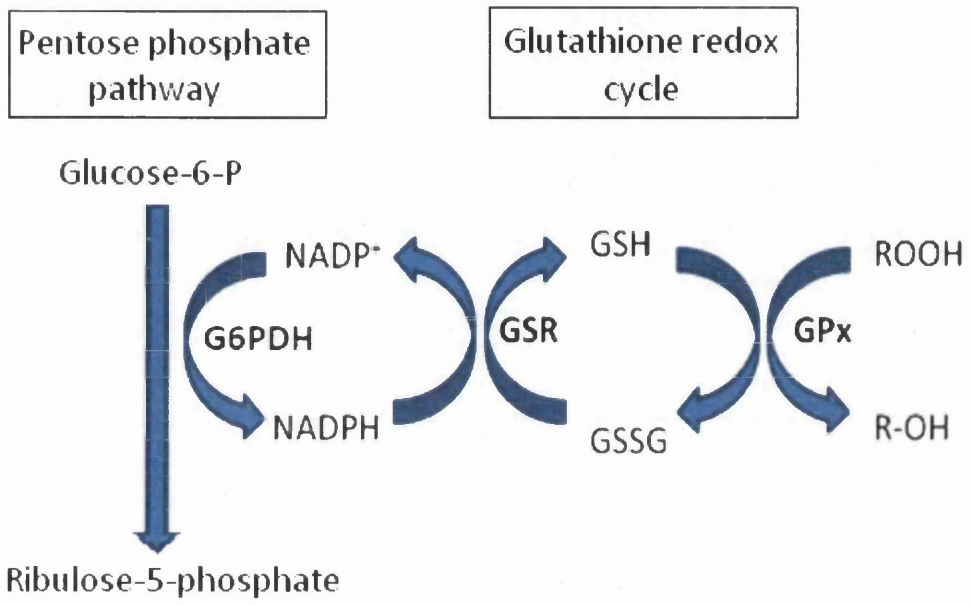

G6PDH; glucose-6-phosphate dehydrogenase, GSR; Glutathione reductase, GPx; Glutathione peroxidise

5.1.2 GPX1

GPX1 is the most common GPX isoform, which is responsible for the detoxification of H_2O_2 in order to prevent oxidative stress (Halliwell *et al*, 1992). Its role in the prevention of oxidative stress has also been determined in mouse models (Brigelis-Flohe and Kipp, 2009). This antioxidant enzyme is involved in the same pathways as GSR and its efficiency in neutralisation of peroxides is reliant on the intact GSH pathway (Hirrlinger and Drignen, 2010). This gene was chosen for further

investigation due to the differences in gene expression, although not statistically significant, observed in the previous chapter as well as its association with GSR within the GSH pathway.

5.1.3 PPARγ

Peroxisome proliferator-activated receptor gamma (*PPARγ)* is a gene that encodes the gamma subtype of PPAR. The PPAR subfamily of nuclear receptors are responsible for transcription regulation of various genes. In particular, PPARγ is an adipocyte specific transcription factor, which plays a role in the regulation of adipocyte function and has been associated with the pathology of obesity (Wagener *et al*, 2010). The main function of PPARγ is to regulate adipocyte differentiation and glucose homeostasis (Vidal-Puig *et al,* 1997). It influences glucose homeostasis, insulin sensitivity and blood pressure in obese patients via its role in adipocyte differentiation, fat deposition and its effect on plasma leptin levels. PPARγ has also been found to regulate macrophage activation, which is important for the synthesis of inflammatory cytokines. The *PPARγ* gene was chosen for investigation due to its regulatory role on AT and its previous association with diabetes, making it an interesting target within this population.

5.1.4 IL-6

IL-6 is a pro-inflammatory cytokine involved in the induction of the acute phase inflammatory response. IL-6 has been associated with β-cell differentiation, fat degradation and inflammatory disorders, such as diabetes (Kritiansen *et al*, 2005), where increased circulating levels are present years prior to diagnosis. IL-6 was

chosen as a target gene in this study due to its association with chronic inflammatory states such as diabetes and obesity.

Due to surprisingly low levels of oxidative stress observed in the study samples, especially ODM subjects, it was decided that these genes would be examined in parallel in an induced pro-oxidative state mouse cell line.. This will allow the comparison of gene expression of the target genes in human and mouse samples.

GSR and *GPX1* gene expression was investigated in the treated 3T3-L1 cells as these genes showed increased expression in O hVAT samples in Chapter 4. The 3T3-L1 murine cell line is commonly used in gene expression studies and was readily available to examine the target gene expression during induced oxidative stress. LPS was chosen as a pro-oxidant agent to induce a state of high oxidative stress within the cell line as it has been widely used in previous literature as a 'stressor' (Kizaki *et al*, 2002). LPS is a component of the outer cell wall of gram-negative bacteria and plays a crucial role in protecting the bacteria against damaging agents. LPS acts as a toxin, actively inducing the host's immune response. In this study, the pro-inflammatory characteristic of LPS was used to induce a high oxidative environment in which the 3T3-L1 cells were grown prior to gene expression analysis.

5.2 Aim

The purpose of the work described in this chapter was firstly to analyse candidate gene expression in hVAT samples. Two genes showing significant expression differences in Chapter 4, *GSR* and *GPX1*, are examined further by RT-PCR analysis,

along with *IL-6* and *PPARγ*, to examine differences between samples from lean, obese and obese patients with T2DM. Secondly, the aim was to culture 3T3-L1 mouse cell line to examine candidate gene expression in response to a 'biochemical stress'. Gene expression of *Gsr* and *Gpx1* was examined further in the mouse 3T3-L1 cell line in a basal state and in a state of 'biochemical stress', induced by LPS treatment. This allows *in vitro* interrogation of the expression and function of the identified genes.

5.3 Methods

5.3.1 RT-PCR gene expression analysis in human samples

RT-PCR analysis was carried out on 48 hVAT samples, including those examined in Chapter 4. RNA was extracted from the hVAT as previously described (Section 2.2.1) and reverse transcribed to cDNA (Section 2.5). Specific primers were designed using gene sequence information from NCBI (www.ncbi.nlm.nih.gov/) or sequences that had been previously published (GPX1 primers, Boutet *et al*, (2009); GSR primers, Corrales *et al*, (2011)) and synthesised by Eurofins MWG Operon.

5.3.2 RT-PCR gene expression analysis in mouse samples

RT-PCR analysis was carried out on 3T3-L1 cells that had undergone pro-oxidant treatment *in vitro* with LPS, as previously described (Section 2.7). The concentration of LPS used was taken from previous literature (Kizaki *et al,* 2002). Experiments were conducted in triplicate. LPS was administered after 3 days of culturing and left for a complete 14 hour cell cycle post treatment. RNA was extracted from cells (Section 2.7.3), reverse transcribed to cDNA (Section 2.5) and resulting cDNA

pooled. Specific primers were designed using gene sequence information from NCBI (www.ncbi.nlm.nih.gov/) and synthesised by Eurofins MWG Operon.

5.3.3 Analysis of results

Results were analysed using the $2^{-\Delta\Delta CT}$ quantification method, previously described in Chapter 2 (section 2.5) to calculate the level of gene expression change between groups in a relative fashion (Livak *et al*, 2001). Hence, for each group the mean C_T values obtained for each gene were determined. The ΔC_T values for each test gene were subsequently calculated normalising gene expression to β-actin, and the factors X_{GSR}, X_{GPX1}, $X_{IL\text{-}6}$ and $X_{PPAR\gamma}$ were established for each group in order for comparisons to take place. Subsequent N-fold differences <0.5 were considered as decreased gene expression, while over expression was defined as >2.0 fold increase in line with the PCR arrays used in the previous chapter. Due to limited comparisons made, P-values were unable to be calculated, so results are expressed as relative fold-change compared to a control group.

5.4 Results

5.4.1 Baseline characteristics

5.4.1.1 L v O v ODM

hVAT samples from 48 subjects, categorised as L, O and ODM (L/O/ODM: 17/15/16), were selected including the same samples that were analysed in Chapter 4. Baseline characteristics of subjects were analysed for differences between groups as this sample set differed from previous chapters, results are shown in Table 5.1. A significant difference was seen in weight (P<0.001) and BMI (P<0.001) between

groups, both being highest in the ODM group. HDL-C levels in the L subjects were significantly higher than O and ODM groups (P=0.019), whilst both creatinine and albumin were seen to be significantly different across groups (P=0.035 and P=0.037 respectively). A significantly higher percentage of the ODM group had hypertension (P=0.027) and OSA (P=0.001) compared to the other groups, as well as a significantly higher percentage of subjects on statin treatment (P=0.040).

Table 5.1 Baseline characteristics compared between groups

	Lean (n=17)	Obese (n=15)	Obese/T2DM (n=16)	P
Age (years)	53.8 (16.7)	51.8 (11.5)	44.4 (9.5)	0.109
Weight (kg)	74.4 (13.3)	116.7 (33.9)	141.9 (25.8)	**<0.001**
BMI (kg/m^2)	26 (2.6)	40 (11.2)	52 (10.7)	**<0.001**
SBP (mmHg)	137 (22.2)	130 (18.6)	142 (18.4)	0.284
DBP (mmHg)	81 (12.5)	79 (12.7)	76 (13.3)	0.478
Glucose (mmol/L)*	5.7 (0.6)	5.8 (0.4)	8.1 (1.5)	0.062
Cholesterol (mmol/L)	5.7 (1.3)	5.8 (1.7)	4.8 (1.2)	0.270
HDL-C (mmol/L)	1.6 (0.3)	1.1 (0.3)	1.1 (0.2)	**0.019**
LDL-C (mmol/L)	3.6 (1.1)	3.7 (1.7)	2.6 (0.7)	0.138
Triglycerides (mmol/L)	1.2 (0.2)	1.9 (0.5)	2.3 (1.3)	0.253
Creatinine (µmol/L)	79.3 (18.2)	81.6 (11.2)	67.6 (15.6)	**0.035**
Albumin (mmol/L)	47.3 (8.7)	43.0 (2.8)	41.7 (4.6)	**0.037**
RNA (ng/µl)	88.1 (52.6)	89.0 (47.2)	61.5 (42.0)	0.205
Males % (n)	52.9 (9)	40.0 (6)	37.5 (6)	0.630
Current smoker % (n)	29.4 (5)	26.7 (4)	18.8 (3)	0.924
Hypertension % (n)	17.6 (3)	33.3 (5)	62.5 (10)	**0.027**
OSA % (n)	0 (0)	13.3 (2)	50.0 (8)	**0.001**
Statins % (n)	5.9 (1)	33.3 (5)	43.8 (7)	**0.040**
ACE inhibitor % (n)	23.5 (4)	13.3 (2)	50.0 (8)	0.066

Baseline characteristics of 48 hVAT samples in L, O and ODM groups. *Log transformed data. Mean and standard deviation shown or geometric mean and approximate standard deviation for log transformed data. Analysis performed by ANOVA after appropriate transformation. χ^2-test was used to compare groups. P-value shows significance where P<0.05

5.4.1.2 L v O+ODM

Prior to analysis, I chose to examine baseline characteristics between L v O+ODM to look at the effects of obesity between groups. Results are detailed in Table 5.2. As expected, weight (P<0.001) and BMI (P<0.001) were significantly different between groups. HDL-C levels were significantly higher in L group compared to O+ODM (P=0.005), as were albumin levels (P=0.011). There were almost three times the number of subjects with hypertension in the O+ODM group (P=0.035) and all subjects with OSA fell into the O+ODM group (P=0.008). A higher proportion of subjects in the O+ODM group were also found to be on statin treatment (P=0.014).

5.4.1.3 L+O v ODM

I chose to examine baseline characteristics between L+O v ODM to look at the effects of non-diabetes (n=32) and diabetes (n=16), results are shown in Table 5.3. Age (P=0.042), weight (P<0.001) and BMI (P<0.001) were all significantly different between groups. Unsurprisingly, blood glucose levels were found to be significantly higher in the subjects with diabetes (P=0.020), whilst LDL-C (P=0.043) and creatinine (P=0.010) were both higher in patients in the non-diabetes group. The co-morbidities hypertension (P=0.011) and OSA (P<0.001) were significantly more prevalent in the subjects with diabetes and more subjects in this group were also on statin and ACE inhibitor treatments, with ACE inhibitor showing a significant difference (P=0.025).

Table 5.2 Baseline characteristics between lean v obese (O+ODM) groups

	Lean (n=17)	Obese + Obese T2DM (n=31)	P
Age (years)	53.8 (16.7)	48.0 (11.0)	0.152
Weight (kg)	74.4 (13.3)	129.7 (32.2)	**<0.001**
BMI (kg/m^2)	26 (2.6)	46 (12.3)	**<0.001**
SBP (mmHg)	137 (22.2)	136 (19.2)	0.863
DBP (mmHg)	81 (12.5)	77 (12.8)	0.304
Glucose (mmol/L)*	5.7 (0.6)	7.3 (1.2)	0.166
Cholesterol (mmol/L)	5.7 (1.3)	5.1 (1.4)	0.448
HDL-C (mmol/L)	1.6 (0.3)	1.1 (0.2)	**0.005**
LDL-C (mmol/L)	3.6 (1.1)	2.9 (1.1)	0.343
Triglycerides (mmol/L)	1.2 (0.2)	2.2 (1.2)	0.144
Creatinine (µmol/L)	79.3 (18.2)	74.1 (15.2)	0.304
Albumin (mmol/L)	47.3 (8.7)	42.2 (4.0)	**0.011**
RNA (ng/µl)	88.1 (52.6)	75.3 (46.1)	0.388
Males % (n)	52.9 (9)	38.7 (12)	0.342
Current smoker % (n)	29.4 (5)	22.6 (7)	0.815
Hypertension % (n)	17.6 (3)	48.4 (15)	**0.035**
OSA % (n)	0 (0)	32.3 (10)	**0.008**
Statins % (n)	5.9 (1)	38.7 (12)	**0.014**
ACE inhibitor % (n)	23.5 (4)	32.3 (10)	0.525

Baseline characteristics between lean and obese (O+ODM) groups to look at effects of obesity between groups. *Log transformed data. Mean and standard deviation shown or geometric mean and approximate standard deviation for log transformed data. Analysis performed by ANOVA after appropriate transformation. χ^2-test was used to compare groups. P-value shows significance where $P<0.05$

Table 5.3 Baseline characteristics between non-diabetic and diabetic groups

	No Diabetes (n=32)	Diabetes (n=16)	P
Age (years)	52.9 (14.3)	44.4 (9.5)	**0.038**
Weight (kg)	94.2 (32.8)	141.9 (25.8)	**<0.001**
BMI (kg/m^2)	32 (10.6)	52 (10.7)	**<0.001**
SBP (mmHg)	134 (20.7)	142 (18.4)	0.214
DBP (mmHg)	80 (12.4)	76 (13.3)	0.270
Glucose (mmol/L)*	5.8 (0.5)	8.1 (1.5)	**0.017**
Cholesterol (mmol/L)	5.8 (1.5)	4.8 (1.2)	0.101
HDL-C (mmol/L)	1.3 (0.4)	1.1 (0.2)	0.084
LDL-C (mmol/L)	3.7 (1.4)	2.6 (0.7)	**0.043**
Triglycerides (mmol/L)	1.6 (0.6)	2.3 (1.3)	0.148
Creatinine (µmol/L)	80.3 (15.2)	67.6 (15.6)	**0.010**
Albumin (mmol/L)	45.6 (7.2)	41.7 (4.6)	0.057
RNA (ng/µl)	88.5 (49.3)	61.5 (42.0)	0.074
Males % (n)	46.9 (15)	37.5 (6)	0.537
Current smoker % (n)	28.1 (9)	18.8 (3)	0.857
Hypertension % (n)	25.0 (8)	62.5 (10)	**0.011**
OSA % (n)	6.2 (2)	50.0 (8)	**<0.001**
Statins % (n)	18.8 (6)	43.8 (7)	0.066
ACE inhibitor % (n)	18.8 (6)	50.0 (8)	**0.025**

Baseline characteristics between non-diabetes (L+O) and diabetes groups to look at the effect of diabetes between groups *Log transformed data. Mean and standard deviation shown or geometric mean and approximate standard deviation for log transformed data. Analysis performed by ANOVA after appropriate transformation. χ^2-test was used to compare groups. P-value shows significance where P<0.05

5.4.2 RT-PCR gene expression analysis in human samples

HumanVAT samples from 48 subjects, categorised as L, O and ODM (L/O/ODM: 17/15/16), were selected, including the same samples that were analysed in Chapter 4, to investigate gene expression of 4 genes, *GSR, GPX1, IL-6* and *PPARγ*, normalised against *ACTB* as a housekeeping gene. Results are shown in Table 5.4.

GSR showed no difference in gene expression in the O group, however did show a increased fold change of 2.28 in ODM, relative to L. In the ODM group, *GSR* showed a 2.36 fold-change when compared to O subjects. *GPX1* gene expression showed no difference between groups. *IL-6* had increased gene expression of 3.01 and 2.03 in the O and ODM groups respectively, relative to L, however, no difference was observed in ODM compared to O subjects. *PPARγ* gene expression showed no difference between groups

When the samples were grouped by obesity (L v O+ODM), *GSR, GPX1* and *PPARγ* showed no difference in gene expression in the obese subjects (O+ODM) relative to L, whilst *IL-6* showed increased gene expression of 2.46 in the obese group (O+ODM). Results were analysed with subjects grouped as having no diabetes and diabetes (L+O v ODM). *GSR* showed increased gene expression of 2.33 in the group with diabetes relative to the no diabetes group. No difference was seen in expression of *GPX1, IL-6* and *PPARγ* between the groups.

Table 5.4 Fold change gene expression in hVAT samples

Compared groups	Gene	Fold change	Expression change
L v O	GSR	0.97	↔
	GPX1	1.12	↔
	IL-6	3.01	↑
	PPARγ	0.65	↔
L v ODM	GSR	2.28	↑
	GPX1	1.97	↔
	IL-6	2.03	↑
	PPARγ	0.66	↔
O v ODM	GSR	2.36	↑
	GPX1	1.77	↔
	IL-6	0.67	↔
	PPARγ	1.03	↔
L v (O + ODM)	GSR	1.51	↔
	GPX1	1.48	↔
	IL-6	2.46	↑
	PPARγ	0.66	↔
(L + O) v ODM	GSR	2.33	↑
	GPX1	1.88	↔
	IL-6	1.21	↔
	PPARγ	0.82	↔

Table 5.3 Summary of hVAT gene expression values showing their status
< 0.5 decreased gene expression (denoted by ↓)
> 2.0 increased gene expression (denoted by ↑)
0.5 – 2.0 no difference in gene expression (denoted by ↔)

5.4.3 RT-PCR gene expression analysis in mouse samples

Mouse 3T3-L1 cells were cultured in conditions of high and low glucose and treated with LPS in order to induce a pro-oxidative environment. Treated cells were analysed to investigate gene expression of 2 genes, *Gsr* and *Gpx1*, normalised against *Actb* as a housekeeping gene, results are shown in table 5.5. In 3T3-L1 cells cultured in medium with high glucose content, *Gsr* and *Gpx1* gene expression showed no difference after LPS treatment relative to untreated cells. In cells grown in medium with low glucose content, *Gsr* showed no difference in gene expression with LPS treatment, whilst *Gpx1* showed decreased expression of 0.33 fold with LPS treatment relative to untreated cells.

Table 5.5 Fold change gene expression in treated 3T3-L1 samples

Treatment	Gene	Fold change	Expression change
High glucose (LPS v No LPS)	Gsr	0.91	↔
	Gpx1	1.27	↔
Low glucose (LPS v No LPS)	Gsr	0.62	↔
	Gpx1	0.33	↓

Table 5.4 Summary of mouse treated 3T3-L1 gene expression values showing their status
< 0.5 decreased gene expression (denoted by ↓)
> 2.0 increased gene expression (denoted by ↑)
0.5 – 2.0 no difference in gene expression (denoted by ↔)

5.5 Discussion

The aim of the work in this chapter was firstly, to analyse gene expression of the antioxidant genes *GSR, GPX1, PPARγ* and *IL-6* in hVAT samples. Forty eight samples from across the three groups (L/O/ODM: 17/15/16) were analysed by RT-PCR to investigate gene expression. No difference in *GSR* expression was observed in the O group compared to the L, although a significant increase in expression was seen in the ODM group when compared to both L and O groups. This does not completely agree with the previous gene expression results in Chapter 4 gathered using a commercial PCR array kit, in which GSR expression was observed to increase significantly in O subjects and a further increase was seen in ODM. The only explanation for this difference lies within the methodology. Firstly, more samples were analysed via RT-PCR than using the commercial arrays, which may shift the overall outcome. Also there are fundamental differences between PCR array kits, such as those used in Chapter 4 which are highly optimised and use different primers and mastermix solutions, and a lab based PCR protocol that may account for these discrepancies.

When looking at *GPX1* gene expression, no difference was observed in expression levels between the three groups. These results do not agree with what was previously seen when examining *GPX1* gene expression via PCR array analysis, which showed an increased *GPX1* expression in obese patients and then decrease in obese patients with T2DM. An increased *GPX1* expression would have been expected due to increased cellular oxidative burden within these samples, which

would be counteracted by the up regulation of antioxidants, such as GPX1, in defence against excess ROS. This was not seen in this part of the study.

In the case of *IL-6*, increased gene expression was observed in the O and ODM groups compared to L, although no significant difference was observed between the O and ODM subjects. In the past, levels of *IL-6* mRNA expression, as well as systemic levels of IL-6 have been observed to increase with adiposity, with approximately a third originating from adipose (Mohamed-Ali *et al,* 1997), predominantly from VAT rather that subcutaneous tissue (Fried *et al,* 1997). Previous observations have recorded different levels of IL-6 gene expression within different tissues and within different adipose depots (Wozniak *et al,* 2009). This may explain the results observed here. Also differences in expression between different parts of AT has been described (Fried *et al,* 1997, Yudkin *et al,* 2000), but as total adipose was used in this study this will not be a defining factor.

Similarly, *PPARγ* showed no change in gene expression between groups. Previous studies have described an increased adipose expression of *PPARγ* mRNA in obesity although a decrease in expression was acknowledged in the case of low calorie dieting in adipose tissue from obese patients (Vidal-Puig *et al,* 1997). This is interesting because all subjects in the ODM category were undergoing bariatric surgery at the time of sample collection. For this type of surgery to be undertaken the patient must undertake a strict, low calorie pre-operative diet, in order to reduce liver size ready for surgery. It would be assumed that a reduced *PPARγ* expression should have been observed here due to this low calorie diet that is

maintained weeks prior to surgery and sample collection, although no decrease in expression was found. There are two mRNA splice variants of *PPARγ*, which are highly expressed in hVAT, both of which are found in equal proportions within the tissue in obese and diabetic patients (Vidal-Puig *et al*, 1997). The limited difference in expression seen in this study may not be attributed to these splice variants as it can be assumed that they are expressed at similar levels in the sample set used here.

When analysing the subjects group by obesity (L v O+ODM) there was no difference in gene expression found for *GSR, GPX1* and *PPARγ,* however, an increased expression of *IL-6* was observed in the obese subjects. Again, this is attributed to increased IL-6 levels with increased adiposity. Interestingly, *GSR* showed an increased expression in patients with diabetes when compared to subjects without diabetes (L+O v ODM), while no change was observed in the other genes. This increased *GSR* expression does not correspond to results from Chapter 4, where no difference in expression was seen in the *GSR* gene when analysing diabetes against non-diabetes groups.

Analysis of gene expression in a mouse cell line focused on *Gsr* and *Gpx1* only. Due to surprisingly low levels of oxidative stress observed in the human population, especially ODM subjects, Gsr and Gpx1 were examined in parallel in an induced pro-oxidative state. The 3T3-L1 mouse cell line was used to examine candidate gene expression of *Gsr* and *Gpx1* in a basal state and under the influence of a 'biochemical stressor', in this case LPS. After one whole cell cycle post treatment

with LPS, no differences in gene expression of *Gsr* were observed in cells grown in high glucose or low glucose conditions. In the human samples, an increased expression was seen, particularly in the ODM subjects, so it would therefore be expected that the LPS induced state of oxidative stress would induce increased expression of *Gsr* in the mouse cell line. This may not have been seen as mouse cells are more resistant to LPS exposure compared to human cells, which are more sensitive as they contain lower levels of circulating antibodies than mice (Warren *et al*, 2010).

Gpx1 gene expression showed no difference in mouse cells grown in high glucose medium, which agrees with the results seen in the human samples via RT-PCR. When grown in low glucose conditions *Gpx1* did show decreased gene expression when treated with LPS.

Results from the RT-PCR array analysis and the lab based RT-PCR gene expression analysis clearly show an increased expression of *GSR* in ODM subjects. Although unexplained, conflicting results have been shown for the O group. It may be that the increased expression of *GSR* is having an overall protective effect against oxidative stress in the ODM subjects, where surprisingly lower levels of oxidative markers were measured. To gain an insight into possible reasons for the increased expression of *GSR* in this group, it would be important to look at the gene at the DNA level to examine the sequence for possible mutations that may explain this observation.

CHAPTER 6

SEQUENCING FOR *GSR* GENE VARIANTS

6.1 Introduction

Throughout the previous chapters increased *GSR* gene expression has been observed in ODM subjects. This suggests a protective effect against oxidative stress, since the results in Chapter 3 show markers of oxidative stress being notably lower in this group. This observation may be simply due to an increased level of oxidative stress in ODM subjects prior to this study, which initiated a high expression of GSR in defence against excess ROS resulting in an overall decrease in oxidative stress at the time samples were collected.

Several methods were considered to investigate GSR expression, including the measurement of GSR activity by monitoring NADPH consumption within a sample. Commercial kits are available to assay the oxidation of NADPH to NADP+, which is monitored by the decrease in absorbance at 340 nm. The rate of decrease in absorbance is directly proportional to the GSR activity in the sample. The measurement of overall GSR activity in AT samples via this method was not carried out due to time restraints and expense.

Another explanation for the increased GSR expression in ODM subjects may be an alteration within the sequence of the *GSR* gene, which may cause this increased expression within this sample group. In order to investigate this in more detail, the *GSR* gene was selected for gene variant sequencing to identify any possible mutations/polymorphisms that may account for the increased expression observed in previous chapters. Several studies have looked at gene variants of other antioxidant genes and have observed differences in enzyme expression and activity

as a result of polymorphisms. An example of which is the Ala16Val polymorphism within the SOD gene, where the TT genotype results in lower activity (Flekac *et al*, 2008). Recent studies focusing on IL-6 polymorphisms have observed an association between gene variants and an individual's susceptibility to T2DM and its complications (Saxena *et al*, 2013). In particular a significant association has been found between the IL-6 gene -572 C/G polymorphism and T2DM risk (Yin *et al*, 2013).

6.1.1 Glutathione antioxidant system

GSR is an antioxidant enzyme, which plays a pivotal role in the glutathione antioxidant system. GSH, along with its related enzymes, makes up the primary defence against oxidative damage by neutralising excess ROS and repairing any damage caused (Pastore *et al*, 2003). As previously described, the glutathione antioxidant system is responsible for maintaining cellular defence against H_2O_2. This occurs due to glutathione peroxidases restoring GSH levels by reducing GSSG, which has been found to be up-regulated by p53 (Hussain *et al*, 2004). GSH homeostasis is dependent on its synthesis, uptake of exogenous GSH and redox recycling.

GSH synthesis consists of two sequential ATP-dependent steps catalysed by GCL and GSH synthetase (GS), which occurs entirely in the cytosol (Meister and Tate, 1976) (Figure 6.1). The cellular concentration of GSH is regulated by the GCL catalysed formation of γ-glutamyl-cysteine, which is feedback-inhibited by GSH (Griffith and Meister, 1979). This reaction is dependent on cellular adenosine triphosphate (ATP)

which is hydrolysed to adenosine diphosphate (ADP) supplying the energy required for the reaction.

Figure 6.1 GSH synthesis

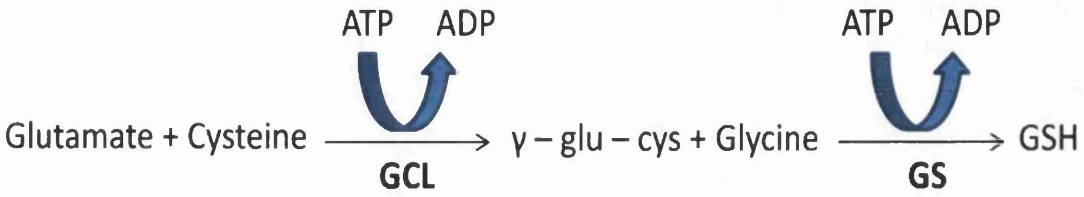

GSH synthesis consisting of two ATP-dependent steps catalysed by glutamate cysteine ligase (GCL) and GSH synthetase (GS)

GSH is principally found in its biologically active reduced thiol form, GSH (Circu and Yee Aw, 2008). In an oxidizing environment there is an increased oxidation of GSH to its disulphide form, GSSG, resulting in a decreased GSH:GSSG ratio. The GSH:GSSG ratio is normally maintained at approximately 100:1, but when affected by oxidative burden can fall as low as 4:1 (Circu and Yee Aw, 2008). This oxidant induced GSH:GSSG imbalance has been found to play a role in the initiation of the apoptotic cascade and can play a vital role in deciding cell fate (Merad-Boudia *et al*, 1998).

A mechanism for cellular GSH regeneration is commonly known as the GSH redox cycle (Figure 6.2), which involves the catalytic conversion of oxidised GSSG to its reduced form, GSH, by NAPDH-dependant GSR (Ahmadpoor *et al,* 2009). GSR is a ubiquitous FAD-containing flavoenzyme (Pai and Schulz, 1983) that is distributed in both the cytoplasm and mitochondria (Circu and Yee Aw, 2008).

Figure 6.2 GSH redox cycle

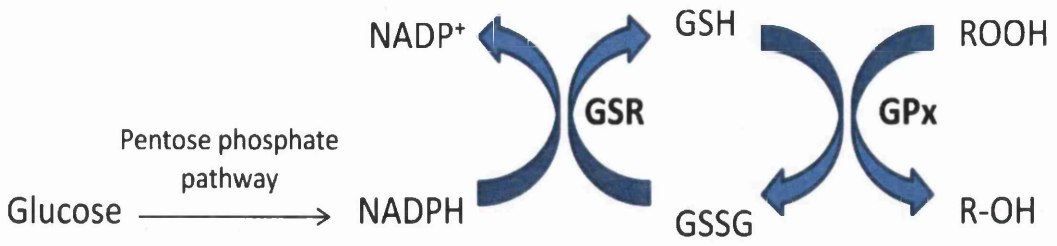

GSR; Glutathione reductase, GPx; Glutathione peroxidase

The reduction of GSSG to GSH via GSR is dependent on the presence of $NADPH/H^+$ as a proton donator, producing $NADP^+$. The required amount for the GSR system is high, with up to 10% of glucose uptake being used to produce sufficient levels of NADPH. However, high amounts of $NADPH/H^+$ are also required for cholesterol synthesis, so in the case of high oxidative stress there may be limited or no free NADPH as it will be used up to a higher degree within the activated GSR system. The result is a decreased total cholesterol level in any environment of oxidative stress and an increase in GSR activity. Therefore, cholesterol levels for production of LDL-C will be reduced. The activity of GSR in environments of oxidative stress is dependent on FAD and ACP1 (Apelt *et al,* 2009). In the event of the GSR system failing due to the lack of FAD during oxidative stress then $NADPH/H^+$ will become available and increased cholesterol production will occur.

The human *GSR* gene is located on chromosome 8 at position p21.1. It is over 4.9kb in size and contains 13 exons (Kelner *et al*, 2000). The complete gene encodes a 522

amino acid long polypeptide. Sequencing of the mRNA sequence of the gene was utilised in order to identify gene variants.

6.2 Aim

The purpose of the work described in this chapter was to analyse the *GSR* gene sequence for variants that may account for the increased gene expression observed in previous chapters. Any variants identified would then be compared between the three sample groups.

6.3 Methods

6.3.1 Sequencing of the *GSR* gene

The sequencing of the *GSR* gene for variants was carried out using specific primers designed to complement the mRNA template in five overlapping segments as described in Chapter 2 (Section 2.6). The method used reverse transcribed mRNA as a template, with resulting PCR products being purified and sent to Source Bioscience (Nottingham, UK) for sequencing. mRNA sequence was successfully gathered for 26 samples. The resulting sequence scores were analysed using Mutation Surveyor to determine potential variants. Samples containing potential variants were sent for re-sequencing for verification.

6.4 Results

6.4.1 Baseline characteristics

6.4.1.1 L v O v ODM

hVAT samples from 26 subjects, categorised as L, O and ODM, were successfully sequenced (L/O/ODM: 9/9/8). Baseline characteristics of subjects were analysed for differences between groups as this sample set differed from the previous chapter, results are shown in Table 6.1. There was no significant difference in age across groups although the L and O subjects were approximately 12 years older than the ODM group. Weight and BMI were significantly higher in the ODM group ($P<0.001$ for both), as was blood glucose ($P=0.044$). HDL-C levels in the L subjects were significantly higher ($P=0.019$), whilst a significantly higher percentage of subjects in the ODM group were on statin ($P=0.025$) and ACE inhibitor ($p=0.024$) treatments.

6.4.1.2 L v O+ODM

Prior to analysis, I chose to examine baseline characteristics between L v O+ODM to look at the effects of obesity between groups. Results are detailed in Table 6.2. Weight and BMI were significantly higher in the O+ODM group ($P<0.001$ for both), whilst HDL-C levels were significantly higher in L group ($P=0.010$). There was a higher proportion of subjects with hypertension and OSA in the O+ODM group, although this was not statistically significant. A higher percentage of subjects in the O+ODM group were on statin treatment and ACE inhibitors, although again this was not significant.

Table 6.1 Baseline characteristics compared between groups

	Lean (n=9)	Obese (n=9)	Obese/T2DM (n=8)	P
Age (years)	53.3 (18.4)	52.3 (9.0)	39.9 (11.1)	0.100
Weight (kg)	72.8 (14.3)	108.7 (30.8)	143.8 (31.7)	**<0.001**
BMI (kg/m^2)	25 (1.7)	37 (9.0)	52 (13.6)	**<0.001**
SBP (mmHg)	130 (21.3)	130 (17.9)	144 (19.9)	0.274
DBP (mmHg)	77 (12.7)	81 (11.0)	77 (10.5)	0.695
Glucose (mmol/L)*	5.1 (0.3)	6.1 (0.4)	9.3 (1.9)	**0.044**
Cholesterol (mmol/L)	7.2 (-)	5.7 (2.4)	5.4 (1.3)	0.613
HDL-C (mmol/L)	1.7 (-)	1.0 (0.2)	1.1 (0.2)	**0.019**
LDL-C (mmol/L)	4.9 (-)	3.8 (2.1)	3.1 (0.7)	0.435
Triglycerides (mmol/L)	1.1 (-)	2.1 (0.5)	2.6 (1.6)	0.604
Creatinine (µmol/L)	74.7 (21.0)	79.5 (9.4)	65.4 (18.8)	0.274
Albumin (mmol/L)	45.2 (4.4)	42.8 (2.9)	40.4 (5.8)	0.128
RNA (ng/µl)	96.8 (61.9)	73.0 (38.5)	64.5 (50.7)	0.412
Males % (n)	44.4 (4)	44.4 (4)	37.5 (3)	0.947
Current smoker % (n)	22.2 (2)	33.3 (3)	25.0 (2)	0.774
Hypertension % (n)	11.1 (1)	22.2 (2)	62.5 (5)	0.057
OSA % (n)	0 (0)	11.1 (1)	25.0 (2)	0.273
Statins % (n)	0 (0)	11.1 (1)	50.0 (4)	**0.025**
ACE inhibitor % (n)	11.1 (1)	11.1 (1)	62.5 (5)	**0.024**

Baseline characteristics of 28 hVAT samples in L, O and ODM groups. *Log transformed data. Mean and standard deviation shown or geometric mean and approximate standard deviation for log transformed data. Analysis performed by ANOVA after appropriate transformation. χ^2-test was used to compare groups. P-value shows significance where P<0.05

Table 6.2 Baseline characteristics between lean and obese (O+ODM) groups

	Lean (n=9)	Obese + Obese T2DM (n=17)	P
Age (years)	53.3 (18.4)	46.5 (11.6)	0.255
Weight (kg)	72.8 (14.3)	125.2 (35.5)	**<0.001**
BMI (kg/m^2)	25 (1.7)	44 (13.4)	**<0.001**
SBP (mmHg)	130 (21.3)	137 (19.6)	0.452
DBP (mmHg)	77 (12.7)	79 (10.6)	0.638
Glucose (mmol/L)*	5.1 (0.3)	8.0 (1.5)	0.069
Cholesterol (mmol/L)	7.2 (-)	5.5 (1.5)	0.326
HDL-C (mmol/L)	1.7 (-)	1.1 (0.2)	**0.010**
LDL-C (mmol/L)	4.9 (-)	3.4 (1.3)	0.281
Triglycerides (mmol/L)	1.1 (-)	2.5 (1.3)	0.359
Creatinine (µmol/L)	74.7 (21.0)	72.4 (16.1)	0.768
Albumin (mmol/L)	45.2 (4.4)	41.4 (4.8)	0.071
RNA (ng/µl)	96.8 (61.9)	69.0 (43.4)	0.193
Males % (n)	44.4 (4)	41.2 (7)	0.873
Current smoker % (n)	22.2 (2)	29.4 (5)	0.823
Hypertension % (n)	11.1 (1)	41.2 (7)	0.114
OSA % (n)	0 (0)	17.6 (3)	0.180
Statins % (n)	0 (0)	29.4 (5)	0.070
ACE inhibitor % (n)	11.1 (1)	35.3 (6)	0.186

Baseline characteristics between lean and obese (O+ODM) groups to look at effects of obesity between groups. *Log transformed data. Mean and standard deviation shown or geometric mean and approximate standard deviation for log transformed data. Analysis performed by ANOVA after appropriate transformation. χ^2-test was used to compare groups. P-value shows significance where $P<0.05$

Table 6.3 Baseline characteristics between no-diabetes and diabetes groups

	No Diabetes (n=18)	Diabetes (n=8)	P
Age (years)	52.8 (14.1)	39.9 (11.1)	**0.031**
Weight (kg)	90.8 (29.7)	143.8 (31.7)	**<0.001**
BMI (kg/m^2)	31 (8.9)	52 (13.6)	**<0.001**
SBP (mmHg)	130 (19.1)	144 (19.9)	0.104
DBP (mmHg)	79 (11.7)	77 (10.5)	0.690
Glucose (mmol/L)*	5.6 (0.4)	9.3 (1.9)	**0.015**
Cholesterol (mmol/L)	6.1 (2.1)	5.4 (1.3)	0.518
HDL-C (mmol/L)	1.2 (0.4)	1.1 (0.2)	0.901
LDL-C (mmol/L)	4.1 (1.8)	3.1 (0.7)	0.261
Triglycerides (mmol/L)	1.9 (0.7)	2.6 (1.6)	0.422
Creatinine (µmol/L)	76.9 (16.3)	65.4 (18.8)	0.128
Albumin (mmol/L)	44.3 (4.0)	40.4 (5.8)	0.070
RNA (ng/µl)	84.9 (51.5)	64.5 (50.7)	0.359
Males % (n)	44.4 (8)	37.5 (3)	0.741
Current smoker % (n)	27.8 (5)	25.0 (2)	0.847
Hypertension % (n)	16.7 (3)	62.5 (5)	**0.019**
OSA % (n)	5.6 (1)	25.0 (2)	0.152
Statins % (n)	5.6 (1)	50.0 (4)	**0.008**
ACE inhibitor % (n)	11.1(2)	62.5 (5)	**0.006**

Baseline characteristics between non-diabetes (L+O) and diabetes groups to look at the effect of diabetes between groups *Log transformed data. Mean and standard deviation shown or geometric mean and approximate standard deviation for log transformed data. Analysis performed by ANOVA after appropriate transformation. χ^2-test was used to compare groups. P-value shows significance where P<0.05

6.4.1.3 L+O v ODM

I chose to examine baseline characteristics between L+O v ODM to look at the effects of non-diabetes (n=18) and diabetes (n=8), results are shown in Table 6.3. Age, weight and BMI were significantly different between groups (P=0.031, P<0.001 and P<0.001 respectively). Blood glucose was significantly higher in subjects with diabetes (P=0.015). There was a higher prevalence of hypertension and OSA in subjects with diabetes, although only hypertension was significant (P=0.019), and a significantly higher percentage of subjects were on statin and ACE inhibitor treatments (P=0.008 and P=0.006 respectively).

6.4.2 Sequencing of *GSR* gene variants

The sequencing of the *GSR* mRNA was successful in 26 hVAT samples. The sequencing was carried out using primers designed to complement the mRNA template in five overlapping segments. The PCR products for the separate fragments were verified using polyacrylamide gel electrophoresis to account for any samples that proved unsuccessful during sequencing. Examples of the gel images are shown in Figure 6.3. They show that products from primer set 1, which were designed to amplify the sequence at the 5' end, were unsuccessful. The sequence amplified using primer set 2 were successful but at a low efficiency, which could still be sequenced, whilst primer set 3 had a high affinity and produced PCR products ideal for sequencing. Intact sequence scores were collected for primer sets 2 and 3. Primer set 4 and 5 were not analysed as they lay outside of the gene coding sequence.

Figure 6.3 Polyacrylamide gel images of PCR products.

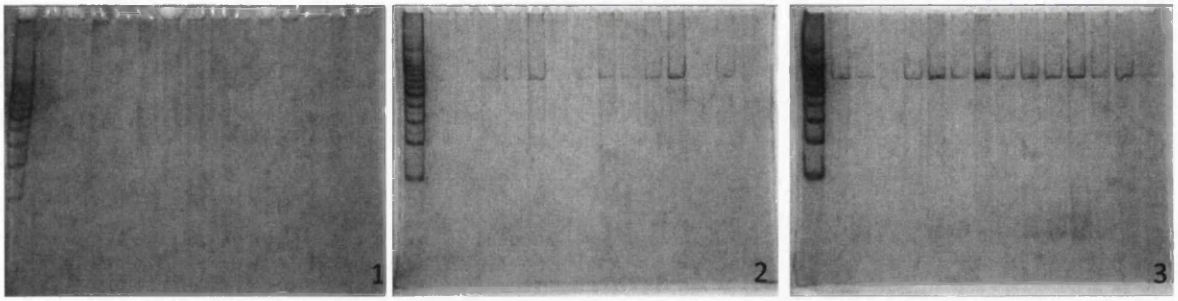

Polyacrylamide gel images showing PCR products for primer set 1 (1), primer set 2 (2) and primer set 3 (3)

Initial analysis showed 1 sample from the O group with a possible variant. This was shown on the resulting chromatograph as a heterozygous base change at position 419 from C→A, which would result in an amino acid change from proline (P) → threonine (T). This P419T variant is shown in Figure 6.4.

Figure 6.4 Chromatograph showing position of P419T variant

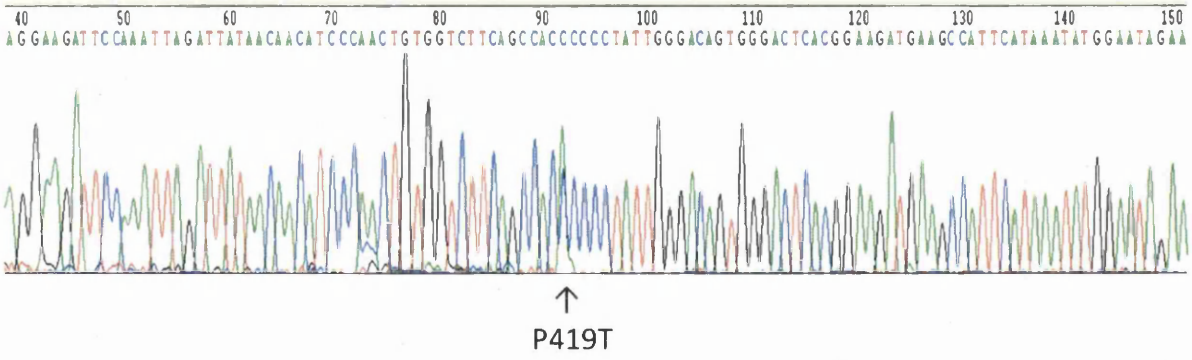

Sequence trace where black peaks denote G, green peaks denote A, red peaks denote T and blue peaks denote C. At position 419 two peaks, one blue and one green, can be seen as a possible heterozygote variant

The sample containing the potential P419T variant was sent for re-sequencing for verification. To be re-sequenced the sample underwent both forward and reverse sequencing to ensure the resulting sequence was correct. The resulting

chromatograph is shown in Figure 6.5. The P419T variant was not observed after re-sequencing.

Figure 6.5 Chromatograph showing position of P419T variant post verification

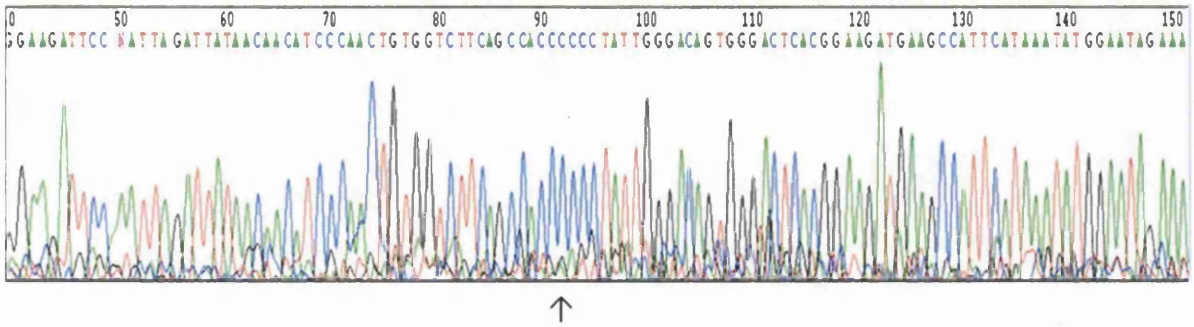

Sequence trace where black peaks denote G, green peaks denote A, red peaks denote T and blue peaks denote C. At position 419 only one blue peak can be seen

6.5 Discussion

The aim of the work in this chapter was to sequence the *GSR* gene for variants. In the previous chapters *GSR* showed an increased expression within the ODM group. It was hypothesised that possible gene variants could be responsible for this increased expression. In order to analyse this in more detail, mRNA for the *GSR* gene was sequenced using specific primers that spanned the gene in 5 overlapping fragments. hVAT from 26 subjects were successfully sequenced for variants, although the 5' end of the mRNA was unable to be sequenced due to primers being unable to bind. This limited affinity seen within the first primer set was due to the 5' sequence being the furthest point from the polyA tail making the binding of primers, although specific, unstable. Primer set 4 and 5 were spanning sequence outside of the coding area so this was left unanalysed.

Initial analysis showed one subject from the O group as having a possible P419T variant, which after searching NCBI was potentially a novel gene variant. This variant was shown as a heterozygous C→A base change, which would result in an amino acid change from proline (P) → threonine (T). The presence of this base change may ultimately cause an alteration in the overall structure and function of the resulting enzyme. However, after verification via re-sequencing this variant was lost. This suggests that the initial variant observed was in fact an anomaly that may have occurred during the PCR reaction.

Gene mutations can be formed at different scales, from small point mutations, through to small deletions of the entire genes or larger deletions that span one or more genes. The latter would not be detectable because the affected cells would not survive (Zhang et al, 2007).

Overall, no gene variants within the *GSR* gene were observed in the mRNA of hVAT samples. This suggests that a gene variation is not the explanation for the increased expression observed in previous chapters. Although no variants were observed within this gene, this still does not rule out DNA alteration as the cause of the increased expression of *GSR* in the ODM group. Alternatively, analysis of splice variants of GSR may hold the key to the gene's increased expression. Splicing of primary transcripts have been shown to play a vital role in the expression of genes, where gene splicing can ultimately result in protein variation and altered expression levels of single genes (Mironov *et al*, 1999).

CHAPTER SEVEN

DISCUSSION

The overall aim of this thesis was to investigate the role of AT in obesity and T2DM focusing on markers of oxidative stress and gene expression in hVAT from subjects categorised as L, O and ODM. This cross-sectional study was carried out to determine any changes in levels of oxidative stress between these groups, as well as identifying particular genes that may contribute to these conditions.

7.1 Biomarkers of oxidative stress

When investigating two biomarkers of oxidative stress ($\Delta ABTS^{+}$ and TBARS) and two markers of DNA damage (telomere length and Comet assay) in hVAT it was expected that oxidative stress levels would increase across groups due to the higher levels of oxidative burden associated with obesity and T2DM. When analysing overall antioxidant capacity in the hVAT, no difference in $ABTS^{+}$ radical formation was observed across the groups suggesting an overall lower level of total antioxidants than was expected to be seen in the O and ODM groups. When measuring levels of lipid peroxidation, there was a significant difference in MDA concentration between the three groups with the ODM group being significantly lower. Telomere length, as a measure of oxidative DNA damage, was significantly longer in subjects with diabetes, which is the opposite to what was expected as telomere shortening is generally associated with T2DM. When measuring DNA damage using the Comet assay no difference was observed between the three groups, although when stratifying by diabetes status there was a significant amount of undamaged DNA remaining in the nucleus of the cells after electrophoresis. This result again is surprising as an increase in DNA damage was expected in the ODM subjects. Overall, there appeared to be a protective mechanism in the subjects with

diabetes as they displayed a decreased level of oxidative stress compared to the other groups, which showed no significant difference in any of the markers. A significant proportion of the subjects in the ODM category were on ACE inhibitor and statin therapy, which may be confounding the results in these experiments as these therapies may be minimising the effects of oxidative stress.

7.2 Gene expression in hVAT

While looking at gene expression differences in obesity and diabetes, via the use of commercial PCR array kits, 19 genes were found to show either increased or decreased expression. In particular, an increase in *GSR* across the groups was observed with a particular significance in both O and ODM when compared to L control. Also a significant difference was seen in the grouped O+ODM subjects when compared to the L controls. It was assumed that this difference in gene expression was due to reduced levels of GSH, within the glutathione redox system, due to hyperglycaemia. As a result of this, there is increased expression of the reducing enzyme, GSR, to maintain a healthy GSH: GSSG ratio and rebalance the redox system. From this it was concluded that in an environment of excessive oxidative burden, depletion of GSH due to increased plasma glucose levels causes increased expression of *GSR*. Although not significant, an increased in gene expression of *GPX1* was observed in O subjects and decrease in ODM subjects. An increased *GPX1* expression would have been expected in the ODM group due to increased cellular oxidative burden within these samples, which would be counteracted by the increased expression of antioxidants, such as GPX1, in defence against excess ROS. This was not seen here.

When investigating gene expression via RT-PCR analysis no difference in *GSR* expression was observed in the O group compared to the L, although a significant increase in expression was seen in the ODM group when compared to both L and O groups. However, GSR expression was increased in patients with diabetes when compared to subjects without diabetes (L+O v ODM). There was no difference in expression of *GPX1* observed between the groups. These results differ from the gene expression results seen via a commercial PCR array kit. The difference was put down to the altered sample set as a greater number of samples were analysed by RT-PCR, which may account for the change in overall results. Also there may be some variance between the two methods of analysis. When utilising a commercial array kit, which is highly optimised and uses different primers and mastermix solutions, results should be expected to differ to a degree when compared to a conventional, lab based PCR protocol. Other than the differences explained here there is no overall conclusion as to why the results for *GPX1* and *GSR* expression may differ between the techniques.

An increased gene expression of *IL-6* was observed in the O and ODM groups compared to L, which was expected due to the association between IL-6 and increased adiposity. No significant difference was observed between the O and ODM subjects, which suggests the IL-6 expression difference is associated with obesity rather than diabetes. When looking at *PPARγ* there was no difference of any significance seen between the three groups.

7.3 Stimulation studies

The aim of this stimulation study was to examine candidate gene expression in response to a 'biochemical stress' in the 3T3-L1 mouse cell line. Gene expression of *Gsr* and *Gpx1* was examined at basal state and in a state of 'biochemical stress', induced by LPS treatment. Cells grown in low glucose conditions showed a decreased expression of *Gpx1* after treatment with LPS. This was in fact the opposite to what should be expected. In an environment of high oxidative stress, induced by LPS treatment, *Gpx1* is expected to increase expression in order to reduce oxidative burden. This unexpected result may be due to the difference in species or because the mouse cells were not an obese model, whereas the human samples were obese with diabetes. The combination of obesity and diabetes may affect the overall gene expression.

7.4 Glutathione reductase sequencing

The previous results had shown a significant difference in the gene expression of the *GSR* gene in ODM subjects. It was suspected that possible gene variants were responsible for this increased expression. In order to analyse this in more detail, mRNA for the *GSR* gene was sequenced in order to identify any causative gene variants. Overall there were no gene variants identified within the coding region of the gene suggesting that an alteration to the DNA sequence of the gene was not the causative factor of the increased expression observed. It may be important in future work to consider the influence of splice variants within the *GSR* gene that may be effecting the overall expression in this population.

7.5 Conclusion

The subjects that make up the ODM group are a unique subset of subjects, both physiologically and biochemically. These patients were under extreme oxidative burden due to not only their excess weight but also elevated blood glucose levels as a result of T2DM and the added burden of existing comorbidities that these inflammatory conditions induce, for example endothelial dysfunction. This study has demonstrated that there are indeed increased levels of oxidative stress within the O group, but may not be to an extent that the current antioxidant systems are overwhelmed and, therefore, need to increase efficiency and production. It has been observed that the ODM subjects had increased levels of oxidative stress to the extreme that the antioxidant systems were required to "kick it up a gear" and increase cellular antioxidant levels. Additionally, the intense drug therapies that these patients are undergoing due to their condition, may be contributing to the overall positive effect on the individuals defence against oxidative stress.

It is difficult to conclude whether the lower levels of oxidative stress measured in the ODM subjects was a result of the increased *GSR* expression observed in the hVAT or if there remains an unseen factor influencing the dramatic expression change seen in this group of subjects.

From these conclusions, it may be hypothesised that within this sample set, the situation of oxidative stress is in fact reversible as the antioxidant capacity in these subjects is evident, and in combination with correct drug therapy it may be possible to combat oxidative burden and reduce the subsequent damage inflicted upon the

cells. Particularly within the ODM subjects in this study, bariatric surgery may play a positive role in the correction of this oxidative state and it would be of interest to be able to follow up this study by repeating this analysis one year post-operative to see if oxidative burden has improved in these subjects. This, however, would not be feasible unless the same patients were undergoing further abdominal surgery for the collection of hVAT.

7.6 Limitations

Although every effort was made to address any problems met within the study, it was unavoidable that some would arise. These are detailed below.

7.6.1 Recruitment of samples

The hVAT samples analysed in this study were collected from the bariatric-obesity clinic and general surgical clinics, Morriston Hospital. As with all surgery there may be reasons for them not being carried out on the scheduled day. For this reason there were many occasions where no samples were successfully collected. Also, the majority of the O samples and all of the ODM samples were collected from bariatric surgery, which in the initial stages of the sample collection were very few making collection very slow. Once WIMOS was established in 2011 there were far more suitable candidates to collect from, although for this reason the completion of sample collections took longer than anticipated.

7.6.2 Baseline characteristics

During sample collections no additional clinical data was gathered directly from the subject at the time of surgery, so all baseline characteristics were gathered from medical notes at a later date. For this reason there are some measures unavailable for particular individuals. There were limited measures of waist circumference for the subjects so this could not be analysed. There was a significant difference in age across the three groups with an older population in the L category and then progressively lower in the O and ODM groups. This may be a confounding factor as age may have an independent impact on the markers measured in this study. This was not taken into consideration during statistical analysis where regression analysis could have been carried out to account for this. It is also important to address the mixture of therapies the subjects were taking. There were a number of subjects on a mixture of oral hyperglycaemic agents, antihypertensive agents and anti-depressive agents, which may have confounding effects on the markers measured in this thesis. Therefore, results must be interpreted with this in mind.

7.6.3 Markers of oxidative stress

When measuring TAOS, the use of hVAT homogenate was experimental. The overall outcome of the use of homogenates was inconclusive, therefore the calculation was altered to calculate relative change in $ABTS^{+}$ radical formation. This is explained in detail in chapter 2 (section 2.3.1).

Initially an in house protocol for the Comet assay was experimented with although due to very strict conditions the optimisation proved difficult in the timescale

allowed. For this reason the protocol was replaced with a commercially available kit to provide reliable results. In the future, I would like to return to the in house protocol and complete its optimisation.

All of the markers adopted for this study are normally measured in blood plasma samples or urine. The use of these techniques with hVAT homogenates was completely experimental. For this reason it would have been advantageous to have corresponding blood plasma samples available to validate these techniques for the use of hVAT.

7.6.4 Gene sequencing

Primer set 1 was not successfully optimised due to the sequence being too far from the poly A tail to bind effectively. Therefore, much of the coding sequence for the *GSR* gene was not sequenced successfully due to primer set 4 and 5 spanning completely non-coding sequence and the ATG stop codon was positioned within the sequence spanned by primer set 3.

7.7 Further work

In the future it would be beneficial to be able to validate these techniques for the use of hVAT by comparison with blood plasma samples. At the time of sample collection, tissue was also collected from the subcutaneous depot in each of the subjects, although these samples were not used in this study. It may be of use to analyse these samples in the same way to compare any differences between depots in this population. A new proposal is being written to follow on from the results of

this study. This work will look at visceral fat, liver and muscle as three important organs that play a crucial role in taking up glucose from the blood in obesity and type 2 diabetes. These organs become "resistant" to insulin resulting in elevated blood glucose levels and ultimately diabetes. The study will examine differences in the behaviour of genes involved in insulin signalling, inflammation and free radical damage within samples of visceral fat, liver and muscle from subjects who are lean, obese and obese with type 2 diabetes. These tissues will be examined using the same techniques as described here. The work could potentially identify proteins and molecules which might lead to new treatments to prevent and treat these common conditions.

APPENDIX 1

Raw data for $\Delta ABTS^{+}$ validation

	Intra-assay variability					
Replicate	A	B	C	D	E	F
1	0.203	0.197	0.201	0.201	0.200	0.200
2	0.198	0.196	0.205	0.197	0.201	0.200
3	0.198	0.201	0.201	0.199	0.203	0.202

	Inter-assay variability		
Replicate	A	B	C
1	0.215	0.230	0.219
2	0.199	0.203	0.226
3	0.185	0.186	0.191
4	0.204	0.194	0.206

These tables contain the intra- and inter-assay variation for ΔABTS+ as described in Chapter 3

APPENDIX 2

Raw data for TBARS validation

	Intra-assay variability							
Replicate	A	B	C	D	E	F	G	H
1	26220	24794	22904	26412	25274	28264	22932	25695
2	23363	24119	23638	25785	24522	24317	24836	27383
3	18390	17226	14878	20338	17858	16626	18205	18783
4	19118	18052	16283	16701	18135	18637	20242	21582

	Inter-assay variability							
Replicate	A	B	C	D	E	F	G	H
1	26220	24794	22904	26412	25274	28264	22932	25695
	18390	17226	14878	20338	17858	16626	18205	18783
2	23363	24119	23638	25785	24522	24317	24836	27383
	19118	18052	16283	16701	18135	18637	20242	21582

These tables contain the intra- and inter-assay variation for TBARS as described in Chapter 3

APPENDIX 3

Raw data for telomere length validation

	Intra-assay variability					
Replicate	A	B	C	D	E	F
1	10.3	10.1	10.4	10.3	10.3	10.3
	9.9	10.1	10.0	10.0	10.0	10.2
	11.1	10.0	9.9	10.5	11.3	10.2
	10.1	10.6	10.9	10.1	10.1	9.8
	10.0	10.7	10.5	10.6	10.4	10.5
	9.7	9.8	9.6	9.9	10.0	9.9
2	19.0	18.9	19.0	18.8	18.8	19.2
	18.9	19.0	19.1	18.9	18.8	19.2
	20.1	19.3	19.3	19.6	20.1	19.4
	19.2	19.6	19.9	18.8	18.8	18.8
	20.4	19.2	18.7	19.5	19.2	19.3
	19.3	19.4	19.0	19.0	19.0	19.2

	Inter-assay variability							
Replicate	A	B	C	D	E	F	G	H
1	9.9	10.1	10.0	10.0	10.0	10.2	10.3	10.1
	10.4	10.3	10.3	10.3	11.1	10.0	9.9	10.5
	11.3	10.2	10.1	10.6	10.9	10.1	10.1	9.8
	10.0	10.7	10.5	10.6	10.4	10.5	9.7	9.8
	9.6	9.9	10.0	9.9	9.8	10.2	10.0	10.0
	10.2	10.0	10.8	10.1	10.7	11.0	10.2	10.8
2	19.0	18.9	19.0	18.8	18.8	19.2	18.9	19.0
	19.1	18.9	18.8	19.2	20.1	19.3	19.3	19.6
	20.1	19.4	19.2	19.6	19.9	18.8	18.8	18.8
	20.4	19.2	18.7	19.5	NA	NA	19.2	19.3
	19.3	19.4	19.0	19.0	19.0	19.2	19.1	19.1
	19.0	19.1	19.6	19.0	19.3	19.5	18.8	19.3

These tables contain the intra- and inter-assay variation for telomere length as described in Chapter 3

APPENDIX 4

Measures of DNA in the Comet assay

Name of measure	Description
Comet length	Total comet length measured at the widest point from the comet head to tail
Comet height	Total comet height measured form the lowest point to highest
Comet area	Total comet area including the comet head, tail and any displacement of DNA in the cell
Comet intensity	Total comet fluorescence intensity representative of total DNA content of the cell
Comet mean intensity	Mean total comet fluorescence intensity across the total comet area
Head diameter	Diameter of the comet head representative of the diameter of the cell's nucleus
Head area	Total area of comet head representative of nucleus area of the cell
Head intensity	Total comet head fluorescence intensity representative of total undamaged DNA content of the cell's nucleus
Head mean intensity	Mean comet head fluorescence intensity across the total comet head area
Head DNA (%)	Percentage of DNA in the comet head representative of the total undamaged DNA in the nucleus
Tail length	Length of the comet tail representative of the migration of damaged DNA in the cell
Tail area	Total comet tail area representative of the total amount of damaged DNA migrated away from the cell's nucleus
Tail intensity	Total comet tail fluorescence intensity representative of total damaged DNA content of the cell
Tail mean intensity	Mean comet tail fluorescence intensity across the total comet tail area
Tail DNA (%)	Percentage of DNA in the comet tail representative of the total damaged DNA migrated away from the cell's nucleus
Tail moment	An overall measure of displacement of damaged DNA from the nucleus of the cell (*Tail DNA% X Length of Tail)*
Olive moment	An alternative measure of 'Tail moment' (*Tail DNA% X Tail Moment Length)*

APPENDIX 5

Array plate layout and list of genes included

	1	2	3	4	5	6	7	8	9	10	11	12
A	ALB	ALOX12	ANGPTL7	AOX1	APOE	ATOX1	BNIP3	CAT	CCL5	CCS	CSDE1	CYBA
B	CYGB	DGKK	DHCR24	DUOX1	DUOX2	DUSP1	EPHX2	EPX	FOXM1	GLRX2	GPR156	GPX1
C	GPX2	GPX3	GPX4	GPX5	GPX6	GPX7	GSR	GSS	GSTZ1	GTF2I	KRT1	LPO
D	MBL2	MGST3	MPO	MPV17	MSRA	MT3	MTL5	NCF1	NCF2	NME5	NOS2A	NOX5
E	NUDT1	OXR1	OXSR1	PDLIM1	PIP3-E	PNKP	PRDX1	PRDX2	PRDX3	PRDX4	PRDX5	PRDX6
F	PREX1	PRG3	PRNP	PTGS1	PTGSE2	PXDN	PXDNL	RNF7	SCARA3	SELS	SEPP1	SFTPD
G	SGK2	SIRT2	SOD1	SOD2	SOD3	SRXN1	STK25	TPO	TTN	TXNDC2	TXNRD1	TXNRD2
H	B2M	HPRT1	RPL13A	GAPDH	ACTB	HGDC	RTC	RTC	RTC	PPC	PPC	PPC

Well	Symbol	Description
A01	ALB	Albumin
A02	ALOX12	Arachidonate 12-lipoxygenase
A03	ANGPTL7	Angiopoietin-like 7
A04	AOX1	Aldehyde oxidase 1
A05	APOE	Apolipoprotein E
A06	ATOX1	ATX1 antioxidant protein 1 homolog (yeast)
A07	BNIP3	BCL2/adenovirus E1B 19kDa interacting protein 3
A08	CAT	Catalase
A09	CCL5	Chemokine (C-C motif) ligand 5
A10	CCS	Copper chaperone for superoxide dismutase
A11	CSDE1	Cold shock domain containing E1, RNA-binding
A12	CYBA	Cytochrome b-245, alpha polypeptide
B01	CYGB	Cytoglobin
B02	DGKK	Diacylglycerol kinase, kappa
B03	DHCR24	24-dehydrocholesterol reductase
B04	DUOX1	Dual oxidase 1
B05	DUOX2	Dual oxidase 2
B06	DUSP1	Dual specificity phosphatase 1
B07	EPHX2	Epoxide hydrolase 2, cytoplasmic
B08	EPX	Eosinophil peroxidase
B09	FOXM1	Forkhead box M1
B10	GLRX2	Glutaredoxin 2
B11	GPR156	G protein-coupled receptor 156
B12	GPX1	Glutathione peroxidase 1
C01	GPX2	Glutathione peroxidase 2 (gastrointestinal)
C02	GPX3	Glutathione peroxidase 3 (plasma)
C03	GPX4	Glutathione peroxidase 4 (phospholipid hydroperoxidase)
C04	GPX5	Glutathione peroxidase 5 (epididymal androgen-related protein)
C05	GPX6	Glutathione peroxidase 6 (olfactory)
C06	GPX7	Glutathione peroxidase 7
C07	GSR	Glutathione reductase
C08	GSS	Glutathione synthetase
C09	GSTZ1	Glutathione transferase zeta 1
C10	GTF2I	General transcription factor IIi
C11	KRT1	Keratin 1
C12	LPO	Lactoperoxidase
D01	MBL2	Mannose-binding lectin (protein C) 2, soluble
D02	MGST3	Microsomal glutathione S-transferase 3
D03	MPO	Myeloperoxidase
D04	MPV17	MpV17 mitochondrial inner membrane protein
D05	MSRA	Methionine sulfoxide reductase A
D06	MT3	Metallothionein 3
D07	MTL5	Metallothionein-like 5, testis-specific (tesmin)
D08	NCF1	Neutrophil cytosolic factor 1

D09	NCF2	Neutrophil cytosolic factor 2
D10	NME5	Non-metastatic cells 5, protein expressed in (nucleoside-diphosphate kinase)
D11	NOS2	Nitric oxide synthase 2, inducible
D12	NOX5	NADPH oxidase, EF-hand calcium binding domain 5
E01	NUDT1	Nudix (nucleoside diphosphate linked moiety X)-type motif 1
E02	OXR1	Oxidation resistance 1
E03	OXSR1	Oxidative-stress responsive 1
E04	PDLIM1	PDZ and LIM domain 1
E05	IPCEF1	Interaction protein for cytohesin exchange factors 1
E06	PNKP	Polynucleotide kinase 3'-phosphatase
E07	PRDX1	Peroxiredoxin 1
E08	PRDX2	Peroxiredoxin 2
E09	PRDX3	Peroxiredoxin 3
E10	PRDX4	Peroxiredoxin 4
E11	PRDX5	Peroxiredoxin 5
E12	PRDX6	Peroxiredoxin 6
F01	PREX1	Phosphatidylinositol-3,4,5-trisphosphate-dependent Rac exchange factor 1
F02	PRG3	Proteoglycan 3
F03	PRNP	Prion protein
F04	PTGS1	Prostaglandin-endoperoxide synthase 1 (prostaglandin G/H synthase and cyclooxygenase)
F05	PTGS2	Prostaglandin-endoperoxide synthase 2 (prostaglandin G/H synthase and cyclooxygenase)
F06	PXDN	Peroxidasin homolog (Drosophila)
F07	PXDNL	Peroxidasin homolog (Drosophila)-like
F08	RNF7	Ring finger protein 7
F09	SCARA3	Scavenger receptor class A, member 3
F10	SELS	Selenoprotein S
F11	SEPP1	Selenoprotein P, plasma, 1
F12	SFTPD	Surfactant protein D
G01	SGK2	Serum/glucocorticoid regulated kinase 2
G02	SIRT2	Sirtuin 2
G03	SOD1	Superoxide dismutase 1, soluble
G04	SOD2	Superoxide dismutase 2, mitochondrial
G05	SOD3	Superoxide dismutase 3, extracellular
G06	SRXN1	Sulfiredoxin 1
G07	STK25	Serine/threonine kinase 25
G08	TPO	Thyroid peroxidase
G09	TTN	Titin
G10	TXNDC2	Thioredoxin domain containing 2 (spermatozoa)
G11	TXNRD1	Thioredoxin reductase 1
G12	TXNRD2	Thioredoxin reductase 2
H01	B2M	Beta-2-microglobulin
H02	HPRT1	Hypoxanthine phosphoribosyltransferase 1

H03	RPL13A	Ribosomal protein L13a
H04	GAPDH	Glyceraldehyde-3-phosphate dehydrogenase
H05	ACTB	Actin, beta
H06	HGDC	Human Genomic DNA Contamination
H07	RTC	Reverse Transcription Control
H08	RTC	Reverse Transcription Control
H09	RTC	Reverse Transcription Control
H10	PPC	Positive PCR Control
H11	PPC	Positive PCR Control
H12	PPC	Positive PCR Control

APPENDIX 6

Raw data for PCR arrays

Appendix 4 PCR array data: Fold change between groups compared to control (L)

		O		ODM	
Position	Symbol	Fold Change (95%CI)	P	Fold Change (95%CI)	P
A01	ALB	1.1179 (0.39, 1.85)	0.40	0.3617 (0.04, 0.68)	0.40
A02	ALOX12	0.9958 (0.52, 1.4)	0.93	1.6753 (0.72, 2.63)	0.16
A03	ANGPTL7	1.0344 (0.15, 1.92)	0.88	1.2265 (0.24, 2.21)	0.61
A04	AOX1	1.284 (0.41, 2.16)	0.33	1.4503 (0.53, 2.37)	0.26
A05	APOE	0.4976 (0.09, 0.90)	0.23	0.4933 (0.15, 0.83)	0.13
A06	ATOX1	1.254 (0.64, 1.87)	0.29	1.0913 (0.57, 1.61)	0.42
A07	BNIP3	1.1702 (0.49, 1.85)	0.35	1.0433 (0.46, 1.62)	0.51
A08	CAT	1.2298 (0.49, 1.97)	0.32	1.2927 (0.50, 2.09)	0.24
A09	CCL5	1.5625 (0.61, 2.52)	0.23	1.6758 (0.81, 2.54)	0.18
A10	CCS	1.0727 (0.61, 1.53)	0.54	1.2317 (0.63, 1.83)	0.33
A11	CSDE1	1.5133 (0.67, 2.35)	0.18	1.8196 (0.64, 3.00)	0.15
A12	CYBA	0.9105 (0.00001, 3.49)	0.52	0.1724 (0.00001, 0.69)	0.99
B01	CYGB	1.2195 (0.39, 2.05)	0.41	1.8125 (0.35, 3.28)	0.17
B02	DGKK	1.7295 (0.14, 3.32)	0.23	2.1521 (0.60, 3.70)	0.25
B03	DHCR24	1.7819 (0.73, 2.84)	0.13	1.6145 (0.60, 2.63)	0.21
B04	DUOX1	1.2612 (0.37, 2.15)	0.35	1.8658 (0.59, 3.15)	0.08
B05	DUOX2	0.9715 (0.19, 1.75)	0.46	2.1072 (0.19, 4.03)	0.27
B06	DUSP1	1.4253 (0.00001, 3.00)	0.34	1.9288 (0.00001, 4.29)	0.25
B07	EPHX2	1.372 (0.52, 2.22)	0.32	1.5073 (0.63, 2.39)	0.17
B08	EPX	1.1322 (0.67, 1.60)	0.61	1.2433 (0.64, 1.85)	0.31
B09	FOXM1	1.2019 (0.55, 1.85)	0.39	1.1309 (0.63, 1.63)	0.57
B10	GLRX2	1.2404 (0.53, 1.95)	0.27	1.2843 (0.62, 1.95)	0.24
B11	GPR156	1.2281 (0.05, 2.40)	0.81	1.8693 (0.12, 3.62)	0.34
B12	GPX1	2.0383 (0.69, 3.38)	0.16	0.6747 (0.00001, 1.96)	0.29
C01	GPX2	0.8685 (0.40, 1.34)	0.75	1.1468 (0.60, 1.69)	0.55
C02	GPX3	1.1353 (0.42, 1.85)	0.44	1.5708 (0.46, 2.68)	0.20
C03	GPX4	1.2254 (0.47, 1.99)	0.32	1.1092 (0.39, 1.82)	0.40
C04	GPX5	1.7268 (0.19, 3.27)	0.35	2.4415 (0.37, 4.51)	0.25
C05	GPX6	0.8715 (0.00001, 1.75)	0.89	2.4817 (0.32, 4.64)	0.19
C06	GPX7	1.1942 (0.63, 1.76)	0.33	1.0485 (0.56, 1.54)	0.46
C07	GSR	2.1519 (1.09, 3.21)	**0.03**	2.5617 (1.18, 3.94)	**0.02**
C08	GSS	1.1348 (0.61, 1.66)	0.36	1.1513 (0.61, 1.70)	0.34
C09	GSTZ1	0.9577 (0.45, 1.46)	0.58	1.0105 (0.50, 1.52)	0.52
C10	GTF2I	1.3588 (0.67, 2.05)	0.21	1.628 (0.75, 2.51)	0.17
C11	KRT1	1.3098 (0.00001, 3.39)	0.27	3.1587 (0.08, 6.24)	0.05
C12	LPO	1.2799 (0.00001, 2.81)	0.80	2.5321 (0.00001, 5.17)	0.31
D01	MBL2	1.7289 (0.00001, 4.09)	0.33	2.4117 (0.11, 4.71)	0.46
D02	MGST3	0.9745 (0.41, 1.54)	0.60	0.8496 (0.36, 1.34)	0.75
D03	MPO	1.75 (0.20, 3.30)	0.27	1.6397 (0.48, 2.80)	0.20
D04	MPV17	1.1417 (0.59, 1.69)	0.35	1.0239 (0.59, 1.46)	0.47
D05	MSRA	1.2396 (0.58, 1.90)	0.31	1.2218 (0.65, 1.80)	0.29
D06	MT3	0.647 (0.00001, 1.36)	0.54	0.6572 (0.17, 1.15)	0.71
D07	MTL5	1.2307 (0.55, 1.92)	0.34	1.3221 (0.68, 1.97)	0.25
D08	NCF1	1.773 (0.51, 3.03)	0.23	2.0089 (0.77, 3.24)	0.16
D09	NCF2	1.574 (0.17, 2.97)	0.27	1.9353 (0.62, 3.25)	0.21
D10	NME5	1.5331 (0.72, 2.34)	0.21	1.3656 (0.78, 1.95)	0.22

D11	NOS2	1.0021 (0.31, 1.69)	0.51	1.2781 (0.57, 1.98)	0.24
D12	NOX5	1.0069 (0.22, 1.79)	0.84	1.4021 (0.14, 2.67)	0.22
E01	NUDT1	1.1948 (0.61, 1.78)	0.33	1.0693 (0.55, 1.59)	0.43
E02	OXR1	1.1867 (0.54, 1.84)	0.30	1.2511 (0.56, 1.94)	0.29
E03	OXSR1	1.4271 (0.57, 2.28)	0.22	1.6217 (0.63, 2.61)	0.19
E04	PDLIM1	1.5253 (0.76, 2.29)	0.18	1.7638 (0.74, 2.79)	0.22
E05	IPCEF1	1.3406 (0.00001, 2.73)	0.28	2.0201 (0.61, 3.43)	0.22
E06	PNKP	1.3042 (0.52, 2.09)	0.27	1.7765 (0.61, 2.94)	0.12
E07	PRDX1	1.3351 (0.71, 1.96)	0.20	1.3653 (0.75, 1.98)	0.23
E08	PRDX2	1.2548 (0.55, 1.96)	0.33	1.0468 (0.43, 1.67)	0.45
E09	PRDX3	1.3641 (0.59, 2.14)	0.22	1.1413 (0.57, 1.71)	0.35
E10	PRDX4	1.492 (0.79, 2.19)	0.16	1.5539 (0.87, 2.24)	0.16
E11	PRDX5	1.0794 (0.62, 1.54)	0.43	0.9967 (0.53, 1.47)	0.48
E12	PRDX6	1.0168 (0.55, 1.48)	0.58	0.9192 (0.37, 1.47)	0.52
F01	PREX1	1.2472 (0.34, 2.16)	0.33	1.8366 (0.54, 3.13)	0.22
F02	PRG3	0.9849 (0.00001, 2.09)	0.93	2.763 (0.07, 5.45)	0.27
F03	PRNP	1.8128 (0.07, 3.56)	0.38	1.373 (0.29, 2.45)	0.83
F04	PTGS1	1.3193 (0.62, 2.02)	0.25	1.2079 (0.59, 1.83)	0.27
F05	PTGS2	1.7331 (0.00001, 4.29)	0.29	1.7102 (0.00001, 3.76)	0.30
F06	PXDN	1.2418 (0.53, 1.95)	0.29	1.1421 (0.54, 1.74)	0.39
F07	PXDNL	0.7038 (0.00001, 1.46)	0.38	0.6323 (0.10, 1.16)	0.15
F08	RNF7	1.1085 (0.59, 1.63)	0.38	0.8882 (0.47, 1.31)	0.60
F09	SCARA3	1.4675 (0.57, 2.37)	0.23	2.0141 (0.61, 3.41)	0.15
F10	SELS	1.2514 (0.63, 1.87)	0.30	1.5521 (0.58, 2.52)	0.24
F11	SEPP1	1.1333 (0.46, 1.80)	0.35	1.3185 (0.66, 1.97)	0.30
F12	SFTPD	1.12 (0.28, 1.96)	0.60	1.3591 (0.40, 2.31)	0.29
G01	SGK2	1.1225 (0.19, 2.06)	0.70	1.4311 (0.15, 2.71)	0.37
G02	SIRT2	1.1415 (0.48, 1.81)	0.40	1.5681 (0.52, 2.62)	0.19
G03	SOD1	1.1593 (0.56, 1.76)	0.37	1.0501 (0.52, 1.58)	0.45
G04	SOD2	1.3707 (0.21, 2.53)	0.29	1.8217 (0.43, 3.21)	0.25
G05	SOD3	1.7483 (0.65, 2.84)	0.15	2.267 (0.53, 4.00)	0.14
G06	SRXN1	1.6644 (0.55, 2.78)	0.18	2.3422 (0.61, 4.08)	0.13
G07	STK25	1.2846 (0.57, 2.00)	0.27	1.4982 (0.55, 2.45)	0.23
G08	TPO	1.9349 (0.66, 3.21)	0.09	2.6356 (0.82, 4.45)	0.06
G09	TTN	1.1465 (0.61, 1.68)	0.34	1.0769 (0.64, 1.51)	0.49
G10	TXNDC2	1.1822 (0.15, 2.22)	0.49	1.9383 (0.56, 3.32)	0.26
G11	TXNRD1	1.8751 (0.81, 2.94)	0.14	1.8898 (1.01, 2.77)	0.11
G12	TXNRD2	1.1818 (0.58, 1.78)	0.34	0.926 (0.49, 1.36)	0.62

Fold change gene expression in hVAT samples. Green text highlights down-regulation by more than 2-fold. Red text highlights up-regulation by more than 2-fold

APPENDIX 7

Raw data for relative gene expression analysis

Mouse gene expression analysis

GSR

High Glucose/No LPS (HG) v High Glucose/LPS (HGL)

$\Delta CT\ (HG) = 18.12 - 10.49$

$= 7.63$

$\Delta CT\ (HGL) = 18.71 - 10.94$

$= 7.77$

$\Delta\Delta CT = HGL\ \Delta CT - HG\ \Delta CT$

$= 7.77 - 7.63$

$= 0.14$

$X = 2^{-\Delta\Delta CT}$

$X = 0.91$

Low Glucose/No LPS (LG) v Low Glucose/LPS (LGL)

$\Delta CT\ (LG) = 18.19 - 11.20$

$= 6.99$

$\Delta CT\ (LGL) = 18.32 - 10.65$

$= 7.67$

$\Delta\Delta CT = LGL\ \Delta CT - LG\ \Delta CT$

$= 7.67 - 6.99$

$= 0.68$

$X = 2^{-\Delta\Delta CT}$

$X = 0.62$

GPX1

High Glucose/No LPS (HG) v High Glucose/LPS (HGL)

$\Delta CT\ (HG) = 19.53 - 10.49$

$= 9.04$

$\Delta CT\ (HGL) = 19.63 - 10.94$

$= 8.69$

$\Delta\Delta CT = HGL\ \Delta CT - HG\ \Delta CT$

$= 8.69 - 9.04$

$= -0.35$

$X = 2^{-\Delta\Delta CT}$

$X = 1.27$

Low Glucose/No LPS (LG) v Low Glucose/LPS (LGL)

$\Delta CT\ (LG) = 19.04 - 11.20$

$= 7.84$

$\Delta CT\ (LGL) = 20.08 - 10.65$

$= 9.43$

$\Delta\Delta CT = LGL\ \Delta CT - LG\ \Delta CT$

$= 9.43 - 7.84$

$= 1.59$

$X = 2^{-\Delta\Delta CT}$

$X = 0.33$

Human gene expression analysis

GSR

L v O

ΔCT (L) = 24.18 – 17.54

= 6.64

ΔCT (O) = 23.94 – 17.25

= 6.69

$\Delta\Delta CT$ = O ΔCT – L ΔCT

= 6.69 – 6.64

= 0.05

$X = 2^{-\Delta\Delta CT}$

X = 0.97

L v ODM

ΔCT (L) = 24.18 – 17.54

= 6.64

ΔCT (ODM) = 22.89 – 17.44

= 5.45

$\Delta\Delta CT$ = ODM ΔCT – L ΔCT

= 5.45 – 6.64

= -1.19

$X = 2^{-\Delta\Delta CT}$

X = 2.28

O v ODM

$\Delta CT\ (O) = 23.94 - 17.25$

$= 6.69$

$\Delta CT\ (ODM) = 22.89 - 17.44$

$= 5.45$

$\Delta\Delta CT = ODM\ \Delta CT - O\ \Delta CT$

$= 5.45 - 6.69$

$= -1.24$

$X = 2^{-\Delta\Delta CT}$

$X = 2.36$

L v (O + ODM)

$\Delta CT\ (L) = 24.18 - 17.54$

$= 6.64$

$\Delta CT\ (O + ODM) = 23.40 - 17.35$

$= 6.05$

$\Delta\Delta CT = (O + ODM)\ \Delta CT - L\ \Delta CT$

$= 6.05 - 6.64$

$= -0.59$

$X = 2^{-\Delta\Delta CT}$

$X = 1.51$

(L + O) v ODM

$\Delta CT\ (L + O) = 24.07 - 17.40$

$= 6.67$

$\Delta CT\ (ODM) = 22.89 - 17.44$

$= 5.45$

$\Delta\Delta CT = ODM\ \Delta CT - (L + O)\ \Delta CT$

$= 5.45 - 6.67$

$= -1.22$

$X = 2^{-\Delta\Delta CT}$

$X = 2.33$

GPX1

L v O

ΔCT (L) = 19.15 – 17.54

= 1.61

ΔCT (O) = 18.70 – 17.25

= 1.45

ΔΔCT = O ΔCT – L ΔCT

= 1.45 – 1.61

= -0.16

$X = 2^{-\Delta\Delta CT}$

X = 1.12

L v ODM

ΔCT (L) = 19.15 – 17.54

= 1.61

ΔCT (ODM) = 18.20 – 17.57

= 0.63

ΔΔCT = ODM ΔCT – L ΔCT

= 0.63 – 1.61

= -0.98

$X = 2^{-\Delta\Delta CT}$

X = 1.97

O v ODM

ΔCT (O) = 18.70 – 17.25

= 1.45

ΔCT (ODM) = 18.20 – 17.57

= 0.63

ΔΔCT = ODM ΔCT – O ΔCT

= 0.63 – 1.45

= -0.82

$X = 2^{-\Delta\Delta CT}$

X = 1.77

L v (O + ODM)

ΔCT (L) = 19.15 – 17.54

= 1.61

ΔCT (O + ODM) = 18.45 – 17.41

= 1.04

$\Delta\Delta CT = (O + ODM)\ \Delta CT - L\ \Delta CT$

= 1.04 – 1.61

= -0.57

$X = 2^{-\Delta\Delta CT}$

X = 1.48

(L + O) v ODM

ΔCT (L + O) = 18.94 – 17.40

= 1.54

ΔCT (ODM) = 18.20 – 17.57

= 0.63

$\Delta\Delta CT = ODM\ \Delta CT - (L + O)\ \Delta CT$

= 0.63 – 1.54

= -0.91

$X = 2^{-\Delta\Delta CT}$

X = 1.88

IL-6

L v O

$\Delta CT\ (L) = 26.78 - 17.54$

$= 9.24$

$\Delta CT\ (O) = 24.90 - 17.25$

$= 7.65$

$\Delta\Delta CT = O\ \Delta CT - L\ \Delta CT$

$= 7.65 - 9.24$

$= -1.59$

$X = 2^{-\Delta\Delta CT}$

$X = 3.01$

L v ODM

$\Delta CT\ (L) = 26.78 - 17.54$

$= 9.24$

$\Delta CT\ (ODM) = 25.66 - 17.44$

$= 8.22$

$\Delta\Delta CT = ODM\ \Delta CT - L\ \Delta CT$

$= 8.22 - 9.24$

$= -1.02$

$X = 2^{-\Delta\Delta CT}$

$X = 2.03$

O v ODM

$\Delta CT\ (O) = 24.90 - 17.25$

$= 7.65$

$\Delta CT\ (ODM) = 25.66 - 17.44$

$= 8.22$

$\Delta\Delta CT = ODM\ \Delta CT - O\ \Delta CT$

$= 8.22 - 7.65$

$= 0.57$

$X = 2^{-\Delta\Delta CT}$

$X = 0.67$

L v (O + ODM)

ΔCT (L) = 26.78 – 17.54

= 9.24

ΔCT (O + ODM) = 25.29 – 17.35

= 7.94

$\Delta\Delta CT$ = (O + ODM) ΔCT – L ΔCT

= 7.94 – 9.24

= -1.30

$X = 2^{-\Delta\Delta CT}$

X = 2.46

(L + O) v ODM

ΔCT (L + O) = 25.90 – 17.40

= 8.50

ΔCT (ODM) = 25.66 – 17.44

= 8.22

$\Delta\Delta CT$ = ODM ΔCT – (L + O) ΔCT

= 8.22 – 8.50

= -0.28

$X = 2^{-\Delta\Delta CT}$

X = 1.21

PPARγ

L v O

$\Delta CT\ (L) = 20.42 - 17.54$

$= 2.88$

$\Delta CT\ (O) = 20.76 - 17.25$

$= 3.51$

$\Delta\Delta CT = O\ \Delta CT - L\ \Delta CT$

$= 3.51 - 2.88$

$= 0.63$

$X = 2^{-\Delta\Delta CT}$

$X = 0.65$

L v ODM

$\Delta CT\ (L) = 20.42 - 17.54$

$= 2.88$

$\Delta CT\ (ODM) = 20.91 - 17.44$

$= 3.47$

$\Delta\Delta CT = ODM\ \Delta CT - L\ \Delta CT$

$= 3.47 - 2.88$

$= 0.59$

$X = 2^{-\Delta\Delta CT}$

$X = 0.66$

O v ODM

$\Delta CT\ (O) = 20.76 - 17.25$

$= 3.51$

$\Delta CT\ (ODM) = 20.91 - 17.44$

$= 3.47$

$\Delta\Delta CT = ODM\ \Delta CT - O\ \Delta CT$

$= 3.47 - 3.51$

$= -0.04$

$X = 2^{-\Delta\Delta CT}$

$X = 1.03$

L v (O + ODM)

ΔCT (L) = 20.42 – 17.54

= 2.88

ΔCT (O + ODM) = 20.84 – 17.35

= 3.49

ΔΔCT = (O + ODM) ΔCT – L ΔCT

= 3.49 – 2.88

= 0.61

$X = 2^{-\Delta\Delta CT}$

X = 0.66

(L + O) v ODM

ΔCT (L + O) = 20.58 – 17.40

= 3.18

ΔCT (ODM) = 20.91 – 17.44

= 3.47

ΔΔCT = ODM ΔCT – (L + O) ΔCT

= 3.47 – 3.18

= 0.29

$X = 2^{-\Delta\Delta CT}$

X = 0.82

APPENDIX 8

List of published abstracts

Jones DA, Prior SL, Baxter JN, Barry JD, Bain SC, Stephens JW (2013) Comet analysis of visceral fat samples from patients with obesity and Type 2 diabetes.

Diabetes UK APC 2013, *Diab. Med.* 2013, 30, Suppl 1, P63

5th International Congress on Prediabetes and the Metabolic Syndrome 2013

Jones DA, Prior SL, Baxter JN, Bain SC, Stephens JW (2012) Oxidative and RNA damage in visceral fat samples from patients with obesity and Type 2 diabetes.

Diabetes UK APC 2012. *Diab. Med.* 2012, 29, Suppl 1, P70

Welsh Endocrine and Diabetes Society Meeting 2012

Jones DA, Prior SL, Baxter JN, Bain SC, Stephens JW (2011) Obesity-related type 2 diabetes is associated with reduced gene expression of GPx1 in visceral adipose tissue.

Diabetes UK APC 2011. *Diab. Med.* 2011, 28, Suppl 1, P47

Welsh Endocrine and Diabetes Society Meeting 2011

APPENDIX 9

Company addresses

Company addresses

Ambion Inc.

http://www.invitrogen.com/site/us/en/home/brands/ambion.html?CID=fl-ambion

Bioline

https://www.bioline.com/h_uk.asp

BioRad

http://www.bio-rad.com

BMG Labtech

http://www.bmglabtech.com

Cambridge Bioscience

http://www.bioscience.co.uk/home

Cell Biolabs

http://www.cellbiolabs.com

Eurofins MWG Operon

http://www.eurofinsgenomics.eu

Invitrogen

http://www.invitrogen.com/site/us/en/home.html

Millipore

http://www.millipore.com

MP Biomedicals

http://www.mpbio.com/GB/Pages/Default.aspx

Qiagen

http://www.qiagen.com

Sigma-Aldrich

http://www.sigmaaldrich.com/united-kingdom.html

Source Bioscience

http://www.sourcebioscience.com

Thermo Scientific

http://www.thermoscientific.com/ecomm/servlet/home?storeId=11152

Zeiss

http://corporate.zeiss.com/country-page/en_gb/home.html

References

Ahmadpoor, P., Eftekhar, E., Nourooz-Zadeh, J., Servat, H., Makhdoomi, K. and Ghafari, A. (2009) Glutathione, glutathione related enzymes and total antioxidant capacity in patients on maintenance dialysis. *IJKD* **3:** 22-27

Anderson, D., Yu, T.W., Wright, J. and Ioannides, C. (1998) An examination of DNA strand breakage in the comet assay and antioxidant capacity in diabetic patients. *Mutat. Res.* **398**: 151-161

Andrulionytè, L., Zacharova, J., Chiasson, J. L., Laakso, M. and STOP-NIDDM Study Group (2004) Common polymorphisms of the PPAR-γ2 (Pro12Ala) and PGC-1a (Gly482Ser) genes are associated with the conversion from impaired glucose tolerance to type 2 diabetes in the STOP-NIDDM trial. *Diabetologia.* **47**: 2176-2184

Apelt, N., De Silva, A. P., Ferreira, J., Albo, I., Monteiro, C., Marinho, C., Teixeira, P., Sardinha, L., Laires, M. J., Mascarenhas, M. R. and Bicho, M. P. (2009) ACP1 genotype, glutathione reductase activity, and riboflavin uptake affect cardiovascular risk in the obese. *Metabolism* **58:** 1415 - 1423

Armstrong, D. and al-Awadi, F. (1991) Lipid peroxidation and retinopathy in streptozotocin-induced diabetes. *Free Radical Bio. Med.* **11:** 433-436

Armstrong D. and Browne, R. (1994) The analysis of free radicals, lipid peroxides, antioxidant enzymes and compounds related to oxidative stress as applied to the clinical chemistry laboratory. *Adv. Exp. Med. Biol.* **366:** 43-58

Astrup, A. S., Tarnow, L., Jorsal, A., Lajer, M., Nzietchueng, R., Benetos, A., Rossing, P. and Parving, H. H. (2010) Telomere length predicts all-cause mortality in patients with type 1 diabetes. *Diabetologia* **53:** 45-48

Ballatori, N., Krance, S. M., Notenboom, S., Shi, S., Tieu, K. and Hammond, C. L. (2009) Glutathione dysregulation and the etiology and progression of human diseases. *Biol. Chem.* **390**: 191-214

Baynes, J.W. (1991) Role of oxidative stress in development of complications in diabetes. *Diabetes* **40:** 405–412

Beck-Nielsen, H. and Hother-Niesen, O. (1996) in Diabetes Mellitus: A Fundamental and Clinical Text, eds. LeRoith, D., Taylor, S. & Olefsky, J. (Lippincott-Raven, Philadelphia), pp. 475–484

Blasiak, J., Arabski, M., Krupa, R., Wozniak, K., Zadrozny, M., Kasznicki, J., Zurawska, M. and Drzewoski, J. (2004) DNA damage and repair in type 2 diabetes mellitus. *Mutat. Res.* **554:** 279-304

Bouchard, C., Despres, J. P. and Mauriege, P. (1993) Genetic and nongenetic determinants of regional fat distribution. *Endocr. Rev.* **14:** 72-93

Boulton, A. J. M., Vinik, A.I., Arezzo, J. C., Bril, V., Feldman, E. L., Freeman, R., Malik, R. A., Maser, R. E., Sosenko, J. M. and Zielgler, D. (2005) Diabetic Neuropathies: A statement by the American Diabetes Association. *Diabetes Care*, **28:** 956- 962

Boutet, M., Roland, L., Thomas, N. and Bilodeau, J. F. (2009) Specific systemic antioxidant response to preeclampsia in late pregnancy: the study of intracellular glutathione peroxidases in maternal and fetal blood. *Am. J. Obstet. Gynecol.* **200:** e1-e7

Brandes, R. P. and Janiszewski, M. (2005) Direct detection of reactive oxygen species ex vivo. *Kidney Int.* **67**: 1662–1664

Bravi, M. C., Armiento, A., Laurenti, O., Cassone-Faldetta, M., De Luca, O., Moretti, A. and De Mattia, G. (2006) Insulin decreases intracellular oxidative stress in patients with type 2 diabetes mellitus. *Metabolism* **55**: 691– 695

Brigelius-Flohe R. and Kipp A. (2009) Glutathione peroxidases in different stages of carcinogenesis. *Biochim. Biophys. Acta* **1790:** 1555–1568

Bukhari, S. A., Rajoka, M. I., Nagra, S. A. and Rehman, Z. U. (2010) Plasma homocysteine and DNA damage profiles in normal and obese subjects in the Pakistani population. *Mol. Biol. Rep.* **37:** 289-295

Calabrese, V., Cornelius, C., Leso, V., Trovato-Salinaro, A., Ventimiglia, B., Cavallaro, M., Scuto, M., Rizza, S., Zanoli, L. and Castellino, P. (2012) Oxidative stress, glutathione status, sirtuin and cellular stress response in type 2 diabetes. *Biochim. Biophys. Acta* **1822:** 729-736

Capurso, C. and Capurso, A. (2012) From excess adiposity to insulin resistance: The role of free fatty acids. *Vasc. Pharmacol.* **57:** 91-97

Catherwood, M. A., Powell, L. A., Anderson, P., McMaster, D., Sharpe, P.C. and Trimble, E. R. (2002) Glucose-induced oxidative stress in mesangial cells. *Kidney. Int.* **61**: 599-608

Cawthon, R. M. (2002) Telomere measurement by quantitative PCR. *Nucleic Acids Res.* **30:** e47

Cerda, H., Delincee, H., Haine, H. and Rupp, H. (1997) The DNA 'comet assay' as a rapid screening technique to control irradiated food. *Mutat. Res.* **375:** 167-181

Chistyakov, D. A., Sayost'anov, K. V., Zotova, E. V. and Nosikov, V.V. (2001) Polymorphisms in the Mn-SOD and EC-SOD genes and their relationship to diabetic neuropathy in type 1 diabetes mellitus. *BMC Med. Genet.* **2:** 4

Cinti, S., Mitchell, G., Barbatelli, G., Murano, I., Ceresi, E., Faloia, E., Wang, S., Fortier, M., Greenberg, A. S. and Obin, M. S. (2005) Adipocyte death defines macrophage localization and function in adipose tissue of obese mice and humans. *J. Lip. Res.* **46**: 2347-2355

Circu, M. L. and Yee Aw, T. (2008) Glutathione and apoptosis. *Free Radic. Res.* **42**: 689-706

Claffey, K. P, Wilkison, K. P. and Spiegelmann, W. O. (1992) Vascular Endothelial Growth Factor: Regulation by cell differentiation and activated second messanger pathways. *J. Biol. Chem.* **267**: 16317-16322

Codoner, P., Valls-Belles, V., Arilla-Codoner, A. and Alonso-Iglasias, E. (2011) Oxidant mechanisms in childhood obesity: the link between inflammation and oxidative stress, *Transl. Res.* **158**: 369-384

Collins, A.R., Raslova, K., Somorovska, M., Petrovska, H., Ondrusova, A., Vohnout, B., Fabry, R. and Dusinska, M. (1998) DNA damage in diabetes: Correlation with a clinical marker. *Free Radical Bio. Med.* **25**: 373-377

Corrales, R. M., Galarreta, D., Herreras, J., Calonge, M. and Chaves, F. (2011) Antioxidant enzyme mRNA expression in conjunctival epithelium of healthy human subjects. *Can. J. Ophthalmol.* **46:** 35-39

Dandana, A., Gammoudi, I., Ferchichi, S., Chahed, H., Limam, H. B., Addad, F., Miled, A. (2011) Correlation of oxidative stress parameters and inflammatory markers in Tunisian coronary artery disease patients. *Int. J. Biomed. Sci.* **7**:6-13

Del Rio, D., Stewart, A. J. and Pellegrini, N. (2005) A review of recent studies on malondialdehyde as toxic molecule and biological marker of oxidative stress. *NMCD* **15:** e328

D'Esposito, V., Passaretti, F., Hammarstedt, A., Liguoro, D., Terracciano, D., Molea, G., Canta, L., Miele, C., Smith, U., Beguinot, F. and Formisano, P. (2012) Adipocyte-released insulin-like growth factor-1 is regulated by glucose and fatty acids and controls breast cancer cell growth in vitro, *Diabetologia* **55:** 2811–2822

Diaz-Llera, S., Podlutsky, A., Osterholm, A. M., Hou, S. M. and Lambert, B. (2000) Hydrogen peroxide induced mutations at the HPRT locus in primary human T-lymphocytes. *Mutat. Res.* **469**: 51-61

Dincer, Y., Alademir, Z., Ilkova, H. and Akcay, T. (2002). Susceptibility of glutathione and glutathione-related antioxidant activity to hydrogen peroxide in patients with type 2 diabetes: effect of glycemic control. *Clin. Biochem.* **35**: 297-301

Dincer, Y., Akcay, T., Alademir, Z. and Ilkiva, H. (2002a) Assessment of DNA base oxidation and glutathione level in patients with type 2 diabetes. *Mutat. Res.* **505**: 75-81

Dronavalli, S., Duka, I. and Bakris, G. L. (2008) The pathogenesis of diabetic nephropathy. *Clin. Pract. Endocrinol. Metab.* **4**: 444–452

Eldor, R. and Raz, I. (2006) Lipotoxicity versus adipotoxicity: The deleterious effects of adipose tissue on beta cells in the pathogenesis of type 2 diabetes. *Diabetes Res. Clin. Pr.* **74**: S3-S8

Farbstein, D., Kozak-Blickstein, A. and Levy, A. P. (2013) Antioxidant vitamins and their use in preventing cardiovascular disease. *Molecules* **15**: 8098–8110

Farooqi, I. S. and O'Rahilly, S. (2005) Monogenic Obesity in Humans. *Annu. Rev. Med.* **56**: 443-458

Flekac, M., Skrha, J., Hilgertova, J., Lacinova, Z. and Jarolimkova, M. (2008) Gene polymorphisms of superoxide dismutases and catalase in diabetes mellitus. *BMC Med. Genet.* **9**: 30

Fraga, C. G, Shigenaga, M. K., Park, J. W., Degan, P. and Ames B. N. (1990) Oxidative damage to DNA during aging: 8-hydroxy-2'deoxyguanosine in rat organ DNA and urine. *Proc. Natl. Acad. Sci. U.S.A.* **87**: 4533-4537

Fried, S. K., Bunkin, D. A. and Greenberg, A. S. (1997) Omental and subcutaneous adipose tissue of obese subjects release interleukin-6: Depot difference and regulation by glucocorticoid. *J. Clin. Endocrin. Metab.* **83**: 847-850

Friedrich, U., Griese, E., Schwab, M., Fritz, P., Thon, K. and Klotz, U. (2000) Telomere length in different tissues of elderly patients. *Mech. Ageing. Dev.* **119:** 89-99

Furukawa, S., Fujita, T., Shimabukuro, M., Iwaki, M., Yamada, Y., Nakajima, Y., Nakayama, O., Makishima, M., Matsuda, M. and Shimomura, I. (2013) Increased oxidative stress in obesity and its impact on metabolic syndrome. *J. Clin. Invest.* **114:** 1752-1761

Gesta, S., Bluher, M., Yamamoto, Y., Norris, A. W., Berndt, J., Kralisch, S., Boucher, J., Lewis, C. and Kahn, C. R. (2006) Evidence for a role of developmental genes in the origin of obesity and body fat distribution. *PNAS* **103**: 6676–6681

Gopaul, N. K., Anggard, E. E., Mallet, A. I., Betteridge, D. J.,Wolj, S. P. and Nourooz-Zadeh, J. (1995) Plasma 8-epi-PGF2-alpha levels are elevated in individuals with non-insulin dependent diabetes mellitus. *FEBS Lett.* **368**: 225-229

Griesmacher, A., Kindhauser, M., Andert, S. E., Schneiner, W., Toma, C., Knoebl, P., Pietschmann, P., Prager, R., Schnack, C., Schernthaner, G. and Mueller, M. M. (1995) Enhanced serum levels of thiobarbituric acid-reactive substances in diabetes mellitus. *Am. J. Med.* **98**: 469–475

Griffith, O. W. and Meister, A. (1979) Potent and specific inhibition of glutathione synthesis by buthionine sulphoximine (S-n-butyl homocysteine sulfoximine). *J. Biol. Chem.* **254**: 7558- 7560

Gross, J. L., de Azevedo, M. J., Silveiro, S. P., Canani, L. H., Caramori, M. L. and Zelmanovitz, T. (2005) Diabetic Nephropathy: Diagnosis, Prevention, and Treatment, *Diabetes Care* **28:** 164-176

Hahn, P. and Novak, M. (1975) Development of brown and white adipose tissue. *J. Lipid Res.* **16**: 79-91

Hajer, GR., van Haeften, TW., Visseren, FLJ. (2008) Adipose tissue dysfunction in obesity, diabetes, and vascular diseases. *Eur. Heart J.* **29**: 2959-2971

Halliwell, B. (1992) Reactive oxygen species and the central nervous system. *J. Neurochem.* **59:** 1609–1623

Hamilton, M.L., Remman, H.V., Drake, J.A., Yang, H., Guo, Z.M., Kewitt, K., Walter, C.A. and Richardson, A. (2001) Does oxidative damage to DNA increase with age? *Proc. Natl. Acad. Sci. U.S.A.* **98**: 10469-10474

Hartz, A. J., Rupley. D. C., Kalkhoff, R. D. and Rimm, A. A. (1983) Relationship of obesity to diabetes: Influence of obesity level and body fat distribution. *Prev. Med.* **12**: 351-357

Helmersson, J., Vessby, B., Larsson, A. and Basu, S. (2004) Association of Type 2 Diabetes With Cyclooxygenase-Mediated Inflammation and Oxidative Stress in an Elderly Population. *Circulation* **109:** 1729-1734

Helmrich, S. P., Ragland, D. R., Leung, R. W. and Paffenbarger, R. S. (1991) Physical activity and reduced occurence of non-insulin-dependent diabetes mellitus. *New Eng. J. Med.* **325**: 147-152

Helton, E. S. and Chen, X. (2007) p53 modulation of the DNA damage response. *J. Cell.Biochem.* **100**: 883-896

Hirrlinger, J. and Dringen, R. (2010) The cytosolic redox state of astrocytes: Maintenance, regulation and functional implications for metabolite trafficking. *Brain Res. Rev.* **63:** 177–188

Hotamisligil, G. S., Shargill, N. S. and Spiegelman, B. M. (1993) Adipose expression of tumor necrosis factor-α: direct role in obesity-linked insulin resistance. *Science* **259:** 87-91

Hotamisligil, G. S. and Erbay, E. (2008) Nutrient sensing and inflammation in metabolic diseases. *Nat. Rev. Immunol.* **8**: 923

Houben, J. M. J., Moonen, H. J. J., van Schooten, F. J. and Hageman, G. J. (2008) Telomere length assessment: Biomarker of chronic oxidative stress? *Free Rad. Biol. Med.* **44**: 235-246

Hruz, T., Wyss, M., Docquier, M., Pfaffl, M. W., Masanetz, S., Borghi, L., Verbrugghe, P., Kalaydjieva, L., Bleuler, S., Laule, O., Descombes, P., Gruissem, W. and Zimmermann, P. (2011) RefGenes: identification of reliable and condition specific reference genes for RT-qPCR data normalization. *BMC Genet.* **12:** 156

Huh, J. Y., Kim, Y., Jeong, J., Park, J., Kim, I., Huh, K. H., Kim, Y. s., Woo, H. A., Rhee, S. G., Lee, K. J. and Ha, H. (2012) Peroxiredoxin 3 is a key molecule regulating adipocyte oxidative stress, mitochondrial biogenesis, and adipokine expression. *Antioxid. Redox Sign.* **16**: 229-243

Hussain, S. P., Amsted, P. and He, P. (2004) p53-induced up-regulation of mn-SOD and GPx but not catalase increases oxidative stress and apoptosis. *Cancer.Res.* **64:** 2350-2356

Ibarra-Costilla, E., Cerda-Flores, R. M., Davilla-Rodriquez, M. I., Samayo-Reyes, A., Calzado-Florez, C. and Cortes-Gutierrez, E. I. (2010) DNA damage evaluated by comet assay in Mexican patients with type 2 diabetes mellitus. *Acta. Diabetol.* **47**: 111-116

Inge, T. H., Jenkins, T. M., Zeller, M., Dolan, L., Daniels, S. R., Garcia, V. F., Brandt, M. L., Bean, J., Gamm, K. and Xanthakos, S. A. (2010) Baseline BMI is a strong predictor of nadir BMI after adolescent gastric bypass. *J Pediatr.* **156:** 103-108

Insenser, M., Montes-Nieto, R., Vilarrasa, N., Lecube, A., Simo, R., Vendrall, J. and Escobar-Morreale HF (2012) A nontargeted proteomic approach to the study of visceral and subcutaneous adipose tissue in human obesity. *Mol. Cell. Endocrinol.* **363:** 10-19

Ibrahim, M. M. (2010) Subcutaneous and visceral adipose tissue: structural and functional differences. *Obes. Rev.* **11:** 11–18

Iyer, A., Fairlie,D. P., Prins,J. B., Hammock, B. D. and Brown, L. (2010) Inflammatory lipid mediators in adipocyte function and obesity. *Nat. Rev. Endocrinol.* **6**: 71–82

Kakkar, R., Kalra, J., Mantha, S.V. and Prasad, K. (1995) Lipid peroxidation and activity of antioxidant enzymes in diabetic rats. *Mol. Cell Biochem.* **151**: 113–119

Kissebah, A. H., Vydelingum, N., Murray, R., Evans, D. J., Kalkhoff, R. K. and Adams, P. W. (1982) Relation of body fat distribution to metabolic complications of obesity. *J. Clin. Endocrin Metab.* **54**: 254

Karge, W. H., Schaefer, E. J. and Ordovas, J. M. (1998) Quantification of mRNA by polymerase chain reaction (PCR) using an internal standard and a nonradioactive detection method. *Methods Mol Biol.* **110:** 43-61

Keaney, J. F., Larson, M. G., Vasan, R. S., Wilson, P. W. F., Lipinska, I., Corey, D., Massaro, J. M., Sutherland, P., Vita, J. A. and Benjamin, E. J. (2003) Obesity and Systemic Oxidative Stress : Clinical Correlates of Oxidative Stress in The Framingham Study. *Arterioscler. Thromb. Vasc. Biol.* **23:** 434-439

Kelner, M. J. and Montoya, M. A. (2000) Structural organization of the human glutathione reductase gene: determination of correct cDNA sequence and identification of a mitochondrial leader sequence. *Biochem. Biophys. Res. Commun.* **269:** 366–368

Kheterpal, I., Ku, G., Coleman, L., Yu, G., Ptitsyn, A. A., Floyd, Z. E. and Gimble, J. M. (2011) Proteome of human subcutaneous adipose tissue stromal vascular fraction cells versus mature adipocytes based on DIGE. *J. Proteome Res.* **10:** 1519-1527

Kiritoshi, S., Nishikawa, T., Sonoda. K., Kukidome, D., Senokuchi, T., Matsuo, T., Matsumura, T., Tokunaga, H., Brownlee, M. and Araki, E (2003) Reactive oxygen

species from mitochondria induce cyclooxygenase-2 gene expression in human mesangial cells: potential role in diabetic nephropathy. *Diabetes* 52: 2570-2577

Kizaki, T., Suzuki, K., Hitomi, Y., Taniguchi, N., Saitoh, D., Watanabe, K., Onoe, K., Day, N. K., Good, R. A. and Ohno, H. (2002) Uncoupling protein 2 plays an important role in nitric oxide production of lipopolysaccharide-stimulated macrophages. *Proc. Natl. Acad. Sci. USA* **99:** 9392-9397

Kowalska, I. (2007) Role of adipose tissue in the development of vascular complications in type 2 diabetes mellitus. *Diabetes Res. Clin. Pr.* **78**: S14-S22

Kristiansen, O. P. and Mandrup-Poulsen, T. (2005) Interleukin-6 and Diabetes: The Good, the Bad, or the Indifferent? *Diabetes* **54: s115-s124**

Kushwaha, S., Vikram, A., Trivedi, P.P. and Jena, G.B. (2011) Alkaline, Endo III and FPG modified comet assay as biomarkers for the detection of oxidative DNA damage in rats with experimentally induced diabetes. *Mutat. Res.* **726**, 242-250

Lee, S. J., Choi, M. G., Kim, D. S. and Kim, T. W. (2006) Manganese superoxide dismutase gene polymorphism (V16A) is associated with stages of albuminuria in Korean type 2 diabetic patients. *Metabolism* **55**: 1-7

Lee, P., Swarbrick, M. M. and Ho, K. K. Y. (2013) Brown Adípose Tissue in Adult Humans: A Metabolic Renaissance. *Endocr. Rev.* **in press**

Lima, S. C. V. C., Arrais, R. F., Almeida, M. G., Souza, Z. M. and Pedrosa, L. F. C. (2004) Plasma lipid profile and lipid peroxidation in overweight or obese children and adolescents. J. Pediatria **80:** 23-28

Livak, K. J. and Schmittgen, T. D. (2001) Analysis of relative gene expression data using real-time quantitative PCR and the 2(-Delta Delta C(T)) Method. *Methods* **25:** 402-408

Lodovici, M., Giovannelli, L., Pitozzi, V., Bigagli, E., Bardini, G. and Rotella, C. M. (2008) Oxidative DNA damage and plasma antioxidant capacity in type 2 diabetic patients with good and poor glycaemic control. *Mutat. Res.* **638:** 98-102

Lyons, T. J. (1991) Oxidized low density lipoproteins: a role in the pathogenesis of atherosclerosis in diabetes? *Diab. Med.* **8**: 411–419

Manfredini, V., Biancini, G.B., Vanzin, C.S., Ribeiro Dal Vesco, A.M., Cipriani, F., Biasi, L., Tremea, R., Decon, M., Peralba, M.C.R., Wajner, M. and Vargas, C.R. (2010) Simvastatin treatment prevents oxidative damage to DNA in whole blood leukocytes of dyslipidemic type 2 diabetic patients. *Cell Biochem. Funct.* **28**: 360-366

Maritim, A. C., Sanders, R.A. and Watkins, J.B. (2003) Diabetes, oxidative stress, and antioxidants: A review. *J. Biochem. Mol. Toxic.* **17**: 24-38

Mathieu, P., Poirier, P., Pibarot, P., Lemieux, I. and Despres, J. P. (2009) Visceral obesity: the link among inflammation, hypertension, and cardiovascular disease. *Hypertension* **53:** 577-584

Mehta, J. L., Rasouli, N., Sinha, A.K. and Molavi, B. (2006) Oxidative stress in diabetes: a mechanistic overview of its effects on atherogenesis and myocardial dysfunction. *Int. J. Biochem. Cell Biol.* **38** 794–803

Meister, A. and Tate, S. S. (1976) Glutathione and related gammaglutamyl compounds: biosynthesis and utalization. *Annu. Rev. Biochem.* **45**: 599-604

Merad-Boudia, M., Nicole, A., Santiard-Baron, D., Saille, C. and Ceballos-Picot, I. (1998) Mitochondrial impairment as an early event in the process of apoptosis induced by glutathione depletion in neuronal cells relevance to Parkinson's disease. *Biochem. Pharmacol.* **56**: 645-655

Mironov, A. A., Fickett, J. W. and Gelfand, M. S. (1999) Frequent Alternative Splicing of Human Genes. *Genome Res.* **9:** 1288–1293

Mohamed-Ali, V., Goodrick, S., Rawesh, A., Katz, D. R. and Miles, J. M. (1997) Subcutaneous adipose tissue releases interleukin-6, but not tumour necrosis factor-α, *in vivo. J. Clin. Endocrin. Metab.***82:** 4196-4200

Nadler, S. T., Stoehr, J. P., Schueler, K. L., Tanimoto, G., Yandell, B. S. and Attie, A. D. (2000) The expression of adipogenic genes is decreased in obesity and diabetes mellitus. *PNAS.* **97**: 11371–11376

Pai, E. F. and Schulz, G. E. (1983) The catalytic mechanism of glutathione reductase as derived from x-ray diffraction analysis of reaction intermediates. *J. Biol. Chem.* **259:** 1752-1757

Palazzo, R. P., Bagatini, P. B., Schefer, P. B., Michelsen de Andrade, F. and Maluf, S. M. (2012) Genomic instability in patients with type 2 diabetes millitus on hemodialysis. *REV. Bras. Hematol. Hemater.* **34**: 31-35

Patrono, C. and Fitzgerald, G.A. (1997) Isoprostanes: Potential marker of oxidative stress in atherothrombotic disease. *Arterioscler. Thromb. Vasc. Biol.* **17**: 2309-2315

Pastore, A., Federici, G., Bertini, E. and Piemonte, F. (2003) Analysis of glutathione: implication in redox and detoxification. *Clinica. Chimica. Acta.* ***333:*** 19-39

Peinado, J. R., Jimenez-Gomez, Y., Pulido, M. R., Ortega-Bellido, M., Diaz-Lopez, C., Padillo, F. J., Lopez-Miranda, J., Vazquez-Martinez, R. and Malagon, M. M. (2010) The stromal-vascular fraction of adipose tissue contributes to major differences between subcutaneous and visceral fat depots. *Proteomics* **10:** 3356-3366

Pfaffl, M. W., Horgan, G. W. and Dempfle, L. (2002) Relative expression software tool (REST) for group-wise comparison and statistical analysis of relative expression results in real-time PCR. *Nucleic Acids Res.* **30:** e36

Poirier, P., Giles, T. D., Bray, G. A., Hong, Y., Stern, J. S., Pi-Sunyer, F. X. and Eckel, R. H. (2006) Obesity and cardiovascular disease: pathophysiology, evaluation, and effect of weight loss. *Arterioscler. Thromb. Vasc. Biol.* **26:** 968-976

Prunet-Marcassus, B., Cousin, B., Caton, D., André, M., Pénicaud, L., Casteilla, L. (2006) From heterogeneity to plasticity in adipose tissues: Site-specific differences. *Exp. Cell. Res.* **312**: 727-736

Qiao, M., Kisgati, M., Cholewa, J. M., Zhu, W., Smart, E. J., Sulistio, M. S. and Asmis, A. (2007) Increased expression of glutathione reductase in macrophage decreases atherosclerotic lesion formation in low-density lipoprotein-deficit mice. *Arterioscler. Thromb. Vasc. Biol.* **27**: 1375-1382

Rehman, A., Nourooz-Zadeh, J., Moller, W., Tritschler, H., Pereira, P. and Halliwell, B. (1999) Increased oxidative damage to all DNA bases in patients with type II diabetes mellitus. *FEBS Lett.* **448**, 120-122

Rehman, J., Traktuev, D., Li, J., Merfeld-Clauss, S., Temm-Grove, C. J., Bovenkerk, J. E., Pell, C. L., Johnstone, B. H., Considine, R. V. and March, K. L. (2004) Secretion of

angiogenic and antiapoptotic factors by human adipose stromal cells. *Circulation* **109:** 1292-1298

Rennie, K. L. and Jebb, S. A. (2005) National prevalence of obesity: Prevalence of obesity in Great Britain. *Obes. Rev.* **6**: 11-12

Ritz, E. (2006) Diabetic nephropathy. Saudi J. Kid. Dis. Trans. **17:** 481-490

Ross, R. (1999) Atherosclerosis – an inflammatory disease. *N. Engl. J. Med.* **340**: 115-126

Rossner, P. and Sram, R. J. (2012) Immunochemical detection of oxidatively damaged DNA. *Free Radic. Res.* **46:** 492-522

Sadi, G. and Guray, T. (2009) Gene expressions of Mn-SOD and GPx-1 in streptozotocin induced diabetes: effect of antioxidants. *Mol. Cell. Biochem.* **327:** 127–134

Saito, M., Okamatsu-Ogura, Y., Matsushita, M., Watanabe, K., Yoneshiro, T., Nio-Kobayashi, J., Iwanaga, T., Miyagawa, M., Kameya, T., Nakada, K., Kawai, Y. and Tsujisaki, M. (2009) High Incidence of Metabolically Active Brown Adipose Tissue in Healthy Adult Humans: Effects of Cold Exposure and Adiposity. *Diabetes.* **58**: 1526-1531

Salpea, K. D., Nicaud, V., Tiret, L., Talmud, P. J. and Humphries, S. E. (2008) The association of telomere length with paternal history of premature myocardial infarction in the European Atherosclerosis Research Study II. *J. Mol. Med.* **86:** 815-824

Salpea, K.D., Talmud, P.J., Cooper, J.A., Maubaret, C.G., Stephens, J.W., Abelak, K. and Humphries, S.E. (2009) Association of telomere length with type 2 diabetes, oxidative stress and UCP2 gene variation. *Atherosclerosis*. **209**, 42-50

Sampson, M. J., Hughes, D. A., Gopaul, N., Carrier, M. J. and Davies, I. R. (2002) Plasma F_2 isoprostanes – direct evidence of increased free radical damage during acute hyperglycemia in type 2 diabetes. *Diabetes Care* **25**: 537-541

Saxena, M., Srivastava, N., Banerjee, M. (2013) Association of IL-6, TNF-α and IL-10 gene polymorphisms with type 2 diabetes mellitus. *Mol. Biol. Rep.* **40:** 6271-6279

Sharma, A., Kharb, S., Chugh, S. N., Kakkar, R. and Singh, G. P (2000) Effect of glycemic control and vitamin E supplementation on total glutathione content in non-insulin-dependent diabetes mellitus. *Ann. Nutr. Metab.* **44**: 11-13

Shin, C. S., Moon, B. S., Park, K. S., Kim, S. Y., Park, S. J., Chung, M. H. and Lee, H. K. (2001) Serum 8-hudroxy-guanine levels are increased in diabetic patients. *Diabetes Care* **24:** 733

Shin, M.J., Cho, E.Y., Jang, Y., Lee, J.H., Shim, W.H., Cho, S.Y., Rim, S.J., Kang, S.M., Ha, J.W., Ko, Y.G., Kim, S.S., Park, H.Y. and Chung, N. (2005) A beneficial effect of simvastatin on DNA damage in 242T allele of the NADPH oxidase p22phox in hypercholesterolemia patients. *Clinica. Chemica. Acta*. **360**, 46-51

Shoelson, S. E., Herrero, L. and Naaz, A. (2007) Obesity, Inflammation, and Insulin Resistance. *Gastroenterology* **132**: 2169–2180

Skyler, J. S. and Oddo, C.(2002) Diabetes trends in the USA. *Diabetes Metab. Res. Rev.* **18 Suppl 3:** S21-26

Sliwinska, A., Blasiak, J., Kasznicki, J. and Drzewoski, J. (2008) In vitro effect of gliclazide on DNA damage and repair in patients with type 2 diabetes mellitus (T2DM). *Chem. Biol. Interact.* **173:** 159-165

Stephens, J.W., Gable, D.R., Hurel, S.J., Miller, G.J., Cooper, J.A. and Humphries, S.E. (2006) Increased plasma markers of oxidative stress are associated with coronary heart disease in males with diabetes mellitus and with 10-year risk in a prospective sample of males. *Clin. Chem*. **52:** 446-452

Stephens, J.W., Dhamrait, S. S., Mani, A. R., Acharya, J., Moore, K., Hurel, S. J., Humphries, S. E. (2007) Interaction between the uncoupling protein 2 -866G>A

gene variant and cigarette smoking to increase oxidative stress in subjects with diabetes. *Nutr Metab Cardiovasc Dis*. **18:** 7-14

Stephens, J. W., Khanolkar, M. P. and Bain, S. C. (2008) The biological relevance and measurement of plasma markers of oxidative stress in diabetes and cardiovascular disease. *Atherosclerosis* **202:** 321-329

Sturgeon, K.M., Feairheller, D.L., Diaz, K.M., Williamson, S.T., Veerabhadrappa, P. and Brown, M.D. (2010) Clinical risk factors demonstrate an age-dependant relationship with oxidative stress biomarkers in African Americans. *Ethn. Dis.* **20:** 403-408

Tatsch, E., Bochi, G. V., Piva, S. J., De Carvalho, J. A. M., Kober, H., Torbitz, V. D., Duarte, T., Signor, C., Coelho, A. C., Duerte, M. M. M. F., Montagner, G. F. F. S., De Cruz, I. B. M. and Moresco, R. N. (2012) Association between DNA strand breakage and oxidative, inflammatory and endothelial biomarkers in type 2 diabetes. *Mut. Res.* **732**: 16-20

Thakkar, N. V. and Jain, S. M. (2010) A comparative study of DNA damage in patients suffering from diabetes and thyroid dysfunction and complications. *Clin. Pharmacol.* **2**: 199-205

Toth, M. J., Tchernof, A., Site, C. K. and Poehlman, E. T. (2006) Menopause related changes in body fat distribution. *Ann. N. Y. Acad. Sci*. **904**: 502-506

Trujillo, M. E. and Scherer, P. E. (2006) Adipose Tissue-Derived Factors: Impact on Health and Disease. *Endocrin. Rev.* **27**: 762–778

Turrens, J. F. (2003) Mitochondrial formation of reactive oxygen species. *J. Physiol.* **552:** 335-344

Urata, Y., Yamamoto, H., Goto, S., Tsushima, H., Akazawa, S., Yamashita, S., Nagataki, S. and Kondo, T. (1996) Long exposure to high glucose concentration impairs the responsive expression of gamma-glutamylcysteine synthetase by interleukin-1beta and tumor necrosis factor-alpha in mouse endothelial cells. *J. Biol. Chem.* **271**: 15146-15152

van Dam, P. S. (2002) Oxidative stress and diabetic neuropathy: pathophysiological mechanisms and treatment perspectives. *Diab. Metab. Res. Rev.* **18:** 176–184

van Gaal, L. F., Mertens, I. L. and De Block, C. E. (2006) Mechanisms linking obesity with cardiovascular disease, *Nature*. **444**: 875-880

van Reyk, D. M., Gillies, M. C. and Davies, M. J. (2003) The retina: oxidative stress and diabetes. *Redox Rep.* **8:** 187–192

Vidal-Puig, A. A., Considine, R. V., Jimenez-Linan, M., Werman, A., Pories, W. J. and Caro, J. F. (1997) Peroxisome proliferator-activated receptor gene expression in human tissues. *J. Clin. Invest.* **99:** 2416-2422

Wagener, A., Goessling, H. F., Schmitt, A. O., Mauel, S., Gruber, A. D., Reinhardt, R. and Brockmann, G. A. (2010) Genetic and diet effects on Ppar-a and Ppar-g signaling pathways in the Berlin Fat Mouse Inbred line with genetic predisposition for obesity. *Lipids Health Dis.* **9:** 99

Warren, H. S., Fitting, C., Hoff, E., Adib-Conquy, M., Beasley-Topliffe, L., Tesini, B., Liang, X., Valentine, C., Hellman, J., Hayden, D. and Cavaillon J. (2010) Resilience to bacterial infection: difference between species could be due to proteins in serum. *J. Infect. Dis.* **201:** 223–232

World Health Organisation (2008) Waist Circumference and Waist–Hip Ratio: Report of a WHO Expert Consultation, Geneva.

Wood, L. G., Gibson, P. G. and Garg, M. L. (2003) Biomarkers of lipid peroxidation, airway inflammation and asthma. *Eur. Respir. J.* **21**: 177–186

Yagi, K. (1998) Simple assay for the level of total lipid peroxides in serum or plasma. *Methods Mol. Biol.* **108:** 101-106

Yin, Y. W., Sun, Q. Q., Zhang, B. B., Hu, A. M., Liu, H. L., Wang, Q., Zeng, Y. H., Xu, R. J., Zhang, Z. D and Zhang, Z. G. (2013) Association between interleukin-6 gene -572 C/G polymorphism and the risk of type 2 diabetes mellitus: a meta-analysis of 11,681 subjects. *Ann. Hum. Genet.* **77**: 106-114

Wozniak, S. E., Gee, L. L., Wachtel, M. S. and Frezza, E. E. (2009) Adipose tissue: The new endocrine organ? A review article. *Dig. Dis. Sci.* **54**: 1847-1856

Ye, J. (2009) Emerging Role of Adipose Tissue Hypoxia in Obesity and Insulin Resistance. *Int J Obes (Lond).* **33**: 54–66

Yin, H., Cox, B. E., Liu, W., Porter, N. A., Morrow, J. D. and Milne G. L. (2009) Identification of intact oxidation products of glycerophospholipids *in vitro* and *in vivo* using negative ion electrospray iontrap mass spectrometry. *J. Mass Spectrom.* 44: 672–680

Yoshida, K., Hirokawa, J., Tagami, S., Kawakami, Y., Urata, Y. and Kondo, T. (1995) Weakened cellular scavenging activity against oxidative stress in diabetes mellitus: Regulation of glutathione synthesis and efflux. *Diabetologia.* **38**: 201-210

Yudkin, J. S., Kumari, M., Humphries, S. E. and Mohamed-Ali, V. (2000) Inflammation, obesity, stress and coronary heart disease: is interleukin-6 the link? *Atherosclerosis* **148:** 209-14

Zalba, G., Fortuno, A. and Diez, J. (2006) Oxidative stress and atherosclerosis in early chronic kidney disease. *Nephrol. Dial. Transplant* **21:** 2686-2690

Zhang, Y., Zhou, J, Wang, T. and Cai, L. (2007) High level glucose increases mutagenesis in human lymphoblastoid cells. *Int. J. Biol. Sci.* **3**: 375-379

Zglinicki, T. (2002) Oxidative stress shortens telomeres. *Trends Biochem. Sci.* **27:** 7

Zimmet, P., Alberti, K. G. M. M. and Shaw, J. (2001) Global and societal implications of the diabetes epidemic. *Nature* **414:** 782-787